Molecular and Preclinical Pharmacology of Nonsteroidal Androgen Receptor Ligands

Dissertation

Presented in Partial Fulfillment of the Requirements for the Degree Doctor of Philosophy in the Graduate School of The Ohio State University

By

Amanda Jones, M.S.

Graduate Program in Pharmacy

The Ohio State University

2010

Dissertation Committee:

James T. Dalton, Advisor

Thomas D. Schmittgen

William L. Hayton

Robert W. Brueggemeier

Abstract

     The androgen receptor (AR) is critical for the growth and development of secondary sexual organs, muscle, bone and other tissues, making it an excellent therapeutic target. Ubiquitous expression of AR impedes the ability of endogenous steroids to function tissue selectively. In addition to the lack of tissue selectivity, clinical use of testosterone is limited due to poor bioavailability and pharmacokinetic problems. Our lab, in the last decade, discovered and developed tissue selective AR modulators (SARMs) that spare androgenic effects in secondary sexual organs, but demonstrate potential to treat muscle wasting diseases. This work reveals the discovery of next generation SARMs to treat prostate cancer and mechanistically characterize a prospective SARM in muscle and central nervous system (CNS).

     Prostate cancer relies on the AR for its growth, making it the primary therapeutic target in this disease. However, prolonged inhibition, with commercially available AR antagonists, leads to the development of mutations in its ligand binding domain resulting in resistance. Utilizing the crystal structure of AR-wild-type and AR-W741L mutant, we synthesized a series of AR pan-antagonists (that inhibit both wild-type and mutant ARs). Structure activity relationship studies indicate that sulfonyl and amine linkages of the aryl propionamide pharmacophore are important for the antagonist activity.

     From a series of potent anabolic SARMs, S-23 was chosen to understand the mechanism for the prevention of glucocorticoid- and hypogonadism-induced myopathy. Muscle mass is maintained by a balance in protein synthesis and degradation pathways. Any alteration in this balance, in favor of the degradation pathway, results in muscle atrophy. Glucocorticoid- and castration-dependent dephosphorylation of Akt and up-regulation of ubiquitin ligases were inhibited by S-23. Interestingly, these results also discovered that hypogonadism inactivates the IGF-1/Akt pathway and glucocorticoids up-regulate ubiquitin ligases to induce muscle atrophy.

     In addition to full anabolic activity, S-23 functioned as an agonist in the CNS, at a dose above its muscle $ED_{50,}$ to suppress the hypothalamus-pituitary-gonadal axis. S-23 effectively and reversibly suppressed spermatogenesis in rats with concomitant beneficial effects on muscle,

bone mineral density, and lean mass. Although the therapeutic window was narrow, coadministration with a progestin to rapidly suppress LH and FSH may broaden the therapeutic window and provide an oral agent for hormonal male contraception. Despite these changes in the HPG axis, S-23 enhanced female motivation in ovariectomized rats utilizing the partner preference paradigm. The effectiveness of SARMs in this study provides definitive proof of the importance of androgen receptor function to female sexual motivation.

Collectively, these studies demonstrate the development of pan-AR antagonists and a novel mechanism for androgen function in muscle and CNS.

Dedication

To my parents, Jerilynn, and Brooke

Acknowledgements

First and foremost, I would like to thank my advisor, Dr. Jim Dalton for his guidance, support, and friendship. With his constant encouragement and wisdom, he has made this journey as exciting as it was challenging.

I would like to express my gratitude to my collaborators, Drs. Duane D. Miller, Charles B. Duke III and Dong-Jin Hwang for synthesizing these wonderful compounds and discussions. I would like to thank my committee members, Drs. Thomas D. Schmittgen, William L. Hayton, and Robert W. Brueggemeier for their time and patience. I would also like to convey my deepest appreciation to Dr. Ramesh Narayanan and other colleagues at GTx, Inc for their wisdom and assistance throughout my graduate studies here.

Finally, I need to thank my parents and family for their endless love. It would not have been possible to reach this stage in my life without their support and guidance. I am deeply grateful for their continuous encouragement and belief in me.

Vita

Sept. 2, 1980……………………….......................Born – Canton, OH

May 2003……………………….........................B.S. Pharmaceutical Sciences

University of Toledo

2003-2005………………………….....................Graduate Teaching Associate

University of Toledo

May 2005…………………….............................M.S. Pharmaceutical Sciences

University of Toledo

2005-2006……………………..............................Graduate Teaching Associate

The Ohio State University

2006-2008………………......................................Graduate Research Associate

The Ohio State University

2008-present……………………..........................Research Associate II, Pharmacology

GTx, Inc., Memphis, TN

Publications

Mohler ML, Bohl CE, **Jones A**, Coss CC, Narayanan R, He Y, Hwang DJ, Dalton JT, Miller DD. 2009 Nonsteroidal Selective Androgen Receptor Modulators (SARMs): Dissociating the Anabolic and Androgenic Activities of the Androgen Receptor for Therapeutic Benefit. J Med Chem 52(12):3597-617.

Jones A, Chen J, Hwang DJ, Miller DD, Dalton JT. 2009 Preclinical Characterization of a (S)-N-(4-Cyano-3-trifluoromethyl-phenyl)-3-(3-fluoro, 4-chlorophenoxy)-2-Hydroxy-2-Methyl-Propanamide: A Selective Androgen Receptor Modulator for Hormonal Male Contraception. Endo 150(1):385-395.

Sharifi N, Hamel E, Lill MA, Risbood P, Kane CT, Hossain MT, **Jones A**, Dalton JT, Farrar WL. 2007 A bifunctional colchicinoid that binds to the androgen receptor. Mol Cancer Ther 6(8):2328-36.

Field of Study

Major field: Pharmacy

Table of Contents

List of Tables

List of Figures

Abbreviations

ADT	Androgen deprivation therapy
AF	Activation function
ANOVA	Analysis of the variance
AR	Androgen receptor
ARE	Androgen response element
AUC	Area under the curve
B_0	Percentage of the specific binding in the absence of the compound of interest
BMC	Bone mineral content
BMD	Bone mass density
BPH	Benign prostate hyperplasia
BW	Body weight
CL	Clearance
CNS	Central nervous system
C_{max}	Maximum concentration
CPA	Cyproterone acetate
C_t	Threshold cycle
DBD	DNA-binding domain
DEX	Dexamethasone
DEXA	Dual energy x-ray absorptiometry
DHT	Dihydrotestosterone
DMEM	Dulbecco's Minimum Essential Medium
DMSO	Dimethylsulfoxide
DPBS	Dulbecco's phosphate buffered saline
E_2	Estradiol
EB	Estradiol benzoate
ED_{50}	50% of the effective dose
EDL	Extensor digitorum longus
EIA	Enzyme-immuno assay
E_{max}	Maximum effect
ER	Estrogen receptor
F	Oral bioavailability
FBS	Fetal bovine serum
FM	Fat mass
FFM	Fat free mass
FoxO	Forkhead box O
FSD	Female sexual dysfunction
FSH	Follicle stimulating hormone
GnRH	Gonadotropin releasing hormone
GR	Glucocorticoid receptor
GSK3β	Glycogen synthase kinase 3β

GST	Glutathione S-transferase
HPG	Hypothalamic-pituitary-gonadal
HPLC	High performance liquid chromatography
HSDD	Hypoactive sexual desire disorder
HSP	Heat shock protein
IC_{50}	Concentration that inhibits 50%
IGF-1	Insulin-like growth factor 1
IM	Intra-muscular
IV	Intravenous
K_d	Dissociation constant
K_i	Inhibitory constant
L	Ligand concentration
LBD	Ligand bindind domain
LBP	Ligand binding pocket
LC/MS/MS	Liquid chromatography/mass spectrometry/mass spectrometry
LH	Luteinizing hormone
LNG	Levonorgestrel
MAFbx	Muscle atrophy F-box
MENT	7α-methyl-19-nortestosterone
MFI	Median fluorescent intensity
MIB	Mibolerone
MuRF1	Muscle ring finger 1
MRI	Magnetic resonance imaging
mRNA	Messenger ribonucleic acid
MRT	Mean residence time
mTOR	Mammalian target of rapamycin
NLS	Nuclear localization signal
NTD	N-terminal domain
ORX	Orchidectomize
OVX	Ovariectomize
p70S6K	p70 ribosomal protein S6 kinase
PCR	Polymerase chain reaction
PD	Pharmacodynamic
PEG	Polyethylene glycol
PI3K	Phosphatidylinositol 3 kinase
PK	Pharmacokinetic
P_o	Oral administration
RBA	Relative binding affinity
RIA	Radio-immuno assay
SC	Subcutaneous
SAR	Structure-activity-relationship
SARM	Selective androgen receptor modulator
SHBG	Sex hormone binding globulin
$t_{1/2}$	Half-life

TB	Testosterone buciclate
TD	Testosterone decanoate
TE	Testosterone enanthate
T_{max}	Time to reach maximum concentration
TP	Testosterone propionate
TU	Testosterone undecanoate
V_{ss}	Steady state volume of distribution
WHO	World Health Organization
WT	Wild-type

Chapter 1
Introduction

1.1.   Testosterone Biosynthesis and the Androgen Receptor

Testosterone is the major circulating androgen in men and is essential for development and maintenance of reproductive tissues, muscle and bone mass, hair growth, libido, and spermatogenesis (1, 2). Testosterone is primarily synthesized by the Leydig cells of the testis and is under the control of the hypothalamic-pituitary-gonadal (HPG) axis. Gonadotropin-releasing hormone (GnRH) is secreted by the hypothalamus, which in turn stimulates secretion of luteinizing hormone (LH) and follicle-stimulating hormone (FSH) from the anterior pituitary gland (Figure 1.1). Testosterone is synthesized in response to both LH and FSH. High levels of endogenous testosterone or exogenous androgens bind the androgen recepetor (AR) in the central nervous system (CNS) and exert negative feedback by inhibiting secretion of GnRH (3). Sertoli cells of the testis also respond to FSH by releasing inhibin and activin, important factors in sperm maturation and HPG regulation.

The AR is activated directly by testosterone or dihydrotestosterone (DHT), the reduced metabolite of testosterone that is produced in male accessory sex organs, skin, and hair follicles (Figure 1.2). The AR is a member of the nuclear hormone receptor superfamily of ligand activated transcription factors. The AR gene, located on the X chromosome, is more than 90 kb long and encodes a protein of 919 amino acids (Figure 1.3) The AR protein follows the consensus nuclear hormone receptor structure with an N-terminal domain (NTD), whose function is still not clear, a DNA binding domain (DBD), responsible for binding to androgen response elements (ARE), a hinge region containing a nuclear localization signal (NLS), and a ligand binding domain (LBD), to which androgens bind and activate the receptor. The activation function 1 (AF-1), located in the NTD, is functionally independent of ligand binding and critical for full transactivation (4). The LBD contains the AF-2 domain that functions in a ligand-dependent manner and takes on a conformation that facilitates the recruitment of co-activators or co-repressors (5).

Unbound, inactive AR is localized in the cytosol in association with heat shock proteins (HSPs) in a high affinity conformation (6). Steroids diffuse through the cell membrane and bind to the AR. Ligand binding causes dissociation of HSPs and alters AR conformation leading to a sequence of events initiated by AR homodimerization and followed by post-translational modification and translocation to the nucleus (7). The translocated receptor-ligand complex binds to the ARE located in the promoter or enhancer regions of AR gene targets. Recruitment of co-activators or co-repressors (8) and other transcriptional machinery (9) regulates the transcription and translation of target genes.

The crystal structure of the AR reveals that the LBD forms 11 α-helices (H1-H12; H2 is absent in AR) and two β-turns, arranged in a three layer, α-helical sandwich (10). Upon agonist binding, H12 repositions to form a "lid" for the ligand binding pocket (LBP) and stabilize the ligand. This conformation positions the functional AF2 region on the surface of the LBD, a prerequisite for co-regulator recruitment. However, binding of an antagonist puts a strain on H12, leaving the LBP open.

In addition to the classical genomic pathway of AR-mediated transcriptional activation, non-genomic pathways, independent of direct DNA binding (11), have also been reported in osteoblasts (12), oocytes (11), prostate cancer cells (13), and skeletal muscle cells (14). The non-genomic actions of AR are characterized by rapidly activating signaling cascades leading to subsequent physiological response within a few seconds to minutes after ligand sensitization (15). The mechanism underlying the nongenomic actions remain unclear although conflicting evidence supports the role of intracellular AR or an obscure G protein-coupled receptor (GPCRs) (11, 14, 16).

1.2. Steroidal Androgens

Traditionally, testosterone has been used to treat androgen insufficiency related disorders such as hypogonadism, cachexia due to cancer, burns and disuse, improve sexual function, cognitive function and even used as a male contraceptive. In women, the physiological role of testosterone is controversial, but theoretically testosterone could be used to improve bone mass, muscle mass, and libido (1, 17).

Originally, an oral preparation of unmodified testosterone was introduced for the treatment of hypogonadism, only to discover its ineffectiveness due to rapid hepatic elimination ((18) Figure 1.4). Addition of a 17α-methyl group to the testosterone backbone (17α – methyltestosterone) delayed metabolism and provided an orally effective preparation. However, use of preparations with this alkyl modification has been discontinued due to apparent

hepatotoxicity (19). Esterification of the 17β-position with a long fatty acid side chain (testosterone undecanoate or TU) improved oral absorption but the serum concentration-time profiles exhibit high inter-individual variability, thus limiting its use (20). To prolong the pharmacologic effects of testosterone, various esters were developed including testosterone enanthate (TE), testosterone buciclate (TB), testosterone decanoate (TD) and testosterone propionate (TP). Administration of these esters is limited to intramuscular (i.m.) injection, transdermal patches or gels, or surgical installation of implants and pellets. However, analogous to the parent steroidal testosterone preparations, these long-acting esters also have limitations including highly fluctuating serum testosterone levels between injections and skin irritations associated with patch use (19). Although some enhancement of the pharmacologic effects were obtained relative to testosterone, it was never possible to adequately dissociate the anabolic (i.e. muscle and bone) and androgenic (i.e. prostate) activities of these compounds. As such, potential long-term use of steroidal testosterone in men and women is negligible because of significant pharmacokinetic (PK) and pharmacodynamic (PD) problems as well as possible risks to reproductive tissues associated with their use.

1.3.   Discovery and Development of Selective Androgen Receptor Modulators (SARMs)

Nonsteroidal AR ligands were first identified as antagonists for the treatment of prostate cancer (21-23). Several pharmacophores with high AR binding affinities were discovered. This included the monoarylpropionamide flutamide (a prodrug of hydroxyflutamide (21-23)), the hydantoin nilutamide (24-26), and the diarylpropionamide bicalutamide ((27-29) Figure 1.5). In pursuit of irreversible AR inhibitors, certain thioether derivatives of bicalutamide with considerable agonist activity *in vitro* were discovered (30). However, extensive hepatic metabolism led to negligible tissue exposure resulting in lack of activity *in vivo* (31). Structural modifications by dehalogenating the B-ring were performed to minimize B-ring reactivity (e.g. replace *p*-chloroacetamide with *p*-acetamide). The resulting compound, acetothiolutamide, possessed potent agonist activity only *in vitro* ((31) Figure 1.5). Metabolite studies revealed that the lack of agonist activity *in vivo* was due to conversion of the thioether to sulfoxides and sulfones, which are present in bicalutamide (31). Further structural modifications were made to the diarylpropionamide backbone, namely converting the thioether to an ether linkage, and the resulting compound (S-4) was identified as a potent AR agonist both *in vitro* and *in vivo* ((32, 33) Figure 1.5).

En route to develop an AR ligand that demonstrates greater anabolic activity than androgenic activity *in vivo*, the successful crystallization of R-bicalutamide and

arylpropionamides in the AR LBD allowed for efficient structure-based design of nonsteroidal AR ligands. Important *in vitro* structure-activity-relationships (SARs) were identified to optimize AR binding affinity and functional activity, including electron-withdrawing groups at the *para* position of the A-ring (e.g. cyano or nitro), an ether bridge, and electron-withdrawing groups at the *ortho*, *meta* and/or *para* positions of the B-ring (e.g. halogens, cyano or nitro). These modifications significantly altered *in vitro* AR binding affinity and functional activity. *In vivo*, these minor modifications led to a spectrum of SARMs that possess antagonist activity (bicalutamide in Table 1.1), anabolic agonist activity with full or partial efficacy in muscle/bone (S-4 and S-1, respectively in Table 1.1), and potent CNS activity that retain peripheral anabolic agonism (S-23 in Table 1.1), thus expanding the gamut of potential clinical applications of SARMs.

The ideal SARM has been described as an orally available, minimally hepatotoxic compound displaying antagonist or weak agonist activity in the prostate, partial to full agonist activity in the pituitary, muscle and bone (34). These characteristics, present in the aryl propionamide SARMs, provide a superior clinical alternative to steroidal androgen preparations. Collectively, SARMs display AR activities comparable to testosterone therapy (osteo- and myoanabolism) but without the major concern of increasing the risk of benign prostate hyperplasia (BPH), prostate cancer, or virilization in women.

The mechanisms by which SARMs dissociate anabolic and androgenic actions, while testosterone cannot, remains unclear. Studies have shown that the conformational change of the AR upon SARM binding is distinct from DHT, thus recruiting different coregulator complexes (35, 36). Additionally, studies from our laboratories indicate that SARMs recruit both co-activators and co-repressors to the PSA promoter in LNCaP prostate cancer cells, raising the possibility that SARMs and DHT recruit similar co-activator complexes in anabolic tissues but distinct complexes in androgenic tissues (37). Secondly, SARMs and DHT may nongenomically mediate intracellular signaling differently. The conformational changes of the AR in the presence of SARMs versus DHT activate distinct combinations of intracellular signaling pathways, leading to different biological responses in AR target tissues (i.e. prostate (37)). Finally, testosterone is converted to a more active metabolite (DHT) in the prostate *via* 5α-reductase, resulting in an amplified effect, rendering testosterone extremely potent in both androgenic and anabolic tissues. SARMs are not substrates for 5α-reductase and may compete with DHT for the AR in androgenic tissues, possibly contributing to their tissue selectivity.

Regardless of the mechanism, the fact remains that SARMs possess important pharmacokinetic and pharmacodynamic advantages over steroidal testosterone preparations. The

well established evidence supporting their *in vivo* tissue selectivity and successful proof-of-concept animal studies has stimulated massive interest in the therapeutic potential of SARMs in humans.

1.4. Therapeutic Potential of SARMs and Nonsteroidal AR Antagonists

1.4.1 Hormonal Male Contraception

The discovery of oral contraceptives for women was a major medical breakthrough of the twentieth century. It provided a relatively safe and reversible method to separate sex and reproduction. Male contraception, however, is limited to unreliable condoms and virtually irreversible vasectomies. The physiologic target for hormonal-based methods for men lies in the HPG axis. Suppression of gonadotropin secretion (LH and FSH), and consequently testosterone, can be achieved by exogenous androgens, GnRH ligands or progestins (38, 39). Sufficient suppression results in a reduction of spermatogenesis, leading to azoospermia, or absence of sperm in the ejaculate. This, however, leads to a state of hypogonadism and therefore requires supplemental androgens to fulfill peripheral needs.

In the 1990's, the World Health Organization (WHO) sponsored two large international studies using TE (200 mg/wk, i.m.). In the first study, azoospermia was achieved in 64% of men (n=271) after 6 months (40). The second study concluded when severe oligozoospermia ($<3x10^6$ sperm/mL) was achieved and proved to be not as effective as azoospermia but better than that of condoms (41). However, injection intervals were too short for complete suppression of spermatogenesis resulting in supraphysiologic levels of serum testosterone. In a study in China utilizing the longer acting TU, 97% of men (n=308) achieved azoospermia or severe oligozoospermia after receiving a loading dose of 1000 mg followed by monthly injections of 500 mg for 6 months (42). However, suppression was achieved in only 67% of Caucasian men (43).

A tissue selective steroidal androgen, 7α-methyl-19-nortestosterone (MENT) was later investigated for use as a hormonal male contraceptive agent (44). MENT is not a substrate for 5α-reductase and thus displays tissue selectivity compared to traditional steroidal preparations. In a clinical trial of 12 eugonadal men, 9 men that received 4 implants delivering a dose of 400 µg/day for 12 months achieved oligozoospermia or azoospermia while 2 did not respond to treatment. However, typical steroid-related side effects, including changes in hematocrit, erythrocyte, hemoglobin, lipid profiles and liver enzymes, were observed.

To increase the success rate of hormonal male contraception and lower the dose of testosterone, especially in Caucasian men, testosterone-based regimens combined with progestins or GnRH antagonists were employed. The GnRH antagonist-testosterone combination provided a

rapid onset of spermatogenic suppression, achieving azoospermia, but the expense of these antagonists limit its feasibility for worldwide use (38). Progestins, on the other hand, are more reasonably priced and commonly used in female contraceptives. When administered as monotherapy in men, rapid and potent gonadotropin suppression was achieved (39). However, as spermatogenesis was suppressed, so was testosterone and therefore libido. The most effective progestins used in combination with testosterone injection include cyproterone acetate (CPA), depot medroxyprogesterone acetate, norethisterone, levonorgestrel (LNG), desogestrel, and etonorgestrel (45). Although the synergy of progestin/testosterone combinations to suppress spermatogenesis is promising, the lack of an orally available regimen prevents widespread acceptance for a hormonal based regimen for male contraception (46, 47).

A novel SARM, C-6, was the first aryl propionamide derivative to be identified as a potent regulator of gonadotropins and testosterone in castrated and intact rats, respectively (48). C-6 displayed 4.5 fold greater anabolic than androgenic activity. In castrated rats, the levator ani muscle was maintained at levels similar to that of intact controls at 1.2 mg/kg/day, whereas the prostate was maintained at 50% of intact control with concomitant suppression of LH and FSH. A follow-up study revealed that C-6, when administered at 4 mg/kg/d, significantly inhibited spermatogenesis while maintaining its tissue selective properties. Collectively, tissue selective SARMs represent a promising candidate for an orally available hormonal male contraception.

1.4.2   Female Sexual Dysfunction

Androgens are involved in a number of physiological roles in women, including maintenance of bone mineral density, muscle mass and strength, libido and sexual response (1, 17, 49). Hypoactive sexual desire disorder (HSDD) is a widespread disorder that afflicts naturally postmenopausal women (50-52) and to a greater extent, those who have undergone bilateral oophorectomy (53-55). It is believed that HSDD is associated with a decline in free testosterone levels following surgically-induced or natural menopause.

Clinical trials in premenopausal women revealed that sexual desire and arousal may be enhanced when administered a once daily spray of a 90 μg metered-dose transdermal testosterone preparation for 16 weeks compared with placebo (56). Likewise, when postmenopausal women received a biweekly 300 μg/day testosterone patch for 24 weeks, the frequency of satisfying sexual events, including desire, arousal, orgasm, pleasure and responsiveness, as well as body image, increased compared to placebo (52). Additionally, clinical trials of a 300 μg/day testosterone patch improved sexual functioning, desire, fantasies and well-being in bilaterally

oophorectomized women receiving concomitant estrogen therapy after 12 (57) or 16 weeks of treatment (58).

Use of anabolic steroids in women is limited due to virilization, which is characterized by the development of male sex phenotypes such as deepening of the voice, hirsutism, male pattern baldness, clitoral enlargement, increased muscle strength and acne (59). With reduced androgenic liability and therefore virilizing potential, SARMs offer hope of androgen therapy in women.

1.4.3   Prostate Cancer

Not only normal prostate growth, but also its transformation into cancer depends on androgens. The most commonly used antiandrogens for the treatment of prostate cancer are flutamide and bicalutamide. Clinical studies have shown the effectiveness of bicalutamide in androgen-dependent prostate cancers, frequently administered in combination with leuprolide or other gonadotropin-releasing hormone agonists to achieve maximum androgen blockade (60, 61). However, after initially responding to treatment, many patients relapse subsequent to developing castration-resistant prostate cancer (antiandrogen withdrawal syndrome) (62). This phenomenon is believed to arise from point mutations in the AR LBD causing some antiandrogens to exhibit androgenic activity (63, 64). Commonly observed mutations include Thr 877→Ala (AR(T877A)), Trp 741→Leu (AR(W741L)), and Trp 741→Cys (AR(W741C). Hydroxyflutamide displays agonist activity in AR(T877A) (65) while bicalutamide is a potent agonist in both AR(W741L) and AR(W741C) (66). The resolved crystal structure of bicalutamide bound to AR(W741L) in the agonist conformation (67) confirms the importance of the antagonistic action of antiandrogens by pushing helix 12 of the AR away from the binding pocket (68). Development of a compound that would prevent closure of helix 12 over the LBP (i.e. agonist conformation) and exhibit antagonist activity across all mutations of the AR (pan-antagonism) would be a major breakthrough in the treatment of androgen-dependent prostate cancer.

1.4.4   Muscle Atrophy

Muscle atrophy is a debilitating condition that may result from burns (69), sepsis (70), aging (71), disuse (72), cancer (73), AIDS (74), as well as long-term glucocorticoid administration for the treatment of rheumatoid arthritis (75) and asthma (76). The anabolic effects of the steroids, testosterone and nandrolone, have been demonstrated under conditions related to aging men (71), long-term glucocorticoid treatment (77, 78), HIV (79), and severe

burns (80). Testosterone administration is associated with a dose-dependent increase in lean muscle mass and maximal voluntary strength and a decrease in fat mass.

S-4, a full efficacy anabolic SARM, not only increases the size of the levator ani muscle but also improves skeletal muscle strength (81). Despite only partial recovery in soleus muscle size, S-4 restored the peak tetanic tension (P_0) of the soleus muscle, a measure of contractile force, to intact levels or better. Castration decreased the P_0 to 0.57N; however, S-4 increased P_0 to 0.86N. At 10 mg/kg, S-4 further increased P_0 to 1.02 N, significantly greater than that observed for intact animals (0.85 N) (81).

The effect of S-4 on bone was also investigated in castrated male rats (81). S-4 reduced osteocalcin levels by 70% suggesting SARMs may exert an antiresorptive mechanism on bone turnover. S-4 also partially restored bone mass density (BMD) and bone mineral content (BMC) as well as prevented loss of whole body and lumbar (L5-L6) vertebrae BMD in female rats (82). With reduced prostate and virilizing liability in men and women, SARMs offer novel treatment options in disease states requiring long-term androgen administration, including muscle wasting disorders and osteoporosis.

1.5.   Scope and Objectives of Dissertation

Previous work in our laboratory examined *in vitro* SARs and identified various novel arylpropionamide SARMs that are full agonists in anabolic tissues but at the same time are prostate sparing, SARMs that exhibit partial agonist activity in anabolic tissues, and SARMs that are CNS agonists, resulting in HPG suppression. This research project utilized several arylpropionamide SARMs in proof-of-concept animal studies, extending the therapeutic potential of SARMs. Specifically, its objectives were the following:

I. To determine if a SARM (S-23) is an effective and reversible agent for hormonal male contraception. We hypothesized that S-23, a SARM with potent CNS agonist activity, will mimic the ability of testosterone to regulate gonadotropin secretion and testosterone biosynthesis and effectively suppress spermatogenesis in male rats while maintaining the peripheral needs of androgens in muscle and bone. We also hypothesized that upon cessation of SARM administration, gonadotropin secretion and testosterone synthesis will return to normal and spermatogenesis will ensue.

II. To determine if a series of arylpropionamide SARMs are effective in maintaining sexual motivation in ovariectomized female rats. Transdermal testosterone preparations have enhanced sexual desire in women. However, this desired outcome is accompanied with unwanted steroid-related side effects. We hypothesized that SARMs will mimic the effects

of transdermal testosterone administration in female sexual motivation and that it is at least partially mediated *via* the AR. This will be determined utilizing the partner preference paradigm.

III. To determine if AR pan-antagonists can be developed by adding bulk to the B-ring. Mutations in the AR often change the binding conformation of antiandrogens to adopt that of an agonist binding, thus conferring agonist activity. Combining knowledge of the R-bicalutamide W741L mutant AR complex with DHT bound wild-type AR, we hypothesized that adding bulky substituents to the B-ring may result in pan-antagonism of the various mutations of the AR.

IV. To determine the mechanism by which SARMs inhibit glucocorticoid-induced and castration-induced muscle atrophy. The tissue selective properties of SARMs are well established; however, the mechanism by which SARMs inhibit muscle catabolism and promote muscle protein synthesis remains largely unknown. We hypothesized that SARMs will inhibit muscle catabolism by reducing the up-regulation of muscle-specific ubiquitin ligases.
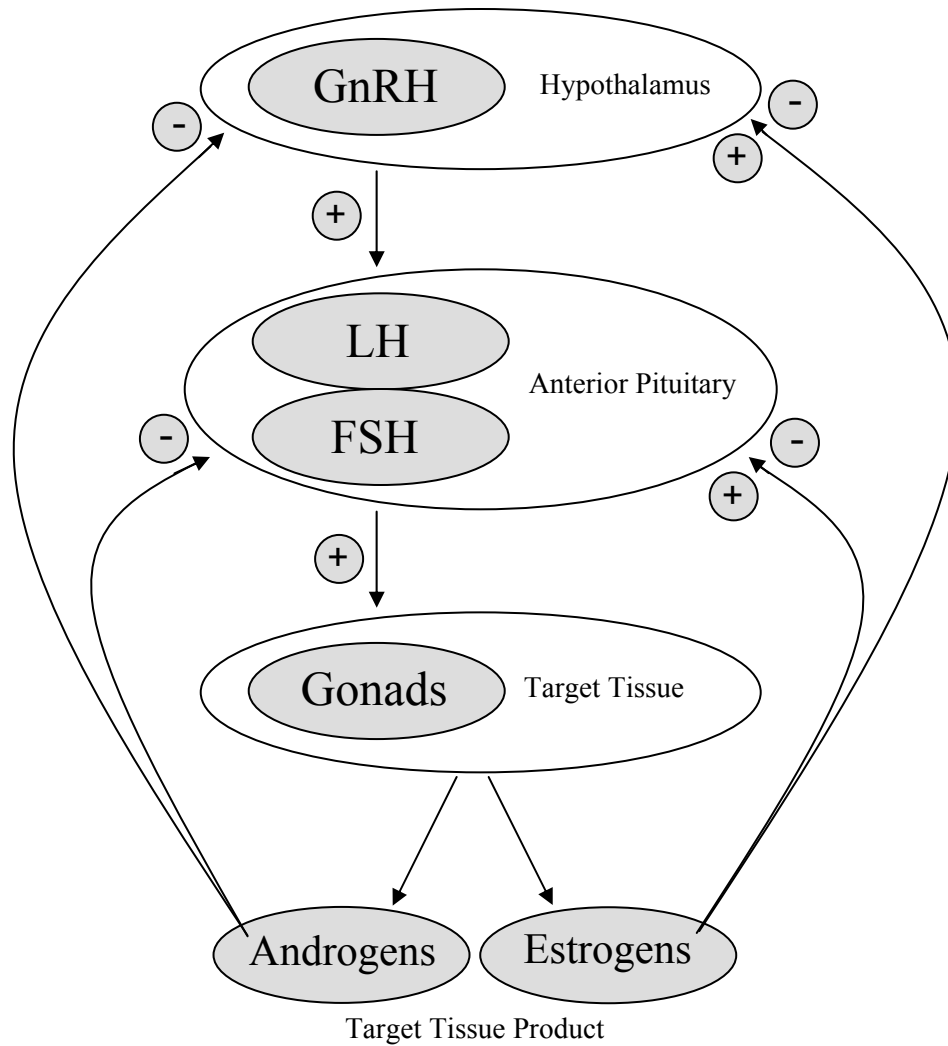
Figure 1.1. Hypothalamus-Pituitary-Gonadal Axis

Production of gonadal steroid hormones is regulated by hormones produced in the hypothalamus (gonadotropin releasing hormone: GnRH) and pituitary (luteinizing hormone: LH; and follicle stimulating hormone: FSH). (+) represents positive feedback and (-) negative feedback. Figure adapted from Goodman and Gilman's Pharmacological Basis of Therapeutics (83).
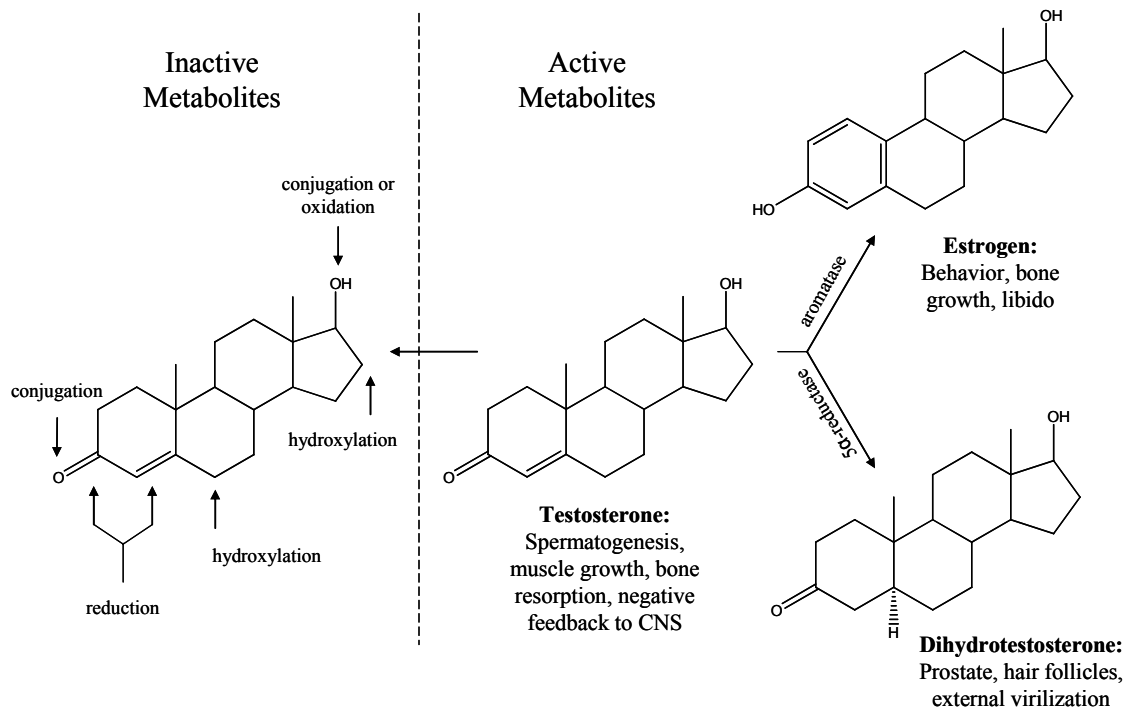
Figure 1.2. Physiological Actions of Testosterone and its Metabolites

Schematic representation of metabolism sites of testosterone and physiological actions of testosterone and its active metabolites. Figure adapted from Neischlag *et al* (84) and Gao *et al* (85).
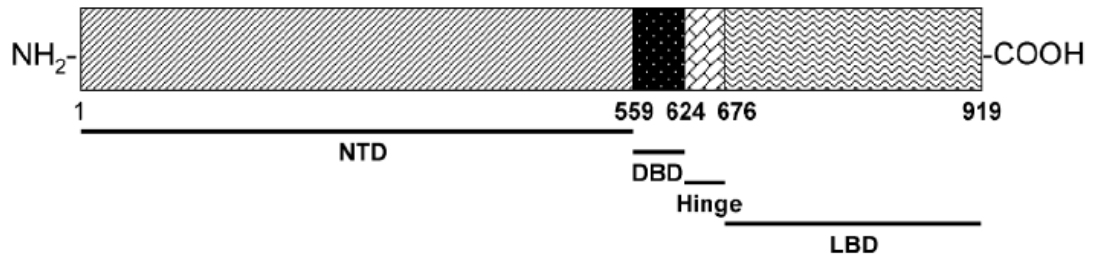
Figure 1.3. Structural Organization of the Human Androgen Receptor

Schematic representation of the 110 kD hAR. NTD: N-terminal domain; DBD: DNA binding domain; LBD: ligand binding domain. Figure adapted from Gao *et al* (85).
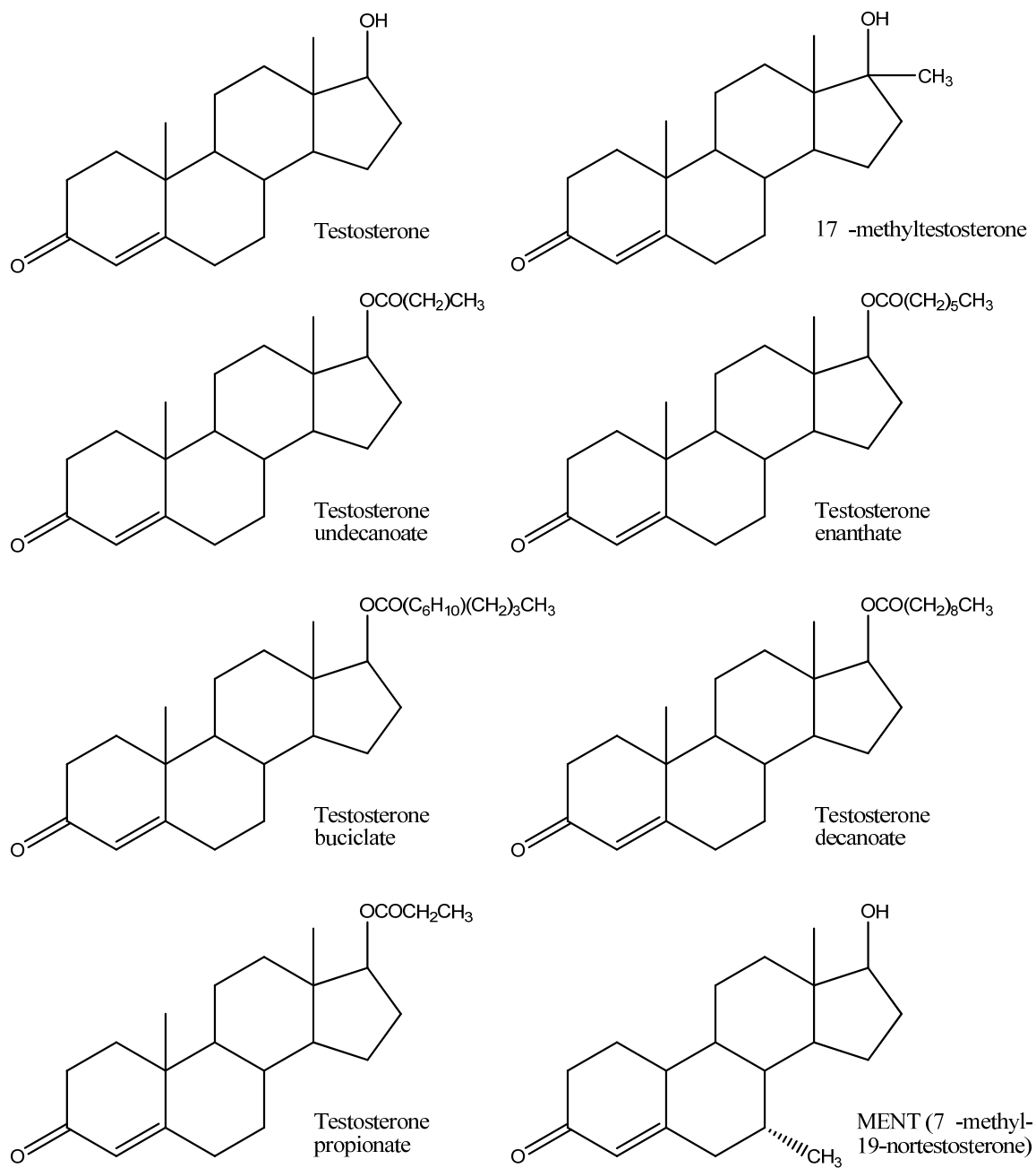
Figure 1.4. Chemical Structures of Steroidal Androgens

13

Name	Chemical Structure	RBA (%)	*In vitro* Activity (%)	E_{max} (LA)	ED_{50} (LA)	E_{max} (VP)	ED_{50} (VP)	F (%)
R-Bicalutamide		0.69	NA	NA	NA	NA	NA	NA
Acetothiolutamide		4.1* (31)	50	NA	NA	NA	NA	NA
S-4		3.3* (32)	93	101 (TP: 104)	0.14 (TP: 0.13)	35.2 (TP: 121)	0.43 (TP: 0.13)	100
S-1		5* (32)	43	74.9	0.44	14.5	0.42	55-60
S-23		26.5	96	139	0.079	138	0.43	96

* RBA calculated assuming the K_i of DHT was 0.2 nM.

Table 1.1. Activity of Steroidal and Nonsteroidal Ligands

Binding affinities (RBAs) are expressed relative to DHT. *In vitro* functional activity is the percentage induced by 10 nM of the respective AR ligand, compared to 1 nM DHT. *In vivo* activity was determined in a 14 day PD study in castrated male rats. LA: levator ani; VP: ventral prostate.

Chapter 2

An Effective and Reversible SARM for Hormonal Male Contraception

2.1.   Introduction

The ultimate goal of hormonal male contraception is to suppress LH and FSH, *via* the HPG axis, resulting in depletion of intratesticular testosterone and suppression of spermatogenesis, while replacing the physiological need for androgens using an androgen preparation (84). Although 90-100% of Asian men receiving testosterone-alone regimens achieved azoospermia, this regimen was not highly effective in non-Asian men (~ 60% azoopermia) (40, 41). As such, clinical trials using testosterone in combination with progestins or GnRH analogs are widely viewed as the most promising approach to hormonal male contraception (86, 87). Identification of orally available androgens with the ability to mimic the beneficial anabolic effects of testosterone at doses that do not support spermatogenesis would be a significant step toward achieving this goal.

We previously synthesized a novel SARM (C-6), which bears a *para*-nitro substituent on the A-ring, a *para*-chloro group and a *meta*-fluoro group on the B-ring (Figure 2.1), that was identified as the first arylpropionamide SARM that exhibited potent ability to regulate gonadotropin and testosterone levels in castrated and intact male rats, respectively (48). Pharmacokinetic studies showed that C-6 is orally bioavailable (76%) with a moderate terminal half-life (6.3 h) at a dose of 10 mg/kg in male rats. Additional pharmacologic studies of C-6 demonstrated its profound effects on spermatogenesis in intact male rats after 70-days of treatment at 1 mg/day (48). However, *in vivo* metabolism studies revealed that the major metabolites arose from step-wise reduction of the nitro group on the A-ring of the arylpropionamide SARM backbone (Figure 2.1). Although structure-activity relationship studies showed that changing the *para*-nitro group on the A-ring to a cyano group (S-23) slightly decreased the AR binding affinity and *in vitro* functional activity (33), this modification significantly improved *in vivo* pharmacokinetic properties and efficacy of closely related arylpropionamide SARMs (88).

In the current studies, we examined the *in vitro* and *in vivo* characteristics of S-23, including *in vitro* AR binding affinity, AR-mediated transcriptional activation, and pharmacologic activity in castrated and intact male rats. Although such an agent is most likely to be used in combination with a progestin for oral male contraception in humans, we first examined the effects of S-23 in male rats when co-administered with a low dose of estradiol benzoate (EB), previously shown to be sufficient to support sexual behavior when administered with DHT (89-91). Male rats require estrogen to maintain normal sexual behavior, while androgen alone appears to be the major determinant of human male sexual behavior (90, 92-94). As such, we assessed the endocrine, pharmacologic, and reproductive effects of S-23 at doses ranging from 0.05 to 0.75 mg/day when combined with EB (5 μg/day) by daily subcutaneous (sc) injection for 70 days. The anti-reproductive activity of S-23 was evaluated by its ability to suppress spermatogenesis and prevent pregnancy in mating trials. The effects of S-23 on body weight, androgen-dependent organ weights, body composition, and endocrine hormones were also determined. In addition, the reversibility of the contraceptive regimen was determined by maintaining the rats for more than a full spermatogenic cycle following treatment with a subsequent mating trial. These studies are the first to demonstrate that an arylpropionamide SARM can be used as a component of an effective and reversible oral male contraceptive regimen.

2.2.   Materials and Methods

2.2.1   Experimental Animals

All male and female Sprague-Dawley rats were purchased from Harlan Bioproducts for Science (Indianapolis, IN). Animals were maintained on a 12hour light/dark cycle with food and water available *ad libitum*. The animal protocols were reviewed and approved by the Institutional Laboratory Animal Care and Use Committee of The Ohio State University.

2.2.2   *In Vitro* AR Binding Affinity

Cytosolic AR was prepared from the ventral prostates of male Sprague-Dawley rats 24 hours after castration. The AR binding affinity of S-23 was determined using a radio-labeled competitive binding assay. Briefly, an aliquot of AR cytosol was incubated with 1 nM [^{3}H]mibolerone (MIB; PerkinElmer, Waltham, MA) and 1 mM triamcinolone acetonide at 4° C for 18 hours in the absence or presence of 10 increasing concentrations of the compound of interest (10^{-1} to 10^4 nM). Nonspecific binding of [^{3}H]MIB was determined by adding excess unlabeled MIB (1000 nM) to the incubate in separate tubes. After incubation, the AR-bound

radioactivity was isolated using the HAP method (95). The bound radioactivity was then extracted from HAP and counted. The specific binding of [^{3}H]MIB at each concentration of the compound of interest was calculated by subtracting the nonspecific binding of [^{3}H]MIB and expressed as the percentage of the specific binding in the absence of the compound of interest (B_0). The concentration of the compound that reduced B_0 by 50% (i.e. IC_{50}) was determined using WinNonlin (Pharsight Corp., Mountain View, CA). The equilibrium binding constant (K_i) of the compound of interest was calculated by $K_i = K_d \times IC_{50}/(K_d + L)$, where K_d is the dissociation constant of [^{3}H]MIB (0.19 ± 0.01 nM) and L is the concentration of [^{3}H]MIB used in the experiment (1 nM). The K_i value of each compound of interest was further compared. Relative binding affinities (RBA) are expressed relative to DHT (100%).

2.2.3 *In Vitro* Transcriptional Activity

The *in vitro* functional activities of nonsteroidal ligands were determined by the ability of each ligand to induce AR-mediated transcriptional activation in a co-transfection system. On day 1, CV-1 cells at 90% confluency were transiently transfected in T-125 flasks. The transfection was carried out in serum-free DMEM (Hyclone, Logan, UT) using LipofectAMINE (Invitrogen, Carlsbad, CA) according to the manufacturer's instruction. Cells in each flask were transfected with 0.8 µg of a human AR expression construct (pCMVhAR), 4 µg of an androgen-dependent luciferase reporter construct (pMMTV-Luc), and 4 µg of a β-galactosidase expression construct (pSV- β- galactosidase; Promega Corp.) for 10 hours. Cells were allowed to recover for 12 hours and were then seeded into 24-well plates at a density of 8×10^4 cells/well and allowed to recover for an additional 10 hours before drug treatment.

Activity of each compound of interest (final concentrations ranging from 1-1000 nM) was determined by incubating cells in the absence of 1 nM DHT. In each experiment, vehicle control and positive control (activity induced by 1 nM DHT) were included. Previous experiments in our laboratory determined that the lowest concentration of DHT (Sigma Aldrich, St. Louis, MO) that produced maximal AR-mediated transcriptional activation was 1 nM (30). Therefore, in the present study, the transcriptional activation induced by this concentration of DHT was set as 100% and used as the reference for quantifying agonist activity of C-6 and S-23. After drug treatment (24 hours), cells were washed with ice-cold PBS twice and lysed with 110 µL/well of passive lysis buffer for 30 minutes at room temperature. An aliquot (50 µL) of cell lysate from each well was used for luciferase assays. Transcriptional activity in each well was calculated as the ratio of luciferase activity to β-galactosidase activity to avoid variations caused

by cell number and transfection efficiency. Transcriptional activity induced by each compound of interest was expressed as the percentage of transcriptional activity induced by 1 nM DHT.

2.2.4   *In Vivo* Pharmacologic Activity of S-23 in Castrated Rats

The *in vivo* pharmacologic activity of S-23 was examined in thirty (n = 5/group) male Sprague-Dawley rats weighing approximately 200 grams. Animals were castrated *via* scrotal incision under anesthesia (87 mg/kg ketamine and 13 mg/kg xylazine in saline, ip) 24 hours prior to drug treatment and received daily subcutaneous (sc) injections of S-23 at dose rates of 0.01, 0.05, 0.1, 0.5, 1, and 3 mg/day for 14 days. S-23 was freshly dissolved in vehicle containing dimethylsulfoxide (DMSO; 5%, v/v; Sigma Aldrich) in polyethylene glycol 300 (PEG 300; Sigma Aldrich) before daily administration. An additional two groups of animals with or without castration received vehicle only and served as castrated or intact control groups, respectively. Animals were sacrificed at the end of treatment. Plasma samples were collected and stored at -80° C until use. The ventral prostate, seminal vesicles, and levator ani muscle were removed, cleared of extraneous tissue, and weighed. All organ weights were normalized to body weight and compared. The weights of prostate and seminal vesicles were used to evaluate androgenic activity, while the levator ani muscle weight was used as a measure of anabolic activity. Non-linear regression analysis was performed to obtain the maximal response (E_{max}) induced by S-23 and the dose of S-23 that induced 50% of the maximal response (ED_{50}), using the sigmoid E_{max} model with a baseline effect parameter and WinNonlin software. No upper or lower boundary was used for this modeling.

2.2.5   Pharmacokinetics of S-23 in Rats

The pharmacokinetics of S-23 was examined in male Sprague-Dawley rats weighing approximately 250 grams after a dose of 10 mg/kg by intravenous injection or oral gavage. A catheter was implanted into the right external jugular vein of each animal 24 hours prior to drug administration. S-23 was dissolved in a vehicle containing DMSO (10%, v/v) in PEG 300 and administered to animals through the jugular vein catheter (iv group) or oral gavage (po group) at a volume of 100 µL per dose. For animals in the iv group, the catheter was flushed three times with saline (3× the volume of the dosing solution) before blood sampling. Blood samples (~ 200 µL) were then withdrawn through the jugular vein catheter at 5, 10, 20, 30, 60, 120, 240, 360, 480, 720, 1440, 1800, 2160, and 2880 minutes after the iv dose and at 20, 30, 60, 90, 120, 180, 240, 360, 480, 720, 1440, 1800, 2160, and 2880 minutes after the po dose. An aliquot of saline equal to the volume of blood withdrawn was administered to each animal after each sample

collection. Blood samples were immediately centrifuged at 1,000 g, 4° C for 10 minutes. Plasma samples were prepared and stored at -20° C until HPLC analysis. Stability of S-23 in plasma at room temperature for 48 hours and at -20° C for 30 days was determined to be within 10% of a fresh analytical sample.

An aliquot (90 µL) of each plasma sample from the pharmacokinetic study was spiked with 10 µL of an internal standard (C-3, a structural analog of S-23), and mixed well with 1 mL of acetonitrile (Sigma Aldrich). After centrifugation at 16,000 g, 4° C for 10 minutes, the supernatant was collected and evaporated. The residues were reconstituted in 200 µL of mobile phase. An aliquot of each sample was injected into a Nova-pak C_{18} column (3.9 × 150 mm, 4 µm particle size; Waters Corporation, Milford, MA). The HPLC system consisted of a solvent pump, a degasser, an autosampler, and a UV detector (model 1100, Agilent Technologies, Palo Alto, CA). HPLC separation was performed using an isocratic mobile phase (water/acetonitrile: 50/50, v/v) at a flow rate of 1 mL/min. The UV absorbance of eluents was monitored at 296 nm. Calibration standards were prepared in blank rat plasma with S-23 concentrations ranging from 0.1 ~ 50 µg/mL with the limit of quantitation at 0.1 µg/mL.

The plasma concentration-time data were analyzed using noncompartmental methods in the WinNonlin software. The terminal half-life ($t_{1/2}$) was calculated as $t_{1/2} = 0.693/\lambda$, where λ was the terminal elimination constant. The area under the plasma concentration-time curve ($AUC_{0-\infty}$) was calculated using the trapezoidal method with extrapolation to time infinity. The plasma clearance (CL) was calculated as $CL = Dose_{iv}/AUC_{0-\infty, iv}$, where the $Dose_{iv}$ and $AUC_{0-\infty, iv}$ were the iv dose and the corresponding area under the plasma concentration-time curve from time 0 to infinity, respectively. The apparent volume of distribution at equilibrium (Vd_{ss}) was calculated as $Vd_{ss} = CL\cdot MRT$, where the MRT was the mean residence time following the iv bolus dose. The peak plasma concentration (C_{max}) and time to reach the peak concentration (T_{max}) after a po dose were obtained directly from the plasma concentration-time curves. Oral bioavailability (F_{po}) was defined as $F_{po} = AUC_{0-\infty, po}/AUC_{0-\infty, iv}$ where the $AUC_{0-\infty, po}$ is the corresponding area under the plasma concentration-time curve from time 0 to infinity after oral administration.

2.2.6   Effects of S-23 on Spermatogenesis and Endocrine Physiology in Intact Rats

Forty-two male Sprague-Dawley rats (90 days old) were randomly assigned to seven groups (n = 6/group). All doses were administered *via* sc injection (100 µL/day). Group 1 was the intact control group and received vehicle alone (5% DMSO + 95% PEG 300). Group 2 was the EB control group and received EB alone at a dose of 5 µg/day. In addition to EB (5 µg/day),

animals in groups 3 through 7 were treated with S-23 at dose rates of 0.05, 0.1, 0.3, 0.5, and 0.75 mg/day, respectively. A pilot study with a structurally similar analog (C-6) alone was tested for hormonal male contraception at a single dose of 1 mg/day. In that study, partial but marked suppression of spermatogenesis was observed after 10 weeks of treatment in intact male rats (48). However, the effects of C-6 alone on fertility could not be evaluated due to the fact that the presence of estrogen is essential to maintain normal sexual behavior in rats. Thus, S-23 was co-administered with a low dose of EB in order to evaluate its contraceptive efficacy and avoid potential confounding effects related to libido.

Compounds were freshly prepared immediately before dosing and delivered to animals daily for 70 days. Although S-23 shows high oral bioavailability, sc dosing was used for these studies to lessen animal handling, stress, and morbidity during long-term treatment. Mating trials were conducted during the last week of treatment for animals in groups 1, 2, 4, and 5 to assure that the animals in each group demonstrated appropriate mounting and copulatory behavior. During the last week of treatment, individual male rats from groups 1, 2, 4, and 5 were cohabitated with two sexually active female rats. The number of mounts, mount latency, and intromissions were recorded. Female rats were individually housed after mating trials with free access to water and standard food chow. The female rats were allowed to bring the pregnancy to term. Upon delivery, the number of successful pregnancies was counted. A male rat was defined as fertile if it impregnated either one or two female partners. Total body composition of each animal was determined using dual energy x-ray absorptiometry (DEXA; GE, Lunar Prodigy™) one day prior to the end of treatment. Body weight (BW), total body BMD, percent fat mass (FM), and fat free mass (FFM) were determined using the small animal software (Lunar enCORE, version 6.60.041). For scanning, animals were anesthetized with ketamine:xylazine (87:13 mg/kg) and positioned in a prone position. The total body data was obtained by selecting an area encompassing the entire animal as the region of interest during data processing.

At the end of treatment, animals were sacrificed under anesthesia. Body weight was recorded at autopsy. Prostate, seminal vesicles, right testis, and right epididymides (divided in the middle of corpus epididymis to caput and cauda epididymis) were collected and weighed. All organ weights were normalized to body weight and compared. Blood samples were collected in Falcon tubes, maintained at room temperature for 40 minutes, and centrifuged at 3,000 g for 10 minutes to prepare serum samples. Serum samples were aliquoted and stored at -80° C until analysis. One testis from each rat was removed and weighed. After decapsulation, testicular parenchyma was homogenized in a volume of phosphate-buffered saline that was equivalent to its weight (assuming a density of 1 g/mL). An aliquot of each testicular homogenate was used to

count advanced spermatids (step 17-19) in each testis using a hemacytometer. Results are expressed as million sperm per testis. The remaining testicular homogenates were centrifuged at 3,000 g for 10 minutes. The supernatant of each sample was collected and used to determine the intratesticular testosterone concentrations.

An additional study was conducted in separate animals to determine the reversibility of S-23. Forty-two male rats were treated identically as that stated above. Every rat was cohabitated with two sexually active females. However, following the mating trial, the rats were maintained for an additional 70 days without treatment, after which a second (day 140) mating trial was performed to establish fertility rates. A third and final mating trial was performed on day 168 for seven animals that were deemed infertile on day 140.

2.2.7   Hormone Assays

Serum levels of LH and FSH and intratesticular testosterone concentrations were measured by the University of Virginia, Center for Research in Reproduction (Charlottesville, VA) using radioimmunoassay (RIA) kits validated for use in rodent samples. The lower limit of quantitation for LH, FSH, and intratesticular testosterone RIA kits were 0.040, 1.0, and 0.025 ng/mL, respectively. Testosterone concentrations in serum were measured with a commercially available enzyme immunoassay (EIA) kit (DSL, Webster, TX) in one study only (i.e. the spermatogenesis and fertility study described in Section 2.2.5 above and serum testosterone data in Table 2.3). The detection limit of the EIA kit is 7.5 pg/mL. Although the EIA was not validated for use with rodent serum samples, serum concentrations of testosterone in this study (Table 2.3) were within expected ranges based on LH and intratesticular concentrations of testosterone measured using the validated RIA method. Testosterone concentrations in serum for the reversibility study (data in Table 2.6) were determined using the validated RIA method.

2.2.8   Statistical Analyses

All statistical analyses were performed using single-factor analysis of the variance (ANOVA) followed by Dunnett's multiple comparison test. Tests in which $p < 0.05$ were considered as statistically significant differences.

2.3.   Results

2.3.1   *In Vitro* AR Binding Affinity and Transcriptional Activity of S-23

AR binding affinity was determined using a competitive binding assay with DHT as the positive control. The K_i of DHT was 0.45 ± 0.2. S-23 had a RBA of 26.5% (Figure 2.1). S-23

was structurally modified from C-6 by changing the *para*-nitro group of the A-ring to a cyano group, resulting in about 2-fold lower binding affinity than that of C-6 (RBA of 9.2%). This result was inconsistent with previous structure-activity relationships for the aryl propionamide SARMs, in which five pairs of compounds with cyano-substituents at the *para*-position of the A-ring exhibited lower AR binding affinity than their corresponding nitro-substituted counterparts (96), but suggested that S-23 would demonstrate promising *in vivo* pharmacologic activity.

The ability of S-23 to induce AR-mediated transcriptional activation was determined using a co-transfection assay in CV-1 cells. Upon binding to the AR, S-23 induced a concentration-dependent increase in AR-mediated transcriptional activation (data not shown). Data listed in Figure 2.1 represents the transcriptional activity induced by each compound at 10 nM and reported as the percentage of activity observed for 1 nM of DHT. Both C-6 and S-23 were identified as full AR agonists *in vitro*. Although the transcriptional activation induced by C-6 was higher than that of S-23, the difference was not statistically significant.

2.3.2   *In Vivo* Pharmacologic Activity of S-23 in Castrated Rats

The *in vivo* pharmacologic activity of S-23 was initially evaluated in castrated male rats after 14-days of treatment. Figure 2.2 shows the androgenic activity (prostate and seminal vesicles) and anabolic activity (levator ani muscle) of S-23 in castrated male rats at doses ranging from 0.01 mg/day to 3 mg/day. After castration, the weight of prostate, seminal vesicles, and levator ani muscle decreased significantly to 5.7%, 6.5%, and 35% of control values in intact animals, respectively. Administration of S-23 to castrated animals caused a dose-dependent increase in androgen-dependent organ weights. At a dose rate of 1.0 mg/day, S-23 was able to maintain the prostate and seminal vesicles at weights equal to or greater than that observed in intact animals. Notably, at a dose rate as low as 0.1 mg/day, S-23 was able to selectively maintain the weight of the levator ani muscle at the intact control level, while its effects on the prostate and seminal vesicles were lower than 30% of that observed in intact controls. The E_{max} of S-23 in the prostate, seminal vesicles, and levator ani muscle was $138 \pm 21\%$, $144 \pm 1\%$, and $139 \pm 4\%$ of those observed in intact controls, respectively (Figure 2.3). Accordingly, the ED_{50} of S-23, calculated by non-linear regression of the dose-response relationship in the prostate, seminal vesicles, and levator ani muscle was 0.43 ± 0.18, 0.41 ± 0.0070, and 0.079 ± 0.010 mg/day, respectively. In comparison to C-6 (48), S-23 demonstrated a 2-fold higher potency (ED_{50}) in all three organs without significantly increasing the efficacy (E_{max}) or changing the androgenic/anabolic activity *in vivo*. The increase in potency of S-23 *in vivo* was possibly due to its higher AR binding affinity as compared to C-6. Another possibility was the improved *in vivo*

drug exposure after administration, which would be verified by results of pharmacokinetic studies.

2.3.3   Pharmacokinetics of S-23 in Rats

Following iv administration, S-23 concentrations were high initially, then declined and remained detectable until 48 hours after the dose (Figure 2.5). The mean terminal $t_{1/2}$ of S-23 in male rats was 10.9 hours (Table 2.1). The systemic clearance (CL) and steady state volume of distribution (Vd_{ss}) were 0.87 mL/min/kg and 655 mL/kg, respectively. S-23 appeared rapidly in the systemic circulation after oral administration. Oral absorption was prolonged with maximum plasma concentrations forming a plateau 6 to 10 hours post-dose. Plasma concentrations of S-23 diminished with a mean terminal $t_{1/2}$ of 11.9 hours. Statistical analyses revealed no significant difference between the two $t_{1/2}$ values observed after iv and po administration. The oral bioavailability of S-23 following administration was 96 %, indicating near to complete absorption after oral dose.

2.3.4   Effects of Treatment on Spermatogenesis and Hormonal Regulation

After identification of S-23 as a more potent SARM than C-6, the *in vivo* contraceptive activity of this compound was investigated in intact male rats. To examine the efficacy of male contraception, mating trials were designed at the end of treatment. Previous studies of the effects of C-6 on masculine mating behavior showed that it maintains mating behavior in sexually experienced rats, but failed to stimulate any mating behavior in sexually naïve male rats after long-term castration when administered alone (data not provided). A small amount of EB in combination with a SARM is effective and sufficient to fully restore mating behavior in long-term castrated male rats. Animals in group 1 served as vehicle control. Animals in groups 2 through 7 were treated with EB at a dose of 5 μg/day in combination with S-23 at doses of 0, 0.05, 0.1, 0.3, 0.5, and 0.75 mg/day, respectively. Maintenance of libido plays a key role in the success of mating. EB was included to assure that any differences in reproductive ability of rats were not due to deficiencies in sexual libido. The doses of S-23 were chosen based on the pharmacological activity of this compound (administered alone) in castrated male rats, which covered the whole range of the therapeutic window (Table 2.2).

Spermatogenesis was evaluated by counting the number of homogenization-resistant advanced (step 17-19) spermatids in the testis from control and drug-treated rats (expressed as the number of spermatids per testis). No differences in the mean sperm counts were observed between EB-treated and vehicle control animals (Figure 2.6). Co-administration of S-23 with EB

caused a biphasic effect on sperm counts in the testis, which was consistent with the androgenic activity of drug treatment in the peripheral tissues and sexual organs. The greatest inhibition of spermatogenesis was observed in animals that received 0.1 mg/day S-23 plus 5 µg/day EB. Four out of six animals in this group showed no sperm in the testis with barely detectable sperm counts in the remaining two animals. Higher doses of S-23 actually supported spermatogenesis in a dose-dependent manner, with 0.75 mg resulting in similar mean sperm counts as those in the EB alone and vehicle control groups.

Intratesticular testosterone levels and serum concentrations of LH, FSH, and testosterone were determined using RIA and ELISA assays (Table 2.3). The average serum concentration of LH in the vehicle control group was 0.21 ± 0.050 ng/mL. Drug treatment caused marked suppression of serum LH levels that were below the limit of quantitation (0.04 ng/mL). The average serum concentration of FSH in the vehicle control group was 5.6 ± 1.2 ng/mL. FSH levels were significantly suppressed at the higher doses of S-23 (i.e. groups 6 and 7). The average serum concentration of testosterone in the vehicle control group was 2.2 ± 1.1 ng/mL. EB alone caused a significant reduction in the average serum testosterone concentrations, reducing it to 0.35 ± 0.37 ng/mL. In the presence of S-23, serum testosterone levels were further suppressed in a dose-dependent manner and were below the detection limit of the assay when doses of 0.1 mg/day or higher of S-23 was combined with EB. Accordingly, drug treatment induced a similar trend in the intratesticular testosterone levels (Table 2.3). The mean intratesticular testosterone concentration of animals in the vehicle, EB, and EB plus 0.05 mg of S-23 groups was 91.4 ± 50.3, 22.8 ± 29.9, and 11.7 ± 14.5 ng/mL, respectively. Although the minimum dose of S-23 to completely suppress intratesticular testosterone was 0.3 mg/day, the most remarkable suppression of spermatogenesis was observed in animals treated with 0.1 mg/day of S-23 plus EB. Sixty-seven percent of animals in this group achieved no sperm in the testis (4/6) while the remaining animals achieved very low sperm counts in the testis (2/6) with an average intratesticular testosterone concentration of 4.4 ± 6.6 ng/mL. Higher doses of S-23 (i.e. groups 5, 6 and 7) completely suppressed intratesticular testosterone concentrations. However, spermatogenesis was either partially or completely maintained due to the androgenic activity of S-23 at doses of 0.3 mg/day and greater.

2.3.5   Effects of Treatment on Body Composition and Androgen-Dependent Organ Weights

All EB-treated groups displayed a significant reduction in total body and prostate weights, while the total body BMD was slightly greater than that observed in the vehicle control group, indicative of the effects of estrogen in the male body (Table 2.4). Although a statistically

significant but small difference was noted at one dose level in each case, co-administration of S-23 did not result in dose-dependent effects on body weight or BMD, similar to previous results when a structurally-related SARM (S-4) was administered alone (i.e., without EB) to rats (82). Of note, weights of the testis were significantly less in all of the animals that received S-23, while the weight of the levator ani muscle was unaffected. For direct comparison, all parameters of body composition and organ weights were normalized to body weight in the current studies. Body composition, as analyzed by DEXA, revealed that treatment with EB alone did not significantly alter FM compared to vehicle control (Figure 2.6). Co-administration of S-23 with EB decreased FM in a dose-dependent manner. FM was significantly less than that of EB control at doses of S-23 equal to or greater than 0.3 mg/day and was significantly less than that of vehicle control at the highest dose (0.75 mg/day) tested. In addition, FM linearly correlated with the dose of S-23, with $R^2 = 0.9825$. Correspondingly, the FFM also exhibited a dose-dependent increase after administration of S-23 and EB (Figure 2.7).

2.3.6   Mating Trials

Our pharmacology study showed that the levator ani muscle in castrated rats was maintained at the intact control level for animals that received S-23 at a dose between 0.1 to 0.5 mg/day for 14 days. As such, we conducted mating studies using doses of 0.1, 0.3, and 0.5 mg/day of S-23 (i.e., the lowest doses of S-23 that were capable of fully maintaining levator ani muscle mass). Mating and behavior trials were performed during the last week of treatment for animals in groups 1, 2, 4, and 5, receiving vehicle, EB alone, EB plus 0.1 mg/day S-23, and EB plus 0.3 mg/day S-23, respectively. There were no differences in the number of mounts, mount latency, number of intromissions, or intromission latency between males in groups 1, 2, 4, and 5, indicating that the combination of EB and S-23 or EB alone maintained normal sexual behavior. The efficacy of hormonal male contraception was evaluated by the fertility rate of male rats in these mating trials. One hundred percent of the animals in the vehicle control group were fertile (Table 2.3). Four out of five (80%) male rats were fertile after treatment with EB alone. All male rats treated with EB plus 0.1 mg/day S-23 were infertile, while only one of the six male rats treated with EB plus 0.3 mg/day S-23 was fertile.

2.3.7   Reversibility

The ability of the rats to restore normal spermatogenesis was determined by maintaining the rats for an additional 70 days following treatment. The body weights and weights of the seminal vesicles and testis were restored to that of control (Table 2.5). In addition, muscle

25

weights were maintained; however, prostate weights remained below that of control. Additionally, serum hormone levels as well as mean intratesticular sperm counts returned to that of control (Table 2.6). As a result, an 83% fertility rate was achieved 70 days after termination of treatment; however, infertility was fully reversible after 100 days, with a 100% pregnancy rate.

2.4.   Discussion

Among the current experimental methods for male contraception, the most promising approach is the hormonal method. Spermatogenesis is tightly regulated by hormones through the hypothalamus-pituitary-testis axis. The rationale of hormonal male contraception is to suppress spermatogenesis by interrupting the action of one or more hormones involved in the hypothalamus-pituitary-testis axis, including GnRH, LH, FSH, and testosterone. Testosterone is a logical choice for hormonal contraception since it not only inhibits LH, FSH, and intratesticular testosterone levels *via* its negative feedback mechanism, but it also provides androgens for peripheral, extra-genital tissues. Although testosterone-alone regimens showed an overall high efficacy in the Asian population, the rate of azoospermia in the Caucasian population was only two thirds of that observed in Asians (40-42). Other anti-gonadotropin substances, such as progestins and GnRH analogs were used in combination with testosterone to achieve more rapid and complete suppression of spermatogenesis (97). For hormonal male contraception, the disadvantages of using testosterone include inconvenient routes of administration (e.g., im injection or implantation) and untoward effects on the prostate, hematologic system, and lipid metabolism.

In our current studies, multiple *in vitro* and *in vivo* assays were used to characterize the feasibility of S-23 for hormonal male contraception. First, S-23 was identified as a potent AR agonist with high AR binding affinity and specificity *in vitro*. In the following *in vivo* study using castrated male rats, S-23 revealed the most potent and efficacious anabolic activity that we have observed among the arylpropionamide SARMs with multiple substituents on the B-ring (96). The levator ani muscle weight was maintained at intact control levels by S-23 at doses as low as 0.1 to 0.3 mg/day in castrated male rats. Previous masculine behavior studies showed that C-6 alone could not fully maintain or induce mating behavior in castrated rats, but that inclusion of 5 μg/day of EB in the dosing regimen with C-6 fully restored mating behavior in long-term castrated rats to the same extent as that observed in intact control animals (data not provided). Baum et al. previously showed that male rats are dependent on estrogen for normal sexual behavior (90), while it appears that estrogens are not essential for human male sexual behavior (98, 99). Likewise, Miner et al. recently reported an orally bioavailable SARM that was efficacious in a

sexual behavior model using rats concurrently treated with estrogen (100). In our current contraception studies, S-23 and EB combination regimens were used in intact male rats to maintain the libido of animals during and after treatment. The pharmacologic endpoints included androgen-dependent organ weights, body composition, total body bone mineral density, spermatogenesis, serum levels of LH, FSH, and testosterone, and intratesticular testosterone concentrations. Consistent with previous literature (101, 102), EB alone significantly decreased serum LH and testosterone levels. Consequently, EB alone caused a significant decrease in the body weight, reproductive organs, and lean muscle weights, which was due mainly to the suppressed circulating levels of testosterone. In animals that received EB and SARM combination regimens, their physiologic needs for androgen were replaced by S-23 as evidenced by the fully maintained levator ani muscle and partially maintained prostate and seminal vesicles. Furthermore, animals treated with EB and S-23 were leaner than intact controls with lower average body weight and significantly less percentage of fat mass. A high inverse correlation existed between the dose rate of S-23 and percentage of fat mass in rats. Androgen levels were negatively associated with leptin concentrations in both man (103) and animals (104, 105). Previous reports of another SARM showed that administration significantly decreased leptin levels in castrated male rats (106). The findings from our current studies and previous studies (107) support the hypothesis that SARMs may mimic the effects of testosterone on body weight and body composition.

In adult species, testicular size is mainly determined by the intratesticular testosterone concentration, which is approximately 30-fold and 100-fold higher than its serum level in rats and men, respectively (108, 109). It is unclear why such a high local concentration of testosterone is physiologically needed. Nevertheless, Zirkin et al showed experimentally that an 80% reduction of intratesticular testosterone (20 ng/mL), only 10-fold higher than its serum level (~ 2 ng/mL), was sufficient to quantitatively maintain spermatogenesis in adult rats (110). In the current studies, EB alone remarkably suppressed intratesticular testosterone levels to 25% of those in intact animals. However, no significant inhibition in the weights of the testis was observed after administration of EB alone, presumably implying that the suppressed intratesticular concentration of testosterone was still sufficient to maintain normal spermatogenesis and testicular size. Indeed, sperm counts of animals treated with EB alone were similar to those of intact animals. In combination with S-23, testosterone levels were further suppressed in a dose-dependent manner. However, the overall effects of such combination regimens on spermatogenesis and testis weight were biphasic. In the absence of testosterone, EB plus higher doses of S-23 fully maintained spermatogenesis, suggesting that S-23 achieved sufficiently high intratesticular concentrations to

support spermatogenesis at these higher doses. However, similar biphasic phenomena in spermatogenesis observed using testosterone-based hormonal male contraception corroborate this conclusion (111). At the highest dose we studied herein (0.75 mg/day), S-23 demonstrated quantitative maintenance of spermatogenesis with an average subnormal testicular weight of $75 \pm 7\%$ of that observed in vehicle-treated animals. This finding is consistent with a number of studies using testosterone to restore spermatogenesis in rats made azoospermic either by hypophysectomy or gonadotropin withdrawal (110, 112-114). A possible explanation is that measurement of homogenization resistant sperm heads overestimates the true sperm counts caused by abnormal retention or failed release of step 19 spermatids beyond stage VIII, the most subtle abnormal changes of spermatogenesis associated with various experimental conditions (115, 116). Decreases in testis size are commonly observed during treatment with exogenous androgens, and appear to be directly related to decreases in sperm count (117). Animals that received EB plus 0.1 mg/day S-23 were infertile as hoped, and testis weights in these animals indeed decreased to 34% of that observed in vehicle control males. Doses of EB plus 0.05 or 0.3 mg/day S-23 resulted in very low sperm counts in the testis and unacceptable rates of infertility, demonstrating that a very narrow therapeutic dose range to achieve no sperm in the testis and infertility exists when using a hormonal contraceptive based on androgen alone. Drug development issues with regard to targeting this narrow therapeutic window (i.e., high enough to stop LH production, but not high enough to support spermatogenesis) in men of differing age, weight, medication compliance, and ethnicity represent a significant challenge toward development of an androgen-only male pill. Our studies suggest that use of an androgen alone (orally or parenterally) for male contraception may be problematic, but that combination of an orally available SARM (i.e. S-23) with an orally available progestin (to suppress LH and thus widen the therapeutic window for SARM action) represents a logical and likely feasible way to achieve oral male contraception.

Furthermore, treatment with EB plus 0.75 mg/day S-23 (group 7) not only suppressed LH levels, but also significantly suppressed FSH concentrations. FSH plays a key role in spermatogenesis by maintaining the amount of sperm produced in adult male rats (118). It is likely that suppression of FSH contributes to the reduction of sperm counts as evidenced by S-23 alone or in combination with EB. Additionally, synergistic effects of testosterone and estradiol on suppression of spermatogenesis were reported both in the rat (119) and man (120). It remains unknown whether a SARM and estradiol have similar synergistic and inhibitory effects on spermatogenesis.

The effect of S-23 on androgen-dependent tissue weights and suppression of spermatogenesis was reversible as evidenced by the ability of these tissues to return to that of control in the absence of exogenous androgen administration. Restoring serum hormones and therefore mean sperm counts to that of control indicates that normal spermatogenesis ensued. Therefore, as expected, all male rats were fertile after termination of treatment with S-23 plus EB.

In summary, S-23 was identified as a potent and efficacious SARM in castrated male rats with significantly higher anabolic activity than androgenic activity. In intact male rats, S-23 plus EB demonstrated potential use for hormonal male contraception. Either no sperm in the testis or very low sperm in the testis was successfully achieved in animals that received combination treatment of EB plus 0.1 mg/day S-23. A 100% infertility rate was observed in the efficacy study. Unlike testosterone, which showed biphasic effects in the testis and eipdidymides and nonselective increases in peripheral reproductive tracts (e.g., prostate and seminal vesicles), S-23 only displayed biphasic effects in the organs mentioned above. Additionally, S-23 selectively increased levator ani muscle weight and decreased the percentage of fat mass. After termination of treatment, serum hormones and mean sperm counts returned to that of control, resulting in 100% pregnancy rates in all treatment groups. These results indicate that the effect of S-23 plus EB on spermatogenesis is completely reversible. In conclusion, this is the first study to show that no sperm in the testis can be induced using an EB-SARM combination therapy in which EB was used to maintain libido without affecting quantitative spermatogenesis. This effective therapy selectively decreased weights of the prostate, seminal vesicles, testis, and epdidymides, retained muscle weight, percent of fat and fat-free mass, and increased BMD. S-23 also demonstrated high oral bioavailability (96%). The identification of a SARM with these promising pharmacologic and pharmacokinetic characteristics represents an important step toward the male pill, but much remains to be done.

2.5.   Acknowledgements
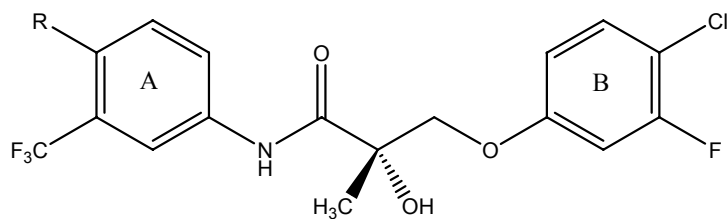
Compound	R	RBA (%)	*In vitro* Activity (% of DHT)
C-6	NO_2	9.2	118 ± 19
S-23	CN	26.5	96 ± 23

Figure 2.1. Chemical Structures, AR Binding Affinity, and *In Vitro* Transcriptional Activity of C-6 and S-23

AR binding affinity was determined using a radioligand competitive assay. The ability of the compound of interest to induce AR-mediated transcriptional activation was determined using a co-transfection assay. The transcriptional activity induced by each compound at a concentration of 10 nM was reported as the percentage of that observed for 1 nM DHT. Data presented as mean $\pm$ SD (n = 3).
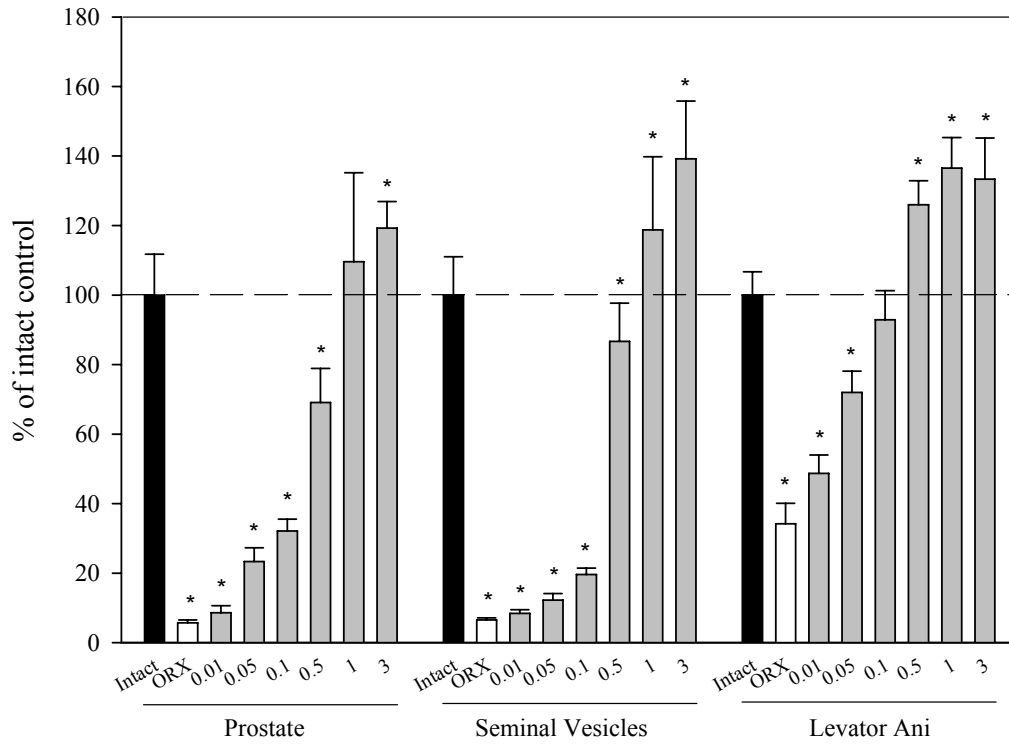
Figure 2.2. Pharmacologic Activity of S-23 in Castrated Male Rats

S-23 was administrated to animals *via* daily sc injections for 14 days with doses ranging from 0.01 mg/day to 3 mg/day. All organ weights were normalized to body weight and presented as the percentage of intact control. Data presented as mean $\pm$ SD (n = 5/group).
* Indicates a significant difference from vehicle-treated, intact control group, with $p < 0.05$.
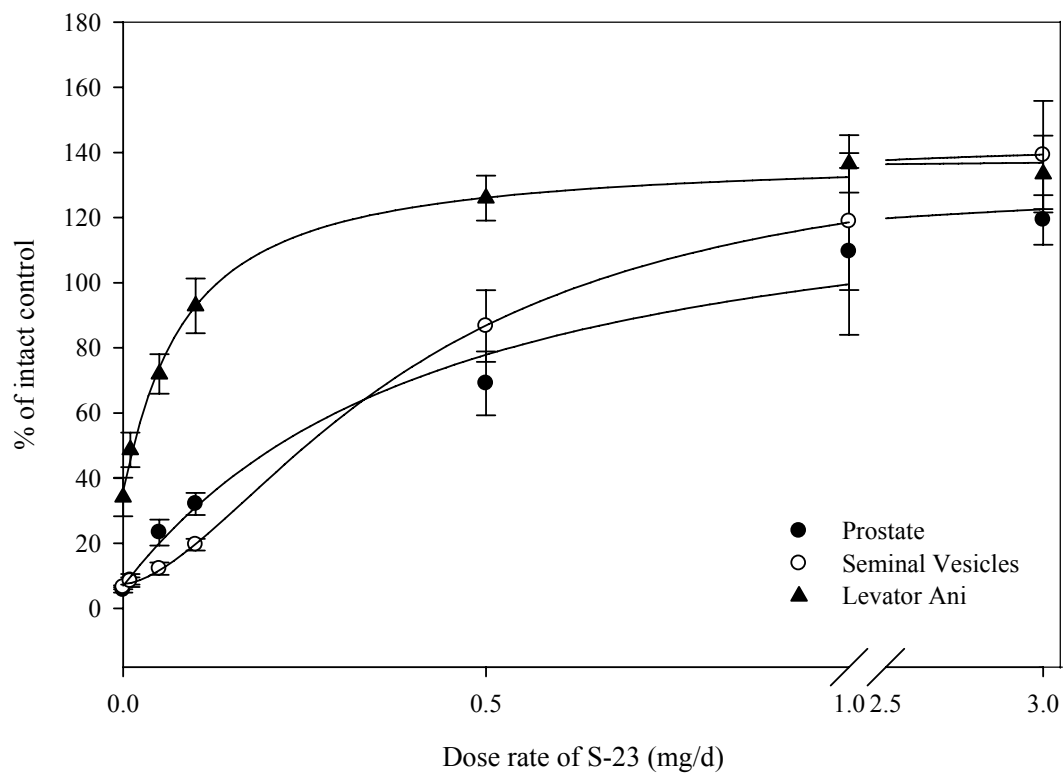
	Prostate	Seminal Vesicles	Levator ani
E_{max}	$138 \pm 21\%$	$144 \pm 1\%$	$139 \pm 4\%$
ED_{50}	0.43 ± 0.18	$0.41 \pm .007$	0.08 ± 0.01

Figure 2.3. Dose-response Curves of S-23 in Castrated Rats

E_{max} and ED_{50} were obtained by nonlinear least-square regression analysis. Data presented as mean $\pm$ SD (n = 5).
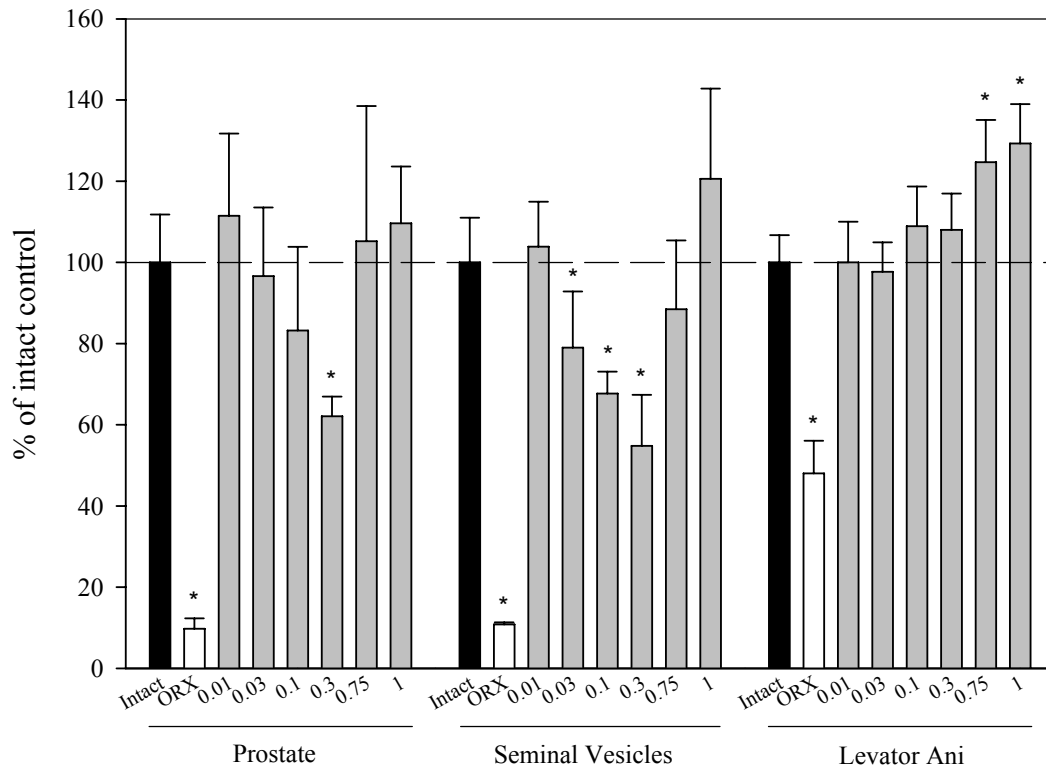
Figure 2.4. Pharmacologic Activity of S-23 in Intact Male Rats

S-23 was administrated to animals *via* daily sc injections for 14 days with doses ranging from 0.01 mg/day to 1 mg/day. All organ weights were normalized to body weight and presented as the percentage of intact control. Each bar represents the mean ± SD (n = 5). * Indicates a significant difference from vehicle-treated, intact control group, with $p < 0.05$.
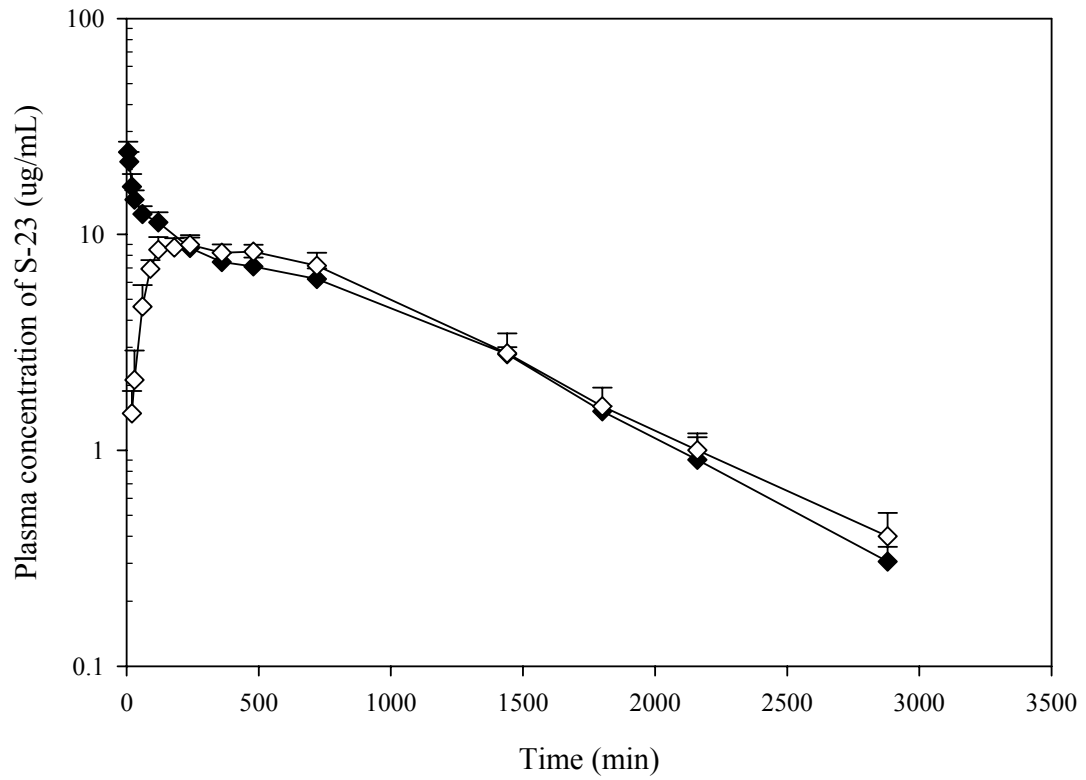
Figure 2.5. Mean Plasma Concentration-Time Profile of S-23 in Rats

Closed and open diamonds represent iv and po routes, respectively. Data presented as mean ± SD (n = 4 or 5/group).

Parameter	10 mg/kg, iv	10 mg/kg, po
$AUC_{0\rightarrow\infty}$ (min, µg/L)	11.3 ± 0.33	10.8 ± 0.66
λz (min^{-1})	0.00153 ± 0.00017	0.0014 ± 0.000156
MRT (min)	751 ± 67	879 ± 61
CL (mL/min·kg)	0.87 ± 0.02	
Vss (mL/kg)	655 ± 78	
F po (%)		95.9
Tmax (min)		252 ± 137
Cmax (µg/mL)		9.4 ± 0.7
CL/F (mL/min·kg)		0.90 ± 0.06
Vss/F (mL/kg)		649 ± 68

Table 2.1. Pharmacokinetic Parameters of S-23 in Male Rats

$AUC_{0-\infty}$: area under the plasma concentration-time curve from time 0 to infinity; λ: terminal elimination constant; CL: plasma clearance; V_{ss}: apparent volume of distribution at equilibrium; $F_{p.o.}$: oral bioavailability; T_{max}: time to reach the peak concentration (C_{max}). Data presented as mean ± SD (n = 4 or 5/group).

Dose	LH (ng/mL)		FSH (ng/mL)	
(mg/d)	Intact	Castrated	Intact	Castrated
	0.58 ± 0.14^C	11.0 ± 1.71^I	5.6 ± 1.1^C	43.4 ± 8.6^I
0.01	0.58 ± 0.15^C	10.9 ± 2.28^I	5.5 ± 1.9^C	42.0 ± 4.7^I
0.03	$0.37 \pm 0.13^{I,C}$	11.45 ± 2.46^I	6.0 ± 1.1^C	52.0 ± 17.9^I
0.1	$0.25 \pm 0.16^{I,C}$	2.29 ± 2.06^C	4.8 ± 0.8^C	$24.3 \pm 14.5^{I,C}$
0.3	$0.08 \pm 0.04^{I,C}$	$0.06 \pm 0.04^{I,C}$	$4.0 \pm 0.6^{I,C}$	6.1 ± 1.4^C
0.75	$<0.04^{I,C}$	$<0.04^{I,C}$	4.2 ± 1.1^C	6.0 ± 0.3^C
1	$<0.04^{I,C}$	$<0.04^{I,C}$	$3.3 \pm 0.5^{I,C}$	6.6 ± 1.1^C

Table 2.2. Effects of S-23 on LH and FSH in Intact and Castrated Rats

Rats were treated for 14 days *via* sc injection and serum LH and FSH concentrations were measured. Data presented as mean ± SE (n = 5/group). [I and C] Indicates a significant difference between the group and intact control group or castrated control group, respectively, with $p < 0.05$.
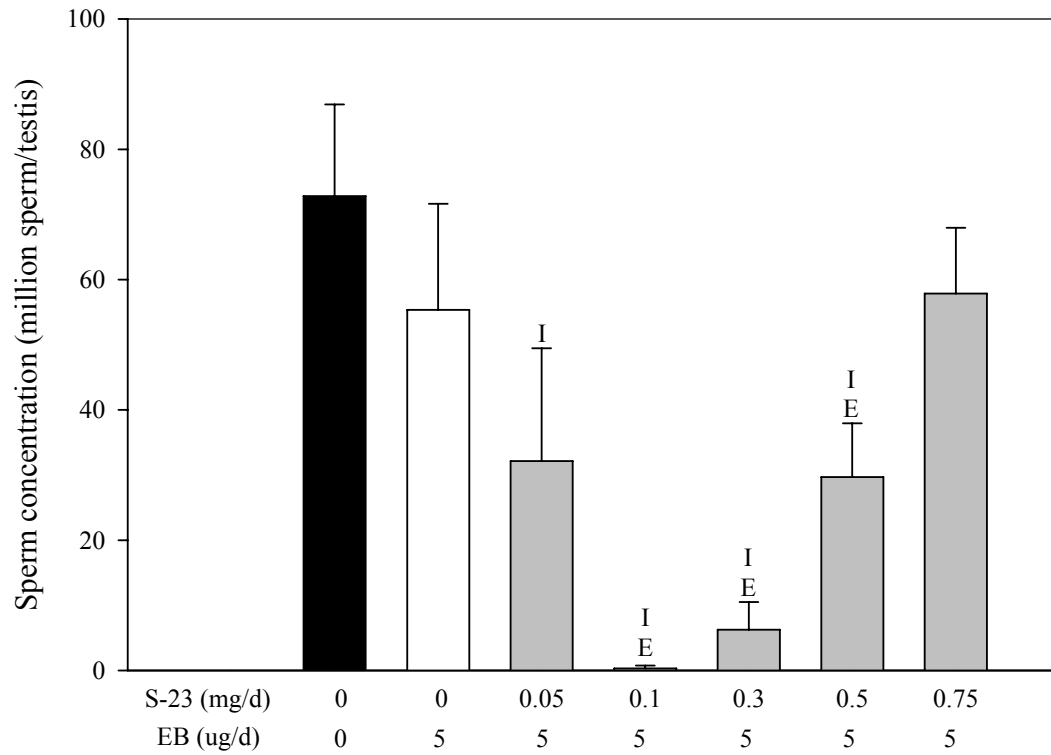
Figure 2.6. Testicular Sperm Concentrations

Rats were treated for 70 days *via* sc injection. Testicular parenchyma was homogenized and advanced spermatids counted. Data presented as mean ± SD (n = 5 or 6/group). [I and E] Indicates a significant difference between the group and vehicle-treated, intact control group and estrogen-treated group, respectively, with $p < 0.05$.

Group	EB (µg/day)	S-23 (mg/day)	Animals	LH (ng/mL)	FSH (ng/mL)	Serum Testosterone (ng/mL)	Intratesticular Testosterone (ng/mL)	Number of Pregnancies
1	--	--	6	0.21 ± 0.050	5.6 ± 1.2	2.2 ± 1.1	91 ± 50	12/12
2	5	--	5	$< 0.04^{\,I}$	5.2 ± 0.43	$0.35 \pm 0.37^{\,I}$	$23 \pm 30^{\,I}$	8/10
3	5	0.05	6	$< 0.04^{\,I}$	4.8 ± 1.4	$0.092 \pm 0.12^{\,I, E}$	$12 \pm 15^{\,I, E}$	ND
4	5	0.1	6	$< 0.04^{\,I}$	4.8 ± 0.90	$< 0.0075^{\,I}$	$4.4 \pm 6.6^{\,I, E}$	0/12
5	5	0.3	6	$< 0.04^{\,I}$	4.3 ± 1.5	$< 0.0075^{\,I}$	$< 2.5^{\,I}$	2/12
6	5	0.5	6	$< 0.04^{\,I}$	$3.4 \pm 0.30^{\,I, E}$	$< 0.0075^{\,I}$	$< 2.5^{\,I}$	ND
7	5	0.75	6	$< 0.04^{\,I}$	$3.6 \pm 0.46^{\,I, E}$	$< 0.0075^{\,I}$	$< 2.5^{\,I}$	ND

Table 2.3. Effects of S-23 on Hormones and Fertility

Rats were treated for 70 days *via* sc injection. Data presented as mean ± SD. ND: not determined. [I and E] Indicates a significant difference between the group and intact control group or EB control group, respectively, with $p < 0.05$.

Group	EB (µg/day)	S-23 (mg/day)	Animals	Body Weight (g)	BMD (g/cm^2)	Prostate (% of intact control)	Seminal Vesicles (% of intact control)	Testis (% of intact control)	Levator Ani Muscle (% of intact control)
1	--	--	6	423 ± 29	0.17 ± 0.006	100 ± 20	100 ± 7.5	100 ± 10	100 ± 15
2	5	--	5	351 ± 8 [I]	0.18 ± 0.004 [I]	46.9 ± 15 [I]	28.1 ± 12 [I]	94 ± 10	62 ± 5.6 [I]
3	5	0.05	6	379 ± 20 [I]	0.19 ± 0.004 [I, E]	34.4 ± 7.6 [I]	23.9 ± 7.6 [I]	69 ± 14 [I, E]	90 ± 11 [E]
4	5	0.1	6	376 ± 26 [I]	0.18 ± 0.004 [I]	31.1 ± 6.6 [I]	21.8 ± 5.3 [I]	34 ± 3.8 [I, E]	97 ± 15 [E]
5	5	0.3	6	387 ± 25 [I, E]	0.19 ± 0.009 [I]	45.1 ± 5.3 [I]	52 ± 8.7 [I, E]	45 ± 3.9 [I, E]	100 ± 3.8 [E]
6	5	0.5	6	351 ± 9 [I]	0.18 ± 0.004 [I]	78.2 ± 5.6 [I, E]	89 ± 4.8 [E]	63 ± 6.3 [I, E]	123 ± 8.5 [I, E]
7	5	0.75	6	344 ± 11 [I]	0.18 ± 0.004 [I]	94.7 ± 89.2 [E]	113 ± 12 [I, E]	75 ± 7.2 [I, E]	131 ± 8.1 [I, E]

Table 2.4. Effects of Treatment on Body Weight, BMD and Androgen-Dependent Tissue Weights

Rats were treated for 70 days *via* sc injection. Data presented as mean ± SD. [I and E] Indicates a significant difference between the group and intact control group or EB control group, respectively, with $p < 0.05$.
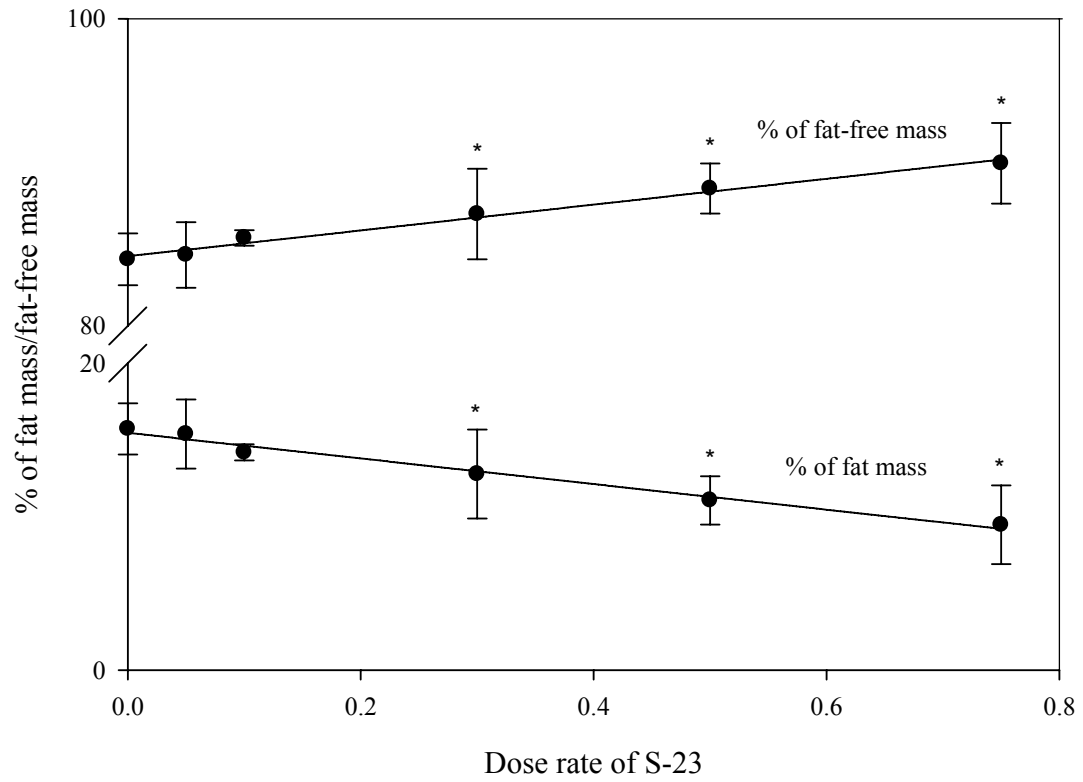
Figure 2.7. Linear Correlation Between the Dose Rate of S-23 and Body Composition (percentage of fat mass and percentage of fat-free mass)

Rats were treated for 70 days *via* sc injection and DEXA scanned. Data presented as the mean ± S.D. (n = 5 or 6/group). [*] Indicates a significant difference between the group and EB control group, respectively, with $p < 0.05$.

Group	EB (µg/day)	S-23 (mg/day)	Animals	Body Weight (g)	Prostate (% of intact control)	Seminal Vesicles (% of intact control)	Testis (% of intact control)	Levator Ani (% of intact control)
1	--	--	6	511 ± 24	100 ± 12.4	100 ± 8.9	100 ± 8.4	100 ± 8.2
2	5	--	5	488 ± 29	99.2 ± 4.1	95.6 ± 18.7	104.8 ± 6.6	102.6 ± 3.3
3	5	0.05	6	504 ± 44	88.2 ± 12.3	95.4 ± 8.4	106.5 ± 5.2	96.5 ± 8.7
4	5	0.1	6	500 ± 35	79.4 ± 12.3 [I, E]	87.7 ± 11.6	99.8 ± 8.6	103.9 ± 14.3
5	5	0.3	6	507 ± 19	68.5 ± 7.7 [I, E]	92.8 ± 9.5	100.3 ± 6.0	85.8 ± 8.3 [I, E]
6	5	0.5	6	491 ± 20	73.7 ± 9.1 [I, E]	96.0 ± 10.3	100.4 ± 7.9	95.6 ± 8.3
7	5	0.75	6	478 ± 16 [I]	86.3 ± 9.4 [E]	105.2 ±10.9	100.5 ± 6.0	98.7 ± 11.0

Table 2.5. Reversible Effects on Body Weight and Androgen-Dependent Tissue Weights

Rats were treated for 70 days *via* sc injection and maintained without treatment for an additional 100 days. Data presented as mean ± SD. [I and E] Indicates a significant difference between the group and intact control group or EB control group, respectively, with $p < 0.05$.

Group	EB (µg/day)	S-23 (mg/day)	Animals	LH (ng/mL)	FSH (ng/mL)	Serum Testosterone (ng/mL)	Sperm (million sperm/testis)	Number of Pregnancies at 70 days	Number of Pregnancies at 140 days
1	--	--	6	0.64 ± 0.47	4.5 ± 1.2	2.7 ± 2.0	72.4 ± 7.7	12/12	12/12
2	5	--	6[a]	0.39 ± 0.16	3.8 ± 0.62	1.1 ± 0.36	65.9 ± 9.5	12/12	10/12
3	5	0.05	6[b]	0.44 ± 0.24	3.9 ± 0.34	1.6 ± 0.92	69.1 ± 8.4	2/12	8/12
4	5	0.1	6[b]	0.41 ± 0.15	3.5 ± 0.84	1.6 ± 1.2	67.6 ± 5.7	0/12	10/12
5	5	0.3	6	0.41 ± 0.10	3.4 ± 0.65	1.6 ± 0.31	65.8 ± 5.7	2/12	10/12
6	5	0.5	6	0.42 ± 0.18	3.2 ± 0.80	1.4 ± 1.1	65.4 ± 4.9	2/12	10/12
7	5	0.75	6	0.39 ± 0.22	3.5 ± 1.0	0.94 ± 0.23	65.4 ± 4.2	6/12	10/12

Table 2.6. Reversible Effects on Serum Hormones, Testicular Sperm Counts and Fertility

Rats were treated for 70 days *via* sc injection and maintained without treatment for an additional 100 days. Data presented as mean ± SD. [I and E] Indicates a significant difference between the group and intact control group or EB control group, respectively, with $p < 0.05$.
[a] Serum was not available for analyses for two animals in this group (n = 4 for hormone values)
[b] Serum was not available for analyses for one animal in this group (n = 5 for hormone values)

Chapter 3

SARMs Enhance Female Sexual Motivation

3.1.   Introduction

Androgens are involved in a number of physiological roles in women, including bone mineral density, muscle mass and strength, libido and sexual response (1, 17, 49). Hypoactive sexual desire disorder (HSDD) is characterized by chronic or recurrent loss or decrease in interest in sexual activity, causing interpersonal distress (121) and severely impacting a female's quality of life. It is believed that the decrease in libido, sexual receptivity, and responsiveness is associated with free testosterone levels that decline following surgically-induced or natural menopause.

Clinical trials in premenopausal women revealed that sexual desire and arousal may be enhanced when administered a transdermal testosterone preparation. The most common side effects associated with transdermal testosterone treatment in women include hirsutism and acne, and some rare occurrences of alopecia, breast pain, weight gain and voice deepening. However, clinical use of transdermal testosterone administration for HSDD has been problematic due to lack of long-term safety data on breast cancer and cardiovascular risks (i.e. increased blood triglycerides) associated with exogenous androgen administration.

Female sexual behavior in rats is characterized by consummatory and appetitive components. Consummatory aspects describe the receptive behavior, including the lordosis reflex to allow copulation by a male. The appetitive components include the soliciting or proceptive behaviors to attract and arouse sexual interest. Henderson *et al* reported that non-aromatizable anabolic steroids inhibits sexual receptivity in hormonally-primed ovariectomized rats; however, the effects of anabolic steroids on proceptive behaviors have not been determined (122).

The development and potential clinical use of tissue selective SARMs may open the door for an androgen-based treatment option in women. In the current studies, we examined the effect of different of B-ring substitutions of arylpropionamide SARMs on AR binding affinity, androgen receptor (AR)- and estrogen receptor (ER)-mediated transcriptional

activation, virilizing potential and pharmacologic activity in orchidectomized male and ovariectomized female rats. Furthermore, we examined the effects of these SARMs on the sexual motivation of progesterone-primed ovariectomized female rats in a partner preference model to evaluate the preference of the female for a sexually active intact male or a sexually inactive orchidectomized male and help clarify if the androgen receptor plays a role in the sexual behavior of females. In unpublished data, a SARM structurally similar to S-23 is able to maintain mating behavior in sexually experienced male rats after long-term castration (123). The dose-dependent effect of S-23 on female sexual motivation as well as a series of SARMs with structural modifications on the B-ring was evaluated at a single, high dose in the partner preference paradigm. The results of these studies provide the first evidence of structurally diverse SARMs in this animal model and provide definitive proof of the importance of AR function to female sexual behavior.

3.2. Materials and Methods

3.2.1 Experimental Animals

Male and female Sprague-Dawley rats were purchased from Harlan Bioproducts for Science (Indianapolis, IN). The animals were maintained on a 12-hour light/dark cycle with food and water available *ad libitum*. All animal studies were conducted under the auspices of animal protocols approved by the Institutional Laboratory Animal Care and Use Committee at the University of Tennessee (male pharmacologic studies, LH/FSH serum concentrations and uterine effects) or The Ohio State University (female behavior studies).

3.2.2 *In Vitro* AR Binding Affinity

The LBD of the AR fused with glutathione-S-transferase (GST) was expressed as a recombinant protein (AR GST-LBD). Basically, an AR-LBD (663-919) was obtained by PCR amplification from a full-length AR expression construct (pCMVhAR) with primers containing flanking restriction sites and inserted into the pGEX6P-1 plasmid vector (Amersham Biosciences). The AR LBD was expressed as a GST fusion protein in *E coli* BL21 (DE3) at 15 °C for 16 h by induction with 30 µM isopropyl 1-thio-β-D-galactopyranoside. Cells were lysed in buffer containing 150 mM NaCl, 50 mM Tris, pH 8.0, 5 mM EDTA, 10% glycerol, 1 mg/mL lysozyme, 10 units/mL DNase I, 10 mM $MgCL_2$, 10 mM DTT, 0.5% CHAPS, and 100 µM phenylmethylsulfonyl fluoride by 3 freeze/thaw cycles.

The K_i of the compounds of interest was determined in a radiolabeled competitive binding assay (124). All SARMs were synthesized in our laboratories using reported methods (125). Chemical purities were confirmed by MS and NMR and determined to be greater than 99%. Increasing concentrations (3 to 10^4 nM) of each compound of interest were incubated with 10 nM [^{3}H]MIB (PerkinElmer, Waltham, MA) and AR GST-LBD at 4 °C for 18h. Protein was also incubated with and without a high concentration (10^{-6} M) of unlabeled MIB (PerkinElmer Life Sciences) in order to determine total and non-specific binding, respectively. The plates were harvested with GF/B filters on the Unifilter-96 Harvester (PerkinElmer) and washed three times with ice-cold buffer. The filter plates were dried at room temperature, Microscint-O cocktail (PerkinElmer) was added to each well, sealed and radioactivity was counted in a TopCount® NXT Microplate Scintillation Counter (PerkinElmer). The specific binding of [^{3}H]MIB at each concentration of the compound of interest was determined by subtracting the nonspecific binding of [^{3}H]MIB, and expressed as a percentage of the specific binding in the absence of competitor. The concentration of the compound of interest that reduced the specific binding of [^{3}H]MIB by 50% (IC_{50}) was determined by non-linear regression with SigmaPlot using the standard four parameter logistic curve. The K_i was calculated by: $K_i = K_d \times IC_{50}/(K_d + L)$, where K_d is the equilibrium dissociation constant of [^{3}H]MIB, and L is the concentration of [^{3}H]MIB (10 nM). The binding affinities of the compounds of interest are expressed relative to DHT (Sigma Aldrich, St. Louis, MO).

3.2.3   *In Vitro* AR- and ER-Mediated Transcriptional Activity

The *in vitro* functional activity of the compounds of interest was determined by the ability of each ligand to induce AR- or ER-mediated transcriptional activation in a cotransfection system (31). At ~ 90% confluency, CV-1 (AR) or HEK 293 cells (ERα and ERβ) were transiently transfected in 15 cm dishes in serum-free DMEM (Hyclone, Logan, UT) using LipofectAMINE (Invitrogen, Carlsbad, CA) according to the manufacturer's instructions. Cells in each dish were transfected with 45 μg GRE-Luc, 1 μg CMV-Luc (renilla luciferase), and 2.5 μg of a CMVhAR, CMVhERα, or CMVhERβ expression vector. Cells were allowed to recover for 12 hours and were then seeded into 24-well plates (8 x 10^4 per well) in DMEM containing 2% charcoal-stripped fetal bovine serum (csFBS; Hyclone) and allowed to recover for an additional 8 hours before drug treatment. Previous experiments in our laboratories determined that the lowest concentration of DHT that maximally induced AR-mediated transcriptional activation was 1 nM (30). Likewise, 1 nM estradiol (E_2; Sigma

Aldrich) was required to maximally induce ERα- and ERβ-mediated transcriptional activation (data not shown). Therefore, in the present study, the transcriptional activation induced by 1 nM DHT or E_2 was set as 100% and used as the reference for quantifying the agonist activity of each test compound. Twenty-four h after drug treatment, cells were washed with Dulbecco's Phosphate Buffered Saline (DPBS; Hyclone) and lysed with 50 μL/well of passive lysis buffer for 30 minutes at room temperature. An aliquot (25 μL) of cell lysate was used for luciferase assays (Dual-Luciferase Reporter Assay System, Promega, Madison, WI). Transcriptional activity in each well was calculated as the ratio of luciferase activity to renilla luciferase activity to avoid variations in transfection efficiency and cell number. Transcriptional activity induced by each compound of interest was expressed as the percentage of that induced by 1 nM DHT (AR) or E_2 (ERα and ERβ).

3.2.4 *In Vitro* N-C Interaction

The amino terminus-carboxy terminus (N-C) interaction of the AR can be identified by a mammalian two hybrid assay. CV-1 cells were maintained and transfected as stated above. Cells in each dish were transfected with 45 μg pG5Luc, 2.5 μg pACT AR-NTD, 2.5 μg pBind AR-LBD and 1 μg CMVLuc. Cells were subsequently plated and treated as described above. Experiments in our laboratories determined that 10 nM DHT was the lowest concentration that maximally induced the N-C interaction (data not shown). Therefore, in the present study, the interaction induced by 10 nM DHT was set as 100% and used as the reference for quantifying the activity of the test compounds. Luciferase assays were performed as described above and the N-C interaction induced by each compound of interest was expressed as the percentage of that induced by 10 nM DHT. If the ligand:receptor complex facilitates interaction between the NTD and the LBD, the close proximity of the activating domain to the DBD results in an increase in luciferase activity.

3.2.5 *In Vivo* Pharmacologic Activity in Castrated Male Rats

The *in vivo* pharmacologic activity of each AR ligand was first determined in castrated male rats. Animals weighing approximately 200 grams were randomly distributed into groups (n = 5/group). Animals were orchidectomized *via* scrotal incision under ketamine/xylazine anesthesia 24 hours before drug treatment and received daily sc injections of the test compound, at a dose rate of 1 mg/day for 14 days. Each AR ligand was freshly dissolved in vehicle containing DMSO (Sigma Aldrich) / PEG300 (Sigma Aldrich) [10/90 (vol/vol)] before daily administration. An additional two groups of animals (n = 5/group)

with or without castration received vehicle only and served as castrate or intact control groups, respectively. Animals were weighed, anesthetized, and sacrificed within 24 hours after the last dose. The ventral prostate, seminal vesicles and levator ani muscle were removed, cleared of extraneous tissue, and weighed. All organ weights were normalized to total body weight and compared. The weights of the prostate and seminal vesicles were used to evaluate androgenic activity while the levator ani muscle weight was used as a measure of anabolic activity. Percent changes were determined by comparison to intact animals.

3.2.6   Effects of SARMs on Sexual Motivation in Female Rats

The effects of SARMs on female sexual motivation were determined in ovariectomized female rats. Female animals weighing approximately 150 grama were randomly distributed into groups (n = 6). Animals were ovariectomized *via* dorsal incision under ketamine/xylazine anesthesia 24 hours before drug treatment and received daily sc injections of the test compound. An additional two groups of animals (n = 6/group) with or without ovariectomization received vehicle only and served as gonadectomized or intact control groups, respectively. Compounds of interest were freshly dissolved in vehicle containing DMSO/PEG300 [5/95 (vol/vol)] and administered at a daily dose of 3 mg/kg/day for 14 days. Doses ranging from 0.05 to 0.75 mg/day were also administered for S-23. TP (Sigma Aldrich) was used as a positive control, while TP co-administered with R-bicalutamide (an antiandrogen) was used to confirm the importance of AR activation to the observed effects.

Behavioral testing was performed in a three compartment chamber with wood shavings covering the floor, and conducted during the early portion of the dark cycle under dim red light within 12 hours after the last dose. Sexually experienced female rats were acclimated to the chamber during three separate 15 minute periods; two the week before behavioral testing and another immediately prior to testing. During this time, the female rats explored the testing chamber in the absence of stimulus male rats. Four hours prior to behavioral testing, female rats received a sc injection of 0.1 mg progesterone (5% DMSO in PEG300; Sigma Aldrich) to facilitate sexual behavior. Following the final 15 minute acclimation period, individual females were restricted to the central compartment while the stimulus male rats, one intact and one castrated (castrated *via* scrotal incision under ketamine/xylazine anesthesia 14 days prior to behavioral testing), weighing greater than 400 grams, were sequestered individually in the lateral compartments. Six different pairs of males (one intact and one castrated) were used for each treatment group, with differing intact

and castrated males being used for each individual female. The rats underwent a 5 minute habituation period with opaque partitions in place. After this period, the opaque partitions were removed and the female rat was able to move freely throughout the three chambers for the 30 minute behavioral testing period. The larger size of the male rats prevented movement between compartments. The duration of time spent in each compartment by the OVX female was recorded. Compartment entries (intact, central, or castrated compartment) were scored when all four paws of the female rat passed through the tube into the compartment. The amount of time (minutes) the female spent with the intact male and castrate are reported. Animals were weighed, anesthetized, and sacrificed within 24 hours after the last dose. The uteri were removed, cleared of extraneous tissue, and weighed. Uterine weights were normalized to body weight and compared. Percent changes were determined by comparison to intact animals. In a separate study, uteri from animals treated with 3 mg/kg/day (14 days) of TP and the most active (S-23 and S-26) and least active (S-25) SARMs were fixed in 4% paraformaldehyde in PBS for histology. The uteri were dehydrated and stained with hematoxalylin and eosin and analyzed.

3.2.7   Effect of SARMs on Serum Hormones

To determine the effect of SARMs (S-23, S-25 and S-26) and TP on serum hormones and uterine growth, a separate animal study was carried out. Female animals weighing approximately 150 grams were randomly distributed into groups (n = 5) and ovariecomized and treated as described above. Serum LH and FSH concentration were determined using the MILLIPLEX™ MAP Rat Pituitary Kit (Millipore, Billerica, MA) according to the manufacturer's instructions. The plate was read on the Luminex 200™ and concentrations were determined using a weighted 5-parameter logistic curve-fitting method using the median fluorescent intensity (MFI) in the xPONENT software. The mimimum detectable concentration in the assay for FSH and LH were 0.0477 and 0.0049 ng/mL, respectively.

3.2.8   Statistical Analyses

All statistical analyses were performed using single-factor ANOVA followed by Dunnett's multiple comparison test. Differences in which $p < 0.05$ were considered statistically significant.

3.3.   Results

3.3.1   *In Vitro* Binding Affinity and Functional Activity

An *in vitro* radiolabeled competitive binding assay was used to determine the relative AR binding affinity of each SARM, and expressed as a percentage relative to DHT (RBA). The series of arylpropionamide analogues showed RBAs ranging from 3-27 % (Table 3.1). The R-isomer of compound S-23 (R-23), bound the AR very weakly with a RBA of 0.1% of DHT, confirming the enantioselective binding of this series of compounds. The *para* mono-substituted halogen derivatives bound the AR with affinity directly varying with the electronegativity of the substituent. The di-substituted derivatives (S-28 and S-29) bound with slightly less affinity than their mono-substituted counterparts (S-24 and S-25). S-22, bearing the cyano group at the *para*-position, bound the AR with a RBA of 16.8%. However, the *meta*-fluoro, *para*-chloro derivative (S-23) displayed the highest binding affinity with a RBA of 26.5%.

The ability of these SARMs to induce AR-, ERα- and ERβ-mediated transcriptional activation was determined in an *in vitro* cotransfection assay. At 100 nM, S-23 displayed the most activity by stimulating AR-mediated transcriptional activation to 101% of that observed for 1 nM DHT (Table 3.1). The cyano-containing compound, S-22, and di-chloro compound, S-29, stimulated the AR similarly, to 94 and 92% of DHT, respectively. The remaining SARMs stimulated AR-mediated transcription to a lesser extent, ranging from 64.8 to 87.6%. The ability of the SARMs to induce ERα-mediated transcriptional activation was also determined. S-23, S-24 and S-25 displayed weak ERα partial agonist activity, by stimulating ERα-mediated transcription to 25, 19 and 24% of that observed for 1 nM E_2, respectively (Table 3.1). S-23 was the only SARM tested that exhibited minimal ERβ-mediated transcription (28.1%), compared to that of the vehicle control (19.3%; Table 1).

The ability of these SARMs to induce interaction between the amino terminus and the carboxy terminus of the AR was determined in a two-hybrid assay. The SARMs displayed a dose-dependent increase in interaction, with S-22 and S-23 maximally inducing the interaction to 115 and 90% of 10 nM DHT, respectively (Figure 3.1). The remaining SARMs only partially induced the N-C interaction, with minimal activity observed up to 100 nM. However, S-22, S-23, S-25 and S-28 induced activity to 32, 27, 16 and 36% of DHT at 10 nM, respectively.

3.3.2   Pharmacologic Activity in Gonadectomized Rats

The *in vivo* androgenic and anabolic activity of these SARMs was first determined in castrated male rats after 14 days of drug administration. Following castration and subsequent depletion of endogenous testosterone, the prostate and levator ani muscle significantly decreased in size to 9 and 39.7% of that observed for intact control, respectively. Previous studies in our laboratories displayed the nonselective nature of TP in castrated male rats, producing an equipotent and equi-efficacious dose-dependent increase in both androgenic and anabolic tissues. The weights of the prostate and levator ani muscle were restored to 121 and 70% of intact control at 0.75 mg/day, respectively (32). Likewise, S-23 displayed only moderate tissue selectivity at 1 mg/day, maximally maintaining the size of the prostate at 110% and the levator ani muscle at 136% of intact control (Table 3.2). S-22 and S-30 displayed the greatest selectivity for anabolic tissues, increasing the size of the levator ani muscle to 136 and 128%, while only maintaining the prostate at 51.1 and 41.4% of that observed in intact control, respectively. S-24 was the least active SARM in this series, maintaining the prostate at only 8% and the levator ani muscle at 70% of intact control. The remaining SARMs displayed tissue selectivity for anabolic tissues, maintaining the levator ani muscle close to that of intact control (ranging from 82% for S-29 to 111% for S-25) and the prostate around 50% (ranging from 33% for S-29 to 60% for S-25). Additionally, the inactive isomer of S-23 (R-23), displayed no *in vivo* activity with tissue weights similar to castrate control, with the prostate and levator ani muscle reducing to 7 and 34% of that observed for intact control, respectively.

The *in vivo* pharmacologic activity of these SARMs in OVX female rats was assessed by uterine weight. Upon excision of ovaries, the uterus reduced to approximately 16% of that observed in intact control. Administration of 3 mg/kg/day TP maintains the uterus at 79%; however, the ability of TP to maintain the size of the uterus was inhibited by co-treatment with bicalutamide, which caused the uterus to reduce to 28% of intact control (Figure 3.2). As S-23 displayed the most androgenic activity in ORX males, it also showed the greatest uterine activity in OVX females, maintaining the uterus at 98.9% of intact control at 3 mg/kg/day. Additionally, the uterus responded in a dose dependent manner to S-23, increasing in size from 37.8% at 0.05 mg/day to 79.5% at 0.75 mg/day, compared to intact control (Figure 3.3). With the exception of S-23, all of the SARMs demonstrated weaker partial agonist activity in the uterus than TP, with the uteri ranging in size from 21% for S-30 to 47% for S-22 at 3 mg/kg/day. R-23 maintained the size of the uterus at 27% of that observed in intact control.

50

The effects of TP and SARMs on endometrial and myometrial thickness were determined by histological analysis. Average thickness of the endometrium and myometrium in the intact control group was 1.23 and 1.08 mm, respectively (Figures 3.5 and 3.6). Ovariectomy reduced these layers of the uterine wall to 0.78 and 0.67 mm, respectively. TP and SARMs selectively increased the myometrial layer, increasing the thickness to greater than that observed for intact control, ranging from 1.34 (S-26) to 1.53 mm (S-23). TP and SARMs maintained the thickness of the endometrium slightly below that of intact control.

3.3.3   Effects of SARMs on Sexual Motivation in Ovariectomized Rats

The influence of SARMs on female sexual motivation in OVX female rats was analyzed in a partner preference paradigm. As expected in this model, the progesterone-primed, vehicle-treated female rats displayed no preference for the sexually active intact male or sexually inactive castrated male, spending on average only 2% more time with the castrated male (Figure 3.7). On the contrary, a significant increase in sexual motivation was observed in progesterone-primed, TP-treated females, displaying a preference for the intact male of 22.6%. When TP was co-administered with bicalutamide, sexual preference was reduced. Six of the nine SARMs caused a significant increase in female sexual motivation, displaying a preference for the intact male over castrate. Although S-26 was the most active of the SARMs tested, the other mono-substituted, para-halogen derivatives (i.e., S-24, S-25 and S-27) showed lesser or no ability to stimulate female sexual motivation. With the unexplained exception of the 0.3 mg/day dose group, all females that received S-23, primed with progesterone, demonstrated a significant increase in female sexual motivation, with similar increases seen at doses ranging from 0.05 mg/day to 3 mg/kg/day (Figure 3.8). It should be noted that although S-30 displayed a significant increase in sexual motivation, it showed the least pharmacologic activity in the uterus. Importantly, treatment with R-23 failed to elicit a significant increase in sexual preference, indicating the stereoselective and AR-dependent nature of these pharmacologic effects.

3.3.4   Effect of SARMs on Serum Hormones

To determine if the inability of S-25 to maintain female sexual motivation is due to lack of CNS penetration, the ability of S-23 and S-26 (both maintain sexual motivation) to suppress LH and FSH was compared to S-25. As expected, ovariectomy significantly increased serum FSH and LH to 158.4 (from 8.2 for intact) and 16.9 (from 0.8) ng/mL, respectively (Table 3.3). TP and all SARMs tested significantly inhibited the ovariectomy-

51

induced rise in LH and FSH, with TP and S-23 displaying the greatest inhibition. Serum FSH measured 27.8 and 24.7 ng/mL for TP and S-23, respectively while LH was below the detectable limit of the assay (0.0049 ng/mL) for both treatments.

3.4.   Discussion

Several clinical trials have displayed the beneficial effects of transdermal testosterone formulations for female sexual dysfunction in women with low serum testosterone levels. Women in these trials reported improvements in sexual desire, pleasure, and orgasms (52, 56-58). However, untoward effects associated with steroidal preparations plague the widespread use of testosterone for many indications, including HSDD. The recent developmental breakthroughs of nonsteroidal SARMs provide an alternative to testosterone for clinical use. SARMs have favorable pharmacokinetic profiles as well as tissue selectivity thereby maintaining the anabolic actions of endogenous androgens without the virilizing consequences associated with traditional steroidal androgen therapies.

The structure activity relationships that define the interaction between novel nonsteroidal ligands and the AR have been extensively studied in our laboratories (30, 33, 88, 96, 125-129) and many others (129-145). In our quest to develop novel SARMs, innumerable structural modifications were made to the arylpropionamide backbone to optimize *in vitro* and *in vivo* activity. Key structural elements include an electron-deficient aromatic A-ring, a methyl group linked to the chiral carbon (S-isomer), an ether linkage, and electronegative substituents in the *meta-* and/or *para-* positions of the aromatic B-ring (Table 1). A series of nonsteroidal AR ligands was developed to study the influence of multiple B-ring substitutions on binding affinity and pharmacologic activity.

In the current study, *in vitro* and *in vivo* assays were used to assess the potential efficacy of SARMs for female sexual dysfunction (FSD). Previous studies revealed the importance of hydrogen bond acceptor groups in the *meta-* and *para-*positions of the A-ring (33, 146). Additionally, previous reports of structure activity relationships demonstrated hydrophilic electron withdrawing groups were favorable on the *para* position of the B-ring, while halogens could be placed at any position (96, 146). Therefore, in the current study, structural modifications were made only to the B-ring since it is critical for AR agonist activity. The inactive isomer of S-23 (R-23) did not bind the AR or induce AR- or ER-mediated transcriptional activity, revealing the stereoselective nature of the AR for these ligands. The *para* mono-substituted halogen derivatives bound the AR with RBAs ranging from 3.2% for the *para*-iodo derivative to 12.1% for the *para*-fluoro derivative,

52

demonstrating that affinity increases with electronegativity (F > Cl > Br > I). Affinity was hindered when the same halogen was added to the *meta*-position of the B-ring (compare S-24 to S-28 and S-25 to S-29). Binding affinity was also negatively influenced by adding extra bulk at the *para-* position, as evidenced by the acetamide on S-30 and the decreasing affinity as bulk increases on the mono-substituted halogen derivatives (I > Br > Cl > F). Modifying the *meta-* and *para*-substituents had a small influence on the ability of each SARM to stimulate AR-mediated transcriptional activation, with maximal transactivation abilities ranging between 80 and 101% for all but one SARM (S-27). Additionally, the SARMs displayed miminal cross-reactivity with the ERα and ERβ, and this was only observed at high concentrations (i.e.1 μM). As a whole, *in vitro* measures of binding affinity and transactivation ability did little to distinguish one compound from another.

The potency of each SARM in androgenic and anabolic tissues is dramatically influenced by modifying B-ring substituents. With the exception of S-23, a halogen-substituted SARM, the nonsteroidal SARMs demonstrated partial agonist activity in androgenic tissues and partial (S-24 and S-29) to full agonist activity in anabolic tissues, in castrated male rats. S-23 bound the AR with the highest affinity and was the least tissue selective SARM, displaying full agonist activity in androgenic and anabolic tissues in castrated rats with the dose-response curve in the prostate shifted slightly towards higher doses. The electronegative cyano group of S-22 also displayed high AR binding affinity; however, the mono-substitution offered more tissue selectivity than the di-substituted S-23. The bulky *para*-acetamide of A-30 significantly reduced AR binding affinity, but was highly tissue selective and exhibited potent anabolic activity.

A separate study showed that a SARM structurally similar to S-23 when combined with EB is able to restore mating behavior in long-term castrated rats (123). Likewise, Miner *et al* reported a bicyclic quinolinone derivative that is able to prevent loss of sexual behavior that occurs after castration (100). The ability of the non-aromatizable SARMs to support male sexual function speaks to the importance of the AR in this gender. However, the role of androgens in female sexual behavior remains questionable.

The partner preference paradigm is frequently used to evaluate the proceptive behavior of female rats. The test animal is given the opportunity to choose between a sexually active intact male and either a receptive female or a sexually inactive ORX male (stimulus animals). Edwards showed that when OVX rats were primed with EB and progesterone, they displayed high levels of proceptive behavior in the presence of sexually active males, but this activity significantly decreased when a sexually inactive male or female

53

was present (147). Estrogen was administered to elicit sexual behavior, however progesterone is required to facilitate both proceptive and receptive behaviors (148). Allan *et al* were the first to report the effectiveness of SARMs in female rats (149), showing that a pyrazoline derived SARM was able to enhance a female's preference for sexually active males.

As women age, androgen production declines, as does sexual desire and activity. Suppressed circulating free testosterone levels may also result from oral estrogen therapy (150), glucocorticosteroid administration (151), chemotherapy, or irradiation. The most accepted indication for transdermal testosterone therapy in women with low circulating testosterone is FSD. The current study was designed to investigate the effects of TP and SARMs on female sexual motivation in the partner preference paradigm. Reduction of endogenous estrogen and testosterone levels following ovariectomy decreased the female's sexual activity, showing no preference for the intact or castrated male. However, progesterone-primed, SARM-treated female rats preferred the company of the intact male, with S-22, S-23 (dose-response), and S-26 being comparable to TP-treated rats, without adversely affecting uterine growth. Females administered low doses of S-23 (0.05 and 0.1 mg/d) displayed a preference for the intact male while maintaining the uterus at less than 40% of intact control. The extent of N-C interaction induced by a ligand appeared to be a reliable predictor of the pharmacologic activity of the ligand in the uterus and the prostate. S-22, S-23, S-25, S-26 and S-27 were the most efficacious *in vitro* by inducing the N-C interaction at 10 and 100 nM. The same SARMs increased the weight of the uterus and prostate to the greatest extent. Importantly, growth observed following TP and SARM administration appears to be due to growth of the myometrium, the smooth muscle of the uterus, and not the endometrium. Additionally, *in vivo* pharmacologic activity in male and female rats is highly correlated, with a correlation coefficient of 0.94 (p = 0.0002) for uterine and prostatic activity.

S-25 and S-26 similarly maintained the weight of the uterus in females and prostate and levator ani muscle in male rats. However, S-26 maintained female sexual motivation while S-25 did not. Serum LH and FSH levels were measured to determine if this discrepancy could be due to their ability (or inability) to penetrate the CNS. However, S-25 and S-26 inhibited OVX-induced elevations in LH and FSH to a similar extent and therefore lack of CNS penetration does not explain the inability of S-25 to maintain female sexual motivation.

There does not appear to be a correlation between B-ring substitutions and the ability of the SARMs to support female sexual motivation. The cyano-substituted (S-22) and the mixed halogen-substituted SARMs (S-23) bind the AR with high affinity, possess potent anabolic activty, and support sexual motivation in female rats. Additionally, mono-substituted halogen containing SARMs bind the AR with varying affinities and display a wide range of *in vivo* activites. However, the ability of S-23 and the inability of S-24 to support female sexual motivation, coupled with their activity in castrated male rats, suggest that the ability of SARMs to support sexual motivation may be associated with their androgenic and anabolic pharmacologic properties. Most SARMs improved sexual motivation of OVX female rats, with potency and efficacy comparable to that of TP. Estrogen is an active metabolite of testosterone, but it is not clear whether the actions of testosterone in women are predominantly mediated *via* the AR, or after aromatization, *via* the ER. However, SARMs are non-aromatizable and do not cross-react with the ER, indicating that the AR plays an important role in female libido. Co-administration of TP with an anti-androgen reduced sexual preference of the female for an intact male also implies that the AR is involved in female sexual behavior. These results suggest that SARMs could be an effective therapy for FSD in women.

In conclusion, the current studies examined binding affinity and activity of a series of nonsteroidal SARMs. Structural modifications to the *meta-* and *para-* positions of the B-ring resulted in a range of *in vitro* AR binding affinities and functional activities. With the exception of S-23, all of the SARMs tested were prostate sparing, selectively maintaining the size of the levator ani muscle in castrated male rats. Most nonsteroidal SARMs improved sexual motivation of OVX female rats in a partner preference paradigm, comparable to TP, while maintaining uterine weights at less than 50% of intact control. These studies indicate that it is possible to develop a SARM that maintains sexual motivation and is selective that does not adversely affect proliferation of the endometrium (e.g. S-30). SARMs, with many advantages over traditional steroidal androgen preparations, could be beneficial in the clinical treatment of hypoactive sexual desire disorder.

3.5. Acknowledgements
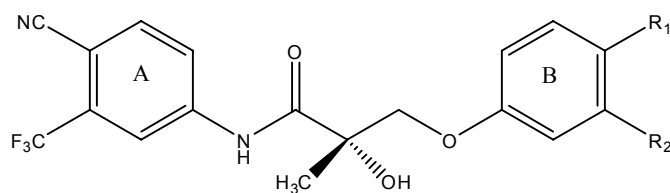
Compound	R$_1$	R$_2$	RBA (%)	AR *in vitro* activity	ERα *in vitro* activity	ERβ *in vitro* activity
S-22	CN	H	16.8 ± 1.3[a]	94 ± 27[a]	11.4 ± 1.6	17.7 ± 0.9
S-23	Cl	F	26.5 ± 2.3[b]	101.2 ± 11.3	25.6 ± 3.5	28.1 ± 0.7
S-24	F	H	12.1 ± 0.3[c]	82.4 ± 9.4	19.6 ± 2.4	18.5 ± 0.6
S-25	Cl	H	11.8 ± 0.3[c]	82.5 ± 4.6	24.1 ± 5.5	21.3 ± 0.4
S-26	Br	H	4.6 ± 3.3[d]	87.6 ± 24.0	8.4 ± 0.5	18.9 ± 0.3
S-27	I	H	3.2 ± 0.3[d]	64.8 ±14.9	11.0 ± 2.3	20.1 ± 0.6
S-28	F	F	9.7 ± 1.4[e]	86 ± 7[e]	8.9 ± 0.9	20.0 ± 0.3
S-29	Cl	Cl	8 ± 2[e]	92 ± 2[e]	8.8 ± 4.9	24.9 ± 0.3
S-30	NHC(O)CH$_3$	H	4.8 ± 5.1	80.5 ± 9.6	4.7 ± 1.9	21.0 ± 0.5
R-23[f]	Cl	F	0.1 ± 0.06	0.19 ± 0.06	6.1 ± 0.7	20.8 ± 0.5

Table 3.1. Chemical Structures, AR Binding Affinities, and *In Vitro* Activities of Nonsteroidal SARMs

AR relative binding affinities were determined using a radiolabeled competitive assay. The ability of the compound of interest to induce AR- or ER-mediated transcription was determined using a cotransfection assay. The transcriptional activity induced by each compound at a concentration of 100 or 1000 nM was reported as the percentage of that observed for 1 nM DHT or E$_2$ for the AR and ER, respectively. Vehicle control for ERα and ERβ was 7.9 and 19.3%, respectively. Data presented as mean ± SD (n = 3). [a] Reported by Kim et al (88); [b] Reported by Jones et al (123), Reported by Fisher (152); [c] Reported by Kim (153); [d] Reported by Chen et al (96), [e] Opposite stereo-chemical conformation to structure shown above.
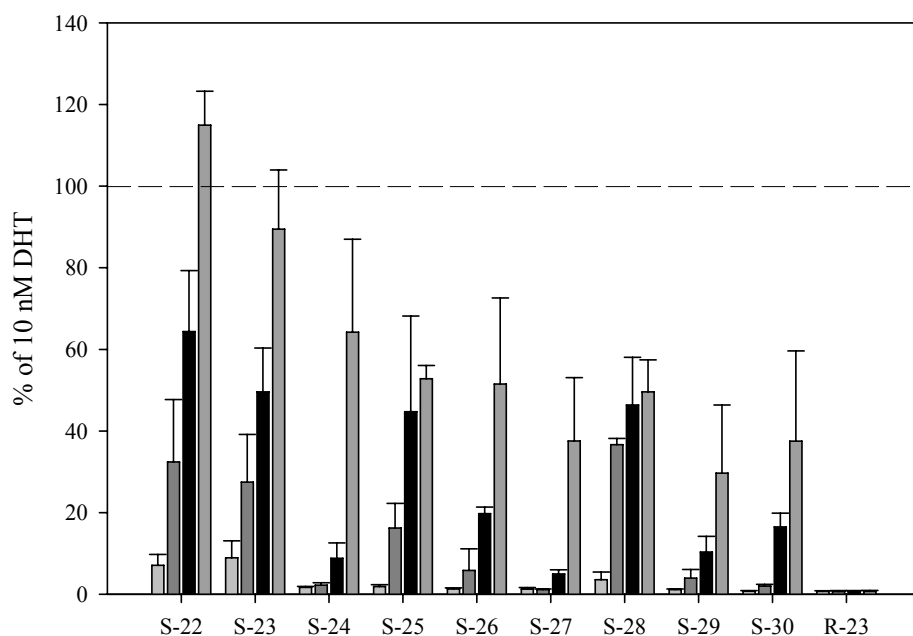
Figure 3.1. *In Vitro* N-C Interaction

The ability of each SARM to induce an interaction between the amino terminus and the carboxy terminus of the AR was determined in a two-hybrid assay. The activity induced by each compound at 1, 10, 100 or 1000 nM was reported as a percentage of that observed for 10 nM DHT. Data presented as mean ± SD (n = 3).

Compound	E_{max} (% of intact control)	
	Prostate	Levator Ani
S-22	51.1 ± 4.2^{a}	136 ± 3.5^{a}
S-23	110 ± 25.6^{b}	136 ± 8.8
S-24	7.7 ± 1.7^{c}	69.9 ± 9.0^{c}
S-25	60.3 ± 1.0^{c}	111 ± 1.8^{c}
S-26	45.4 ± 7.2	97.1 ± 9.8
S-27	41.8 ± 8.9	94.2 ± 8.1
S-28	39.2 ± 6.3	98.7 ± 4.4
S-29	33.4 ± 7.0	82.2 ± 6.2
S-30	41.4 ± 8.8	128 ± 12.7
R-23	6.7 ± 0.3	34.4 ± 4.5

Table 3.2. Pharmacologic Activity of SARMs in Castrated Male Rats

Castrated male rats were treated with SARMs (1 mg/day) for 14 days *via* sc injection. Vehicle-treated intact and castrate groups were also included as controls. Prostate and levator ani muscle weights were normalized to body weight and presented as a percentage of the vehicle-treated, intact control group. Data presented as mean ± SD (n = 5). [a] Reported by Kim et al (88); [b] Reported by Jones et al (123), [c] Reported by Fisher (152).
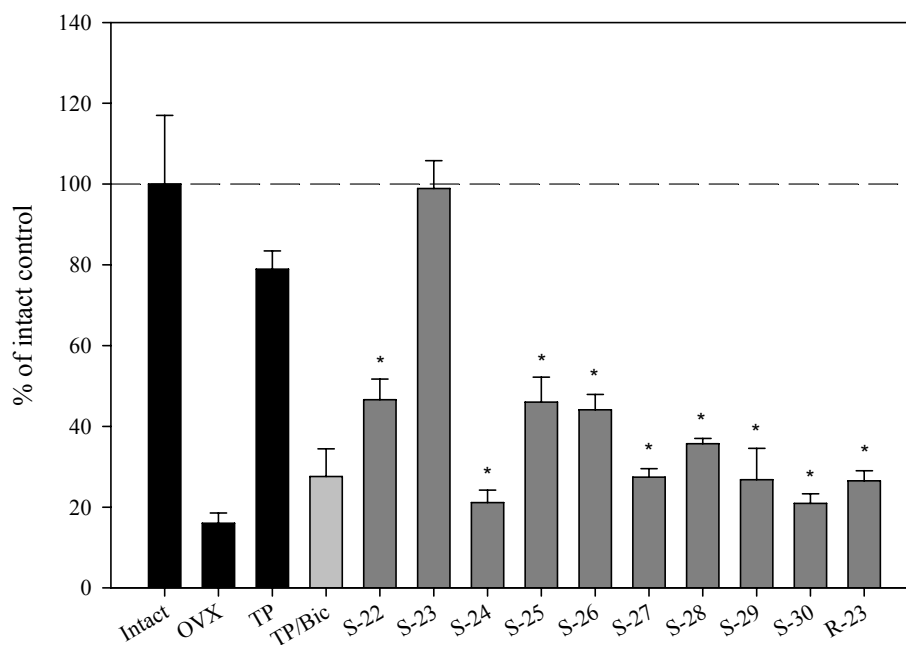
Figure 3.2. Pharmacologic Activity of a Series of SARMs in OVX Female Rats

OVX female rats were treated with TP, TP/Bicalutamide, or a SARM (3 mg/kg/day) for 14 days. Vehicle-treated intact and OVX groups were also included as controls. Uterine weights were measured at the end of the treatment period, normalized to body weight, and presented as a percentage of the vehicle-treated, intact control group. Data presented as mean $\pm$ SD (n = 6). * Indicates a significant difference compared with the vehicle-treated, intact control group, with $p < 0.05$.
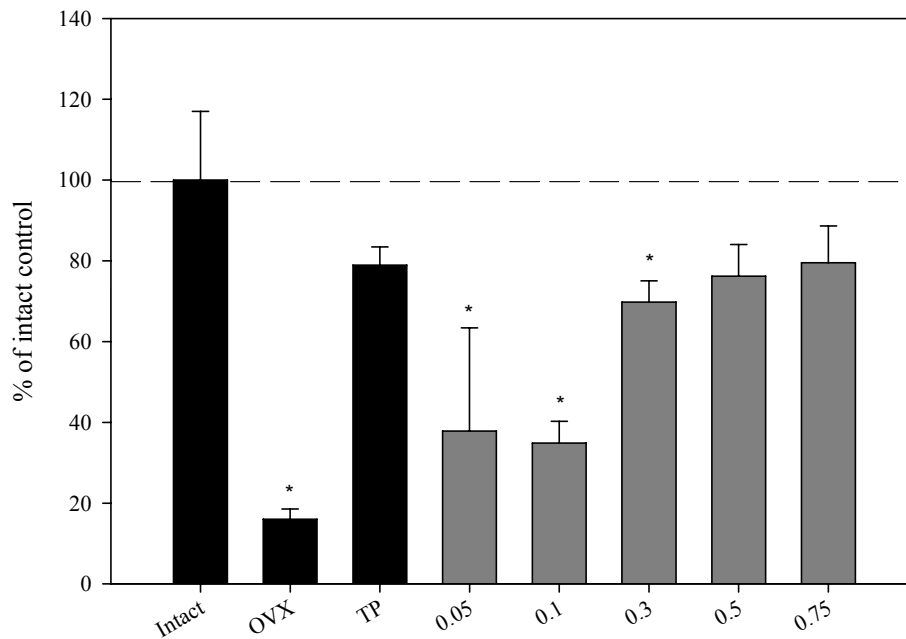
Figure 3.3. Pharmacologic Activity of S-23 in OVX Female Rats

OVX female rats were treated with TP (3 mg/kg/day) or S-23 (0.05, 0.1, 0.3, 0.5, 0.75 mg/day) for 14 days. Vehicle-treated intact and OVX groups were also included as controls. Uterine weights were measured at the end of the treatment period, normalized to body weight, and presented as a percentage of the vehicle-treated, intact control group. Data presented as mean $\pm$ SD (n = 6). * Indicates a significant difference compared with the vehicle-treated, intact control group, with $p < 0.05$.
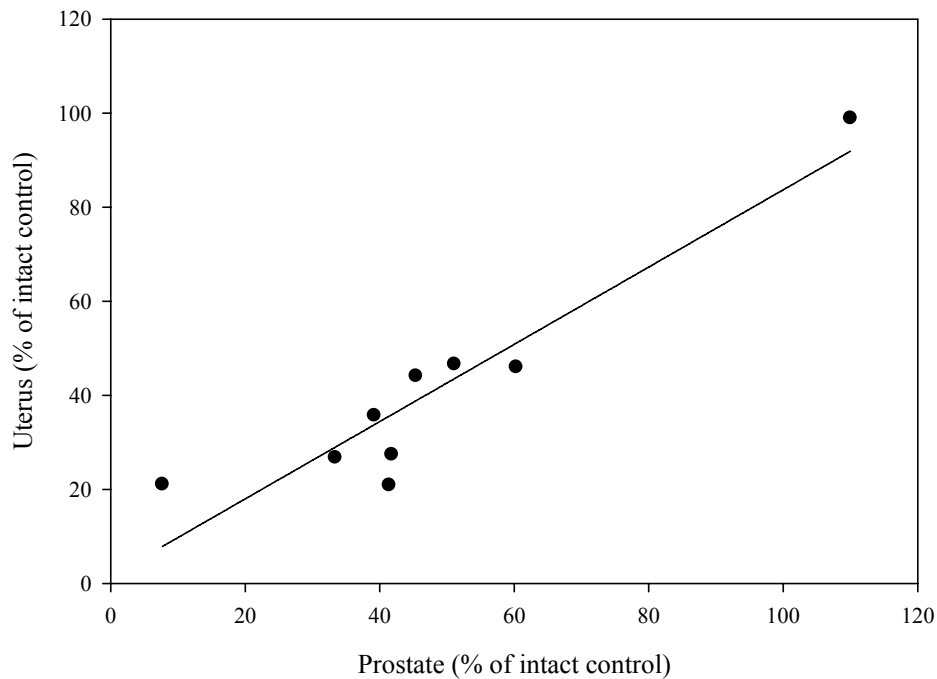
Figure 3.4. Linear Correlation of Male and Female Pharmacologic Activity

OVX female rats and ORX male rats were treated with a SARM at a dose rate of 3 mg/kg/day or 1 mg/day, respectively, for 14 days. Uterine and prostate weights were measured at the end of the treatment period, normalized to body weight, and presented as a percentage of the vehicle-treated, intact control group. Uterine and prostatic activity of each SARM was compared and nonlinear regression performed. Correlation coefficient = 0.94 ($p = 0.0002$).
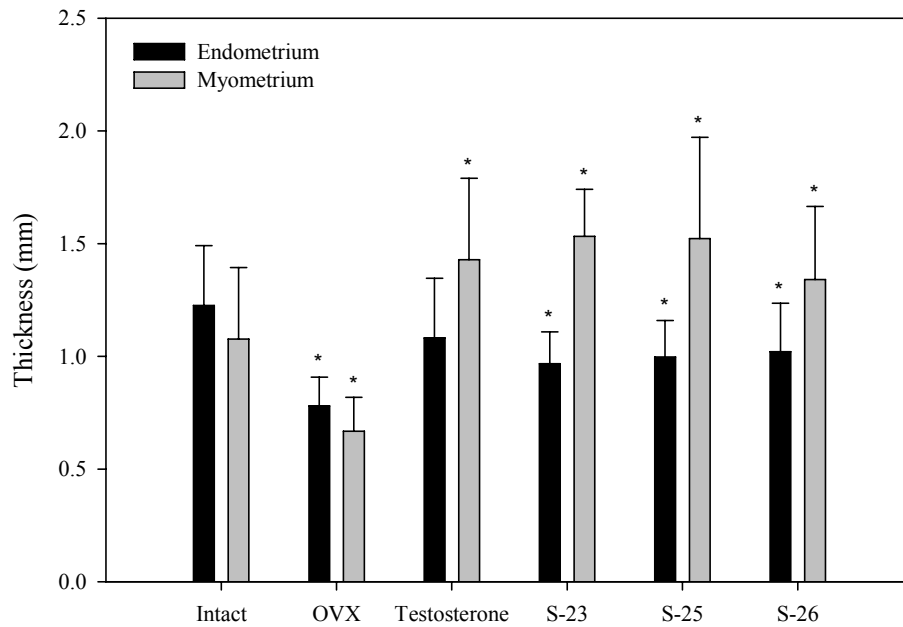
Figure 3.5. Effects of SARMs on Uterine Growth

OVX female rats were treated with TP or a SARM (3 mg/kg/day) for 14 days. Vehicle-treated intact and OVX groups were also included as controls. Data are presented as mean ± SD (n = 5). * Indicates a significant difference compared with the vehicle-treated, intact control group, with $p < 0.05$.
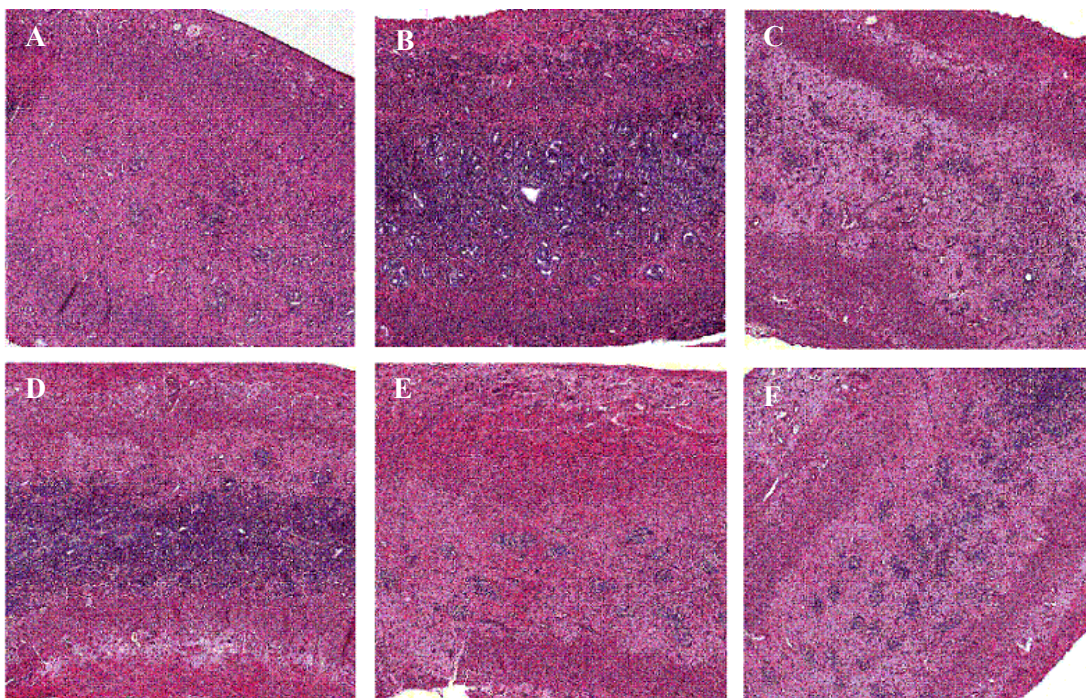
Figure 3.6. Effects of SARMs on Uterine Histology

Rats were treated for 14 days *via* sc injection. Uteri were fixed in 4% paraformaldehyde in PBS for histology. The uteri were dehydrated and stained with hematoxalylin and eosin and analyzed. A-F, Magnified views (2.5x) of the endometrial and myometrial layers in intact, OVX, TP, S-23, S-25 and S-26-treated animals, respectively.
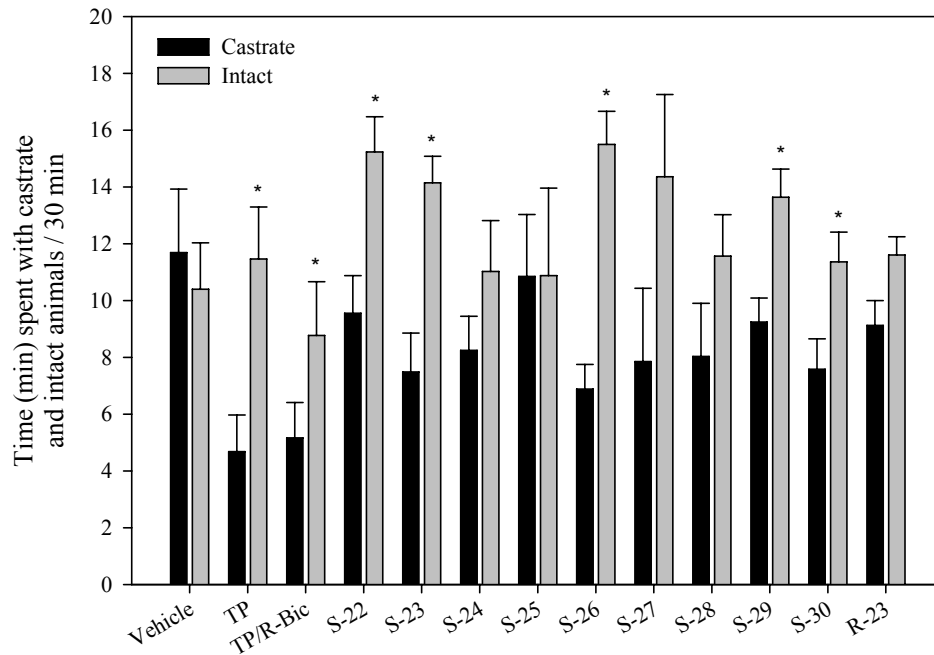
Figure 3.7. Effects of SARMs on Sexual Motivation in OVX Female Rats

OVX female rats were treated with TP, TP/Bicalutamide, or a SARM (3 mg/kg/dat) for 14 dats. A vehicle-treated OVX group was also included as control. Behavioral testing was performed in a three compartment chamber for 30 minutes. The duration of time spent in each compartment by the female was recorded. The total time spent with the castrate and intact males are reported. Data are presented as mean ± SD. * Indicates a significant difference between the time spent with the intact animal compared to the castrate for each group, with $p < 0.05$..

Figure 3.8. Effects of S-23 on Sexual Motivation in OVX Female Rats

OVX female rats were treated with TP (3 mg/kg/day) or S-23 (0.05, 0.1, 0.3, 0.5, 0.75 mg/day) for 14 days. A vehicle-treated OVX group was also included as control. Behavioral testing was performed in a three compartment chamber for 30 minutes. The duration of time spent in each compartment by the female was recorded. The duration of time spent in each compartment by the female was recorded. The total time spent with the castrate and intact males are reported. Data are presented as mean ± SD. * Indicates a significant difference between the time spent with the intact animal compared to the castrate for each group, with $p < 0.05$.

Group	FSH (ng/mL)	LH (ng/mL)
Intact	8.2 ± 2.7^{O}	0.8 ± 0.2^{O}
OVX	158.4 ± 34.2^{I}	16.9 ± 2.4^{I}
TP	$27.8 \pm 7.2^{I, O}$	$< 0.0049^{I, O}$
S-23	$24.7 \pm 5.1^{I, O}$	$< 0.0049^{I, O}$
S-25	$34.9 \pm 9.9^{I, O}$	$0.38 \pm 0.2^{I, O}$
S-26	$40.2 \pm 10.4^{I, O}$	$0.43 \pm 0.08^{I, O}$

Table 3.3. Effects of TP and SARMs on FSH and LH in OVX Female Rats

OVX female rats were treated with TP, S-23, S-25 or S-26 (3 mg/day) for 14 days *via* sc injection. Vehicle-treated intact and ovariectomized groups were also included as controls. Serum LH and FSH were measured. Data presented as mean ± SD (n = 5/group). [I and O] Indicates a significant difference between the group and intact control group or ovariectomized control group, respectively, with $p < 0.05$.

Chapter 4

In Vitro **Structure Activity Relationships of Nonsteroidal Antiandrogens**

4.1. Introduction

Androgens are involved in the normal growth, development and neoplastic transformation of the prostate. Androgen deprivation therapy (ADT) remains to be the foundation of intervention in the treatment of advanced-stage prostate cancer. Flutamide (Eulexin™) and bicalutamide (Casodex™) are nonsteroidal antiandrogens that bind AR and recruit co-repressors to inhibit prostate cancer. Recently, two antiandrogens of the diarylthiohydantoin class, RD162 and MDV3100, were demonstrated to bind the AR with greater affinity than bicalutamide, reduce AR nuclear translocation, and impair binding of AR to androgen response elements (ARE) (154). These orally available AR antagonists are in Phase III clinical trials.

Patients treated with antiandrogens often develop drug resistance due to mutations that develop in the AR-LBD. These mutations allow the AR-LBD to adopt an agonistic conformation, thus conferring agonist activity of antiandrogens (67, 155, 156). However, at this point, termination of treatment may result in antiandrogen withdrawal syndrome, in which patients' tumors regress (66, 157). It is believed that the receptor compensates for the structural perturbations of the antagonist, relative to agonist, by developing these mutations.

Common mutations include Thr 877→Ala (AR(T877A)), Trp 741→Leu (AR(W741L)), and Trp 741→Cys (AR(W741C). While the AR(T877A) mutation adopts an agonist conformation upon binding to hydroxyflutamide (65), AR(W741L) and AR(W741C) convert bicalutamide into a potent agonist (66). Our laboratory solved the x-ray crystal structure of SARMs bound to AR(WT) (129, 156) and R-bicalutamide bound to AR(W741L) (67) providing insight for structure-based drug design.

The three-dimensional crystal structure of R-bicalutamide bound to the AR(W741L) mutant reveals that the B-ring of R-bicalutamide occupies the same position that the indole ring of Trp 741 does when the AR(WT) is bound to DHT (67). In the AR(WT), the presence of the Trp 741 indole ring sterically hinders the binding of bicalutamide such that the B-ring

of R-bicalutamide cannot be accommodated. For the most part, when R-bicalutamide is bound to the W741L mutant AR, residues are positioned similar to that observed for the complexed DHT AR(WT) LBD (Figure 4.1). Additionally, at the position of the chiral hydroxyl group of R-bicalutamide, R-bicalutamide bends and orients itself such that it makes direct contacts with residues of helix 12, a region not occupied by DHT in the AR(WT) ((67) Figure 4.2). Met 895 on helix 12 is considerably shifted by bulk from the sulfonyl linkage group of R-bicalutamide and is accommodated near Leu 741 in the mutant, compared to the complexes of DHT or nonsteroidal AR agonists (ether linkage) bound in the AR(WT) (67). Loss of bulk in this mutation provides room for the larger R-bicalutamide molecule and allows for the same fold seen with other agonist bound steroidal ligands in the AR(WT). Conversely, R-bicalutamide maintains its antagonistic properties in the AR(T877A) due to the bulky structure by sterically inhibiting folding of the receptor (156). Encroachment of the space occupied by helix 12 and partial unfolding of the receptor due to the large molecule likely causes antagonism of R-bicalutamide in AR(WT) (67).

To overcome the widespread problem of antiandrogen resistance, our laboratory sought to develop pan-antagonists that exhibit antagonist activity across all AR mutations. Combining knowledge of the crystal structures of agonist-bound AR(WT) and R-bicalutamide-bound AR(W741L), we investigated the possibility of increasing bulk on the B-ring that would sterically disrupt formation of the AF2. This strategy could be used to inhibit all mutations of the AR and subsequently prostate cancer.

4.2. Materials and Methods

4.2.1 *In Vitro* AR Binding Affinity

In vitro AR binding affinity was determined in a radioligand competitive assay. Preparation of the AR GST-LBD and the method of performing the competitive binding assay were described in Section 3.2.2. Binding affinities are expressed relative to DHT (RBA; 100%).

4.2.2 *In Vitro* AR-Mediated Transcriptional Activity

The agonist and antagonist activities of the compounds in the wild-type AR (AR(WT)), AR(W741L) and AR(T877A) were determined using cell-based transient transactivation assays, as described in Section 3.2.3 (31). Cells were transfected with 45 μg GRELuc, 1 μg CMVLuc (renilla luciferase), and 2.5 μg of a CMVhAR, CMVhAR-W741L or CMVhAR-T877A expression vector. Previous experiments in our laboratory identified that 1

(30), 100 and 1 nM (156) are the lowest concentrations of DHT to induce AR(WT), AR(W741L) and AR(T877A) transactivations, respectively. The *in vitro* functional activity of each compound of interest (final concentrations ranging from 1-1000 nM) was determined by incubating cells in the absence (agonist assays) or presence (antagonist assays) of the indicated concentrations of DHT. Transcriptional activity induced or suppressed by each compound is expressed as the percentage of activity induced by DHT.

4.2.3   Cloning, Expression and Purification of AR-LBD

AR LBD was prepared as described in Section 3.2.2. Mutations were created in pGEX6P-AR (663-919) and pCMVhAR *via* the Stratagene QuikChange mutagenesis kit according to the manufacturer's instructions. Cells were lysed in the buffer containing 150 mM NaCl, 50 mM Tris, pH 8.0, 5 mM EDTA, 10% glycerol, 1 mg/mL lysozyme, 10 units/mL DNase I, 10 mM $MgCL_2$, 10 mM DTT, 0.5% CHAPS, 100 µM phenylmethylsulfonyl fluoride, and 100 µM ligand by 3 freeze/thaw cycles. The supernatant from ultracentrifugation was incubated for 1 h at 4 °C with glutathione-Sepharose (Amersham Biosciences) and washed with 150 mM NaCl, 50 mM Tris, pH 8.0, 5 mM EDTA, 10% glycerol, 10 µM ligand, 0.1% *n*-octyl-β-glucoside and 1 mM DTT. The GST-LBD fusion protein was cleaved in a buffer containing 150 mM NaCl, 50 mM Tris, pH 7.0, 5 mM EDTA, 10% glycerol, 100 µM ligand, 0.1% *n*-octyl-β-glucoside, 1 mM DTT and 5 units of PreScission Protease (Amersham Biosciences) at 4 °C overnight releasing the AR LBD from the glutathione-Sepharose resin. The supernatant was then diluted 3-fold in 10 mM Hepes, pH 7.2, 10% glycerol, 10 µM ligand, 0.1% *n*-octyl-β-glucoside and 1 mM DTT and loaded onto an HP SP cation exchange-column (Amersham Biosciences). Protein was eluted with a gradient of 50 to 500 mM NaCl in the same dilution buffer. The buffer was exchanged in a Millipore 10 kDa cut-off concentrator to a buffer containing 150 mM Li_2SO_4, 50 mM Hepes, pH 7.2, 10% glycerol, 10 µM ligand, 0.1% *n*-octyl-β-glucoside and 10 mM DTT. Protein was concentrated to 8 mg/mL.

4.2.4   Crystallization, Data Collection and Structure Determination

The sitting drop vapor diffusion method was used to obtain AR LBD crystals in reservoirs containing 0.1 M Hepes, pH 7.5, and 0.75 M Li_2SO_4 and was transferred to a solution consisting of 0.1 M Hepes, pH 7.5, 0.75 M Li_2SO_4 and 25% ethylene glycol before being flash frozen in liquid nitrogen. Diffraction data were collected using a Rigaku RU300 rotating anode generator and an R-axis IV[++] image plate (Rigaku, The Woodlands, TX) and

processed with Crystal Clear software (Molecular Structure Corp., The Woodlands, TX). The x-ray crystal structure of the AR(T877A) LBD in complex with A-12 (PDB code 2AXA) was used as a starting structure for refinement using the Crystallography & NMR System (158). Subsequently, electron density maps allowed for accurate fitting of the ligand. Model building and water molecules were added using the program O (159) and further rounds of refinement were performed using rigid body, torsion angle simulated annealing, and individual temperature factor modules of the Crystallography & NMR System. The figures were prepared with PyMOL[3].

4.2. Results

4.2.1 *In Vitro* AR Binding Affinity

S-22, a lead SARM, bearing an ether linkage and a B-ring *para*-cyano group exhibits high AR binding affinity, with a RBA of 5.5%, while R-bicalutamide binds approximately 10-fold less (RBA of 0.62%; Table 4.1). Maintaining the sulfonyl linkage of R-bicalutamide but replacing the *para*-fluoro with a cyano group did not alter binding affinity (A-1). However, introducing an amine linkage significantly decreased the binding affinity and appeared to decrease regiospecificity for the cyano substituent in the B-ring (A-2 – A-4). When an ether linkage is present, the position of the B-ring cyano substituent has a greater effect on AR binding (compare S-22 and A-7 to A-5 and A-6) and replacing the cyano group with a trifluoromethyl resulted in high AR binding affinity (3.0%; A-8). Conversely, introduction of more bulk to the B-ring by adding a naphthyl group decreased the binding affinity of ether-linked (compare A-12 to S-22) and sulfonyl-linked derivatives (compare A-9 to A-1). Presence of an amine linkage, however, increased the binding affinity from 0.16% for A-2 to 1.5% for A-11 when incorporated with a naphthyl B-ring. Adding a more flexible, bulky bi-phenyl substituent, while still maintaining the B-ring *para*-cyano group, decreased the binding affinity approximately 3-fold (A-13 and A-14) compared to the naphthyl substituted compound. However, the RBA of these compounds was still higher than that of the monosubstituted derivative (*para*-cyano), A-2. When the ether linkage was present, adding the bulk and flexibility of a phenyl, benzyl, or phenoxy substituent at any position (A-15 – A-20) did not alter binding affinity compared to the ether-linked derivative lacking a *para*-cyano group (A-10). However, binding affinities were significantly lower compared to ether-linked derivatives bearing a B-ring *para*-cyano group. Both the amine-linked and ether-linked *meta*-phenyl substituted compounds (A-13 and A-16) displayed similar binding affinities, while the amine-linked *ortho*-substituted compound (A-14) bound with greater

70

affinity than the ether-linked derivative (A-17). Finally, addition of a propyl group off the amine linkage (A-22) increased binding affinity compared to its amine-linked counterpart (A-2), but was substantially decreased by addition of a methyl group (A-23).

4.2.2 *In Vitro* AR(WT) Activity

S-22 is a very potent and efficacious SARM in the AR(WT), with maximum agonist activity of $140 \pm 15.1\%$ (E_{max}) and potency of 1.4 nM (EC_{50}; Table 4.1). On the other hand, presence of a sulfonyl linkage and *para*-fluoro substituent on the B-ring in R-bicalutamide results in antiandrogenic activity, with an IC_{50} of 22.4 nM and 90% inhibition of DHT-dependent activity. Replacing the *para*-fluoro of R-bicalutamide with a cyano group (A-1) significantly reduced the antagonist activity in the AR(WT). Incorporation of an amine linkage (A-2) introduced partial agonist activity and improved antagonist activity, although still 5-fold less potent than R-bicalutamide. However, the potency significantly improved (IC_{50} of 6.7 nM) and was better than that of R-bicalutamide when the B-ring *para*-cyano group was shifted to the *meta*-position (A-3). *Meta*- and *ortho*-cyano groups on molecules possessing ether linkages displayed weak AR(WT) agonist and antagonist activity (A-5 and A-6). Only partial agonist activity was observed in the presence of a *para*-cyano group (like S-22) in combination with a *meta*-cyano group (A-7). In addition to very weak antagonist activity, potent partial agonist activity was also observed with a *para*-trifluoromethyl group (A-8).

Introduction of bulk to the B-ring (naphthyl group) of A-1, which also bears a B-ring *para*-cyano group, compromised the IC_{50} and displayed antagonist activity only at high concentrations (A-9). Comparing A-10 and A-12, ether-linked compounds without and with a *para*-cyano group, respectively, demonstrated that though addition of a *para*-cyano group reduced the antagonistic potential, it increased the partial agonist activity. Presence of an amine linkage produced weak agonist and antagonist activity (A-11). Adding flexibility to the B-ring bulk by addition of a phenyl ring at the *meta*-position, as seen in A-13, greatly improved the antagonist activity of the amine-linked compounds, with comparable potency (20.5 nM) and efficacy (88.2%) as R-bicalutamide. Weak antagonist activity was observed in the ether-linked compounds with an aromatic ring off the *para*-, *meta*- and *ortho*-positions of the B-ring (A-16 to A-20). Incorporation of a substitution to the amine linkage exhibited similar efficacy (83.3% inhibition for A-21 to 92.7% for A-22) as that of R-bicalutamide (90.9%). However, potency reduced 5 to 6-fold for the benzyl-substituted (A-21) and propyl-

71

substituted amine-linked compounds, and 10-fold for the methyl-substituted amine-linked compound (A-23).

4.2.3   *In Vitro* AR(W741L) Activity of Nonsteroidal AR(WT) Antagonists

R-bicalutamide is a very potent agonist in the AR(W741L) mutant, with an EC_{50} and E_{max} of 1.1 nM and 273%, respectively (Table 4.2). Replacing the *para*-fluoro with a cyano group, as seen in A-1, significantly reduced agonist activity but still did not exhibit any antagonist activity. Replacing the sulfonyl linkage with an amine maintained similar agonist activity but introduced very weak antagonist activity, although only at high concentrations (A-2). Shifting the *para*-cyano group to the *meta*-position slightly improved the antagonist activity (A-3); however, full agonist activity returned with an *ortho*-cyano group on the B-ring (A-4). Ether-linked compounds A-5, A-6 and A-7, bearing *meta*-cyano, *ortho*-cyano, or *para*-trifluoromethyl group on the B-ring, respectively, exhibited very weak to no antagonist activity. These derivatives did however display varying agonist activity, with the greatest potency observed with A-7 bearing the *para*-trifluoromethyl group. Of the naphthyl-containing compounds, the sulfonyl-linked derivative, A-9, displayed minimal antagonist activity, the ether-linked derivatives A-10 and A-12, exhibited partial and full agonist activity, respectively, as did the amine-linked derivative, A-11. Phenyl-substituted B-ring derivatives, A-13, A-14 and A-15 displayed weak to partial agonist activity, and A-14 alone, which bears an amine linkage and an *ortho*-phenyl substituted B-ring, exhibited weak antagonist activity (305 nM). A-21, the benzyl-subtstituted amine, displayed weak agonist and antagonist activity. Reducing the bulk to a propyl group improved antagonist activity, with the most potent and effective antagonist, A-22, bearing a B-ring *para*-cyano group and a propyl-substituted amine. The IC_{50} and percent inhibition of DHT-dependent activity for A-22 was 151 nM and 81.8%, respectively.

4.2.5.   *In Vitro* AR(T877A) Activity of Nonsteroidal AR(WT) Antagonists

In the AR(T877A) mutant, R-bicalutamide maintained antagonist properties with an IC_{50} of 228.8 nM and inhibited DHT-dependent activity by 73.7% (Table 4.2). Replacing the *para*-fluoro with a cyano group (A-1) weakened antagonist activity and also displayed very weak partial agonist activity. However, changing the linkage group of A-1 to an amine abolished antagonist activity and resulted in full agonist activity, with an EC_{50} and E_{max} of 47.0 nM and 121.9%, respectively (A-2). Moving the *para*-cyano group of the B-ring to the *meta*- and *ortho*-positions (A-3 and A-4, respectively), weakened agonist activity yet gained

weak antagonist activity. A-5, bearing an ether linkage with a B-ring *meta*-cyano group exhibited weak agonist and antagonist activity. However, potent agonist activity resulted from an *ortho*-cyano group as in A-6, or a *para*-trifluoromethyl group as in A-7. All of the naphthyl-containing compounds exhibited weak to partial agonist activity, with the greatest antagonist activity observed with the sulfonyl-linked A-9, with an IC_{50} and inhibition of DHT-induced activity of 604 nM and 74.2%, respectively. The amine-linked molecule, A-11, also displayed weak antagonist activity. Very weak partial agonist activity was observed by adding bulk with flexibility, as observed with B-ring phenyl substituents (A-13, A-14, and A-15). However, the amine-linked *ortho*-phenyl substituted B-ring (A-14) exhibited potent antagonist activity, with an IC_{50} of 34.3 nM and 94.0% inhibition of DHT-dependent activity. The amine-linked substituted compounds all displayed very weak agonist as well as antagonist activity. The larger the substitution on the linker, the less antagonist activity it possesses. The benzyl-substituted amine-linked derivative, A-21, displayed the weakest antagonist activity, with an IC_{50} of 470 nM and 74.8% inhibition of DHT-dependent activity followed by the propyl-substituted amine-linked derivative, A-23. The greatest activity was observed with the methyl-substituted amine-linked derivative (A-22) that had an IC_{50} and percent inhibition of 80.6 nM and 70.9%, respectively.

4.2.5. Binding of A-12 to AR(T877A)

Of the naphthyl-containing compounds, A-12 bound AR(WT) with the greatest affinity and was a potent and efficacious agonist in the mutants. Therefore, a crystal structure was obtained for the complex of A-12 bound in the AR(T877A) mutant (Figures 4.3 and 4.4). The overlay of A-12 in the AR(T877A) and S-22 in the AR(WT) are very similar (Figure 4.3). Interestingly, the A-12/AR(T877A) crystal structure revealed that the distal ring of the naphthyl group is opposite helix 12, between Trp 741 and Met 745, experiencing an edge-to-face π-π interaction with the A-ring. Additionally, Met 745 shifts compared to the S-22/AR(WT) complex to accommodate the bulk of A-12 in the agonist conformation (Figure 4.4), setting off a cascade of effects; Met 742 reorients as a result of the distal naphthyl ring, which pushes Met 745 towards the A-ring. This causes a steric interaction of the 5-position of the A-ring with the amide oxygen of Gln 711 on helix 3.

4.3.   Discussion

Through numerous SAR studies of nonsteroidal AR ligands (30, 88, 96, 125), we identified the cyano- or nitro groups at the *para*-position (hydrogen bond acceptor groups)

and hydrophobic substituents at the *meta*-position (trifluoromethyl) as key structural features on the A-ring of the arylpropionamide backbone to be beneficial for *in vitro* AR(WT) binding. Additionally, hydrophilic, electron-withdrawing substituents at the *para*-position of the B-ring, such as halogens or a cyano group, are also important for high *in vitro* AR binding affinity. These important structural features were therefore preserved in the current study.

The present study demonstrates that novel AR antagonists with a wide range of *in vitro* activities in the AR(WT), AR(W741L) and AR(T877A) can be designed through structural modifications of R-bicalutamide (R-bicalutamide has a 30-fold greater AR binding affinity than the S enantiomer). Increased bulk of the *para*-cyano group in A-1 increased binding affinity but decreased antagonist activity (Table 4.1). Activity was, however, superior to R-bicalutamide by changing the linker to an amine (instead of a sulfonyl) and shifting the cyano group to the *meta*-position of the B-ring. Mono- or di-substituted ether-linked arylpropionamide derivatives were not potent or effective in antagonizing the effects of the AR(WT).

We investigated the possibility of increasing bulk on the B-ring to inhibit receptor folding following ligand binding, a mechanism of AR antagonism. The amine-linked naphthyl derivative displayed the greatest potency when incorporating this substitution, although its potency (IC$_{50}$) was weak at 193 nM, approximately 10-fold less than R-bicalutamide. However, when bulk was introduced with flexibility through a phenyl ring, the result was a molecule that exhibited potency and efficacy comparable to R-bicalutamide (A-13).

The crystal structure of agonist bound A-12 in the AR(T877A) showed that the naphthyl ring does not appear to interact with the T877/T877A space. Therefore, the antagonist properties of A-12 in the AR(WT) were not due to the added bulk on the B-ring. However, it does suggest that the antagonist conformation of these compounds containing naphthyl groups would be conserved in the AR(WT) and the linker must therefore explain the differences in agonist and antagonist activity of these nonsteroidal ligands. Upon binding of A-12 in the mutant AR, a series of conformational changes occur to accommodate the bulk of the naphthyl ring. Met 742 reorients, which pushes Met 745 towards the A-ring, causing a steric interaction, which explains the weaker binding affinity of A-12 compared to S-22.

Since adding bulk to the B-ring *via* naphthyl or phenyl substituents did not result in an antiandrogen with greater potency than R-bicalutamide and the crystal structure of A-12 showed that the linker is likely the determinant of antagonist activity, we attempted to displace helix 12 by adding a substitution to the amine linkage. However, antagonist activity

of the amine-linked molecules in the AR(WT) was weak. The benzyl-substituted amine displayed the greatest potency, but was still approximately 6-fold lower than that of R-bicalutamide.

In the AR(W741L) mutant, R-bicalutamide displayed full agonist activity due to its ability to allow the receptor to adopt the agonist conformation resulting from lack of bulk in the mutation at the location of the indole ring of Trp 741 in the AR(WT) (67). A-13 and A-14 displayed potent antagonist activity in the AR(WT). The B-ring phenyl-substitution of these molecules may rotate and orient such that it pushes on Trp 741 and result in partial unfolding of the receptor. Additionally, none of the B-ring-substituted derivatives displayed any substantial AR(W741L) antagonist activity. Only when bulk extended from the amine linkage was there any significant activity (IC$_{50}$ of 151 nM with 82% inhibition). In the AR(T877A) mutant, however, R-bicalutamide displays antagonist activity in the 200 nM range. Antiandrogenic activity in this mutant appears to be greatest with a B-ring *para*-cyano group and either a *meta*- or *ortho*-phenyl group (A-13 and A-14) or a methyl-substituted amine derivative (A-22). These three molecules possess AR(T877A) antagonist activity below 100 nM.

Crystal structures of nonsteroidal AR ligands in different receptors have provided major insight into structure-based drug design. The most effective R-bicalutamide derived pan-antagonist possessed a substitution off the amine linkage. These studies suggest that replacing the sulfonyl linkage of bicalutamide with a substituted amine may provide feasible template for the development of pan-antagonists for the AR. With further knowledge of how these molecules bind in the AR(WT), AR(W741L) and AR(T877A), more potent and efficacious AR pan-antagonists could be developed and would be a major breakthrough in the treatment of prostate cancer.

4.4. Acknowledgements
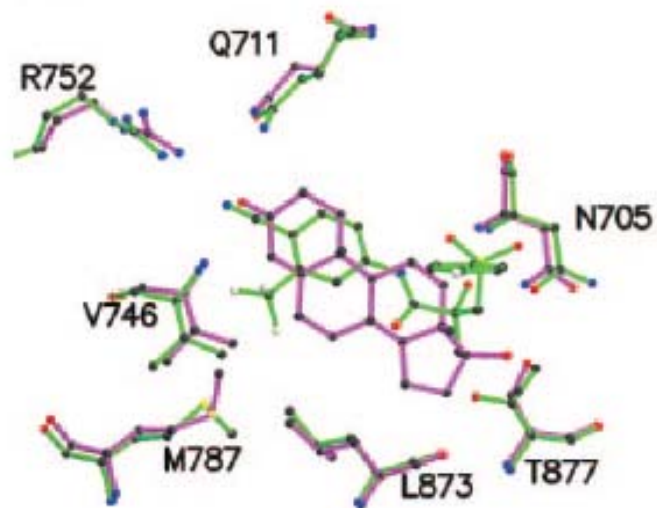
Figure 4.1. Overlay of the R-bicalutamide-W741L Complex (green) and DHT-WT Complex (magenta) – Overview of the Steroidal Plane (67).
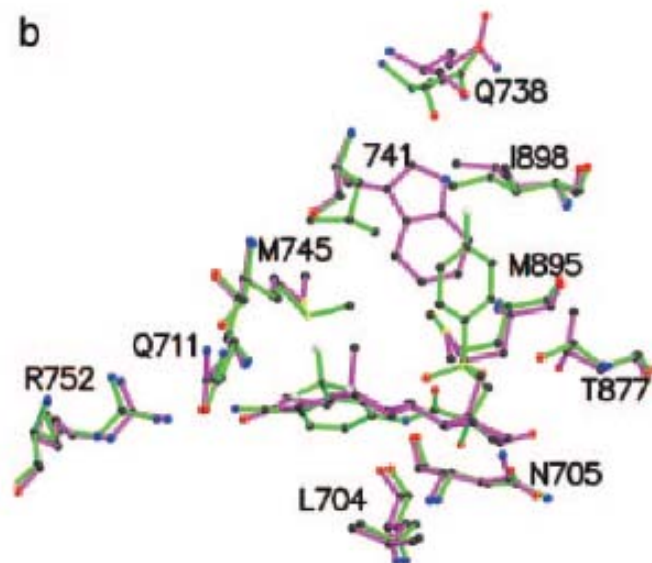
Figure 4.2. Overlay of the R-bicalutamide-W741L Complex (green) and DHT-WT Complex (magenta) – Side View of the Steroidal Plane (67).
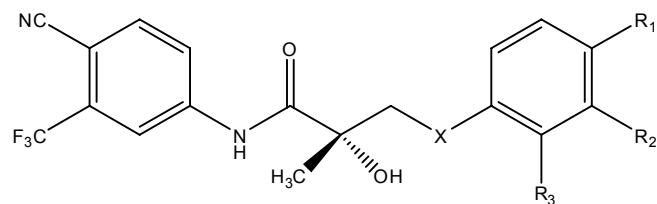
Compound	X	R_1	R_2	R_3	RBA (%)	WT Agonist		WT Antagonist	
						EC_{50} (nM)	E_{max} (%)	IC_{50} (nM)	% inhibition at 1 μM
S-22	O	CN	H	H	5.5 ± 1.8	1.4	140 ± 15.1	NA	NA
R-Bicalutamide	SO_2	F	H	H	0.62 ± 0.06	NA	NA	22.4 ± 6.7	90.9 ± 0.83
A-1	SO_2	CN	H	H	0.62 ± 0.07	NA	NA	743	61.9 ± 10.4
A-2	NH	CN	H	H	0.16 ± 0.01	626	156 ± 213.	119	89.9 ± 0.4
A-3	NH	H	CN	H	0.27 ± 0.01	NA	NA	6.7	93.7 ± 3.1
A-4	NH	H	H	CN	0.20 ± 0.06	>1000	47.6 ± 10.4	151	56.4 ± 3.2
A-5	O	H	CN	H	0.49 ± 0.02	>1000	22.3 ± 1.3	178	60.8 ± 2.6
A-6	O	H	H	CN	0.58 ± 0.07	>1000	43.7 ± 5.8	>1000	37.3 ± 1.9
A-7	O	CN	CN	H	2.4 ± 0.4	104	72.9 ± 8.9	NA	NA
A-8	O	CF_3	H	H	3.0 ± 0.6	6.4	67.0 ± 8.6	>1000	45.6 ± 9.4
A-9	SO_2	CN	-(CH)4-		0.25 ± 0.01	NA	NA	>1000	42.6 ± 8.9
A-10	O	H	-(CH)4-		0.68 ± 0.01	NA	NA	583	71.4 ± 4.1
A-11	NH	CN	-(CH)4-		1.5 ± 0.05	>1000	48.3 ± 7.4	193	63.0 ± 1.2
A-12	O	CN	-(CH)4-		1.9 ± 0.7	340	113 ± 61.3	>1000	43.7 ± 5.7
A-13	NH	CN	Phenyl	H	0.56 ± 0.03	NA	NA	20.5	88.2 ± 1.1
A-14	NH	CN	H	Phenyl	0.65 ± 0.06	>1000	22.6 ± 6.4	81.3	92.2 ± 1.0
A-15	O	Phenyl	H	H	0.62 ± 0.02	>1000	20.4 ± 0.7	239	62.8 ± 3.2
A-16	O	H	Phenyl	H	0.53 ± 0.01	NA	NA	>1000	24.0 ± 4.4
A-17	O	H	H	Phenyl	0.38 ± 0.02	NA	NA	898	55.9 ± 2.4
A-18	O	$CH_2(C_6H_5)$	H	H	0.68 ± 0.1	NA	NA	667	78.2 ± 5.9
A-19	O	H	Phenoxy	H	0.36 ± 0.1	NA	NA	>1000	23.4 ± 4.5
A-20	O	H	H	$CH_2(C_6H_5)$	0.52 ± 0.02	NA	NA	>1000	44.8 ± 7.5

Table 4.1. AR(WT) Binding Affinities and Functional Activity of Nonsteroidal AR Ligands

Table 4.1 continued

A-21	NCH$_2$(C$_6$H$_5$)	CN	H	H	ND*	NA	NA	119	92.7 ± 1.8
A-22	N(CH$_2$)$_2$CH$_3$	CN	H	H	1.1 ± 0.1	NA	NA	151	83.3 ± 13.8
A-23	NCH$_3$	CN	H	H	0.39 ± 0.07	NA	NA	209	77.6 ± 4.1

Binding affinities (RBAs) were determined in a radiolabeled competitive assay and expressed relative to DHT (100%). The functional activity of each compound was determined by the ability of each ligand to induce (agonist) or suppress (antagonist) AR(WT)-mediated transcriptional activation in a co-transfection system and expressed as a percentage of that induced by DHT. * The RBA was not able to be determined. NA: Not applicable

image of chemical structure
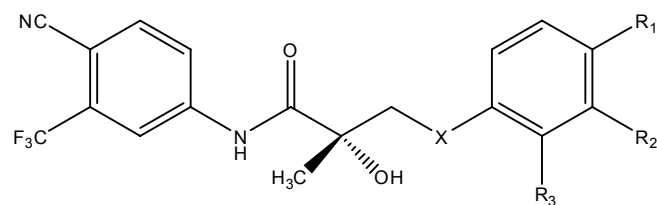
Compound	X	R_1	R_2	R_3	W741L Agonist		W741L Antagonist		T877A Agonist		T877A Antagonist	
					EC_{50} (nM)	E_{max} (%)	IC_{50} (nM)	% inhibition at 1 μM	EC_{50} (nM)	E_{max} (%)	IC_{50} (nM)	% inhibition at 1 μM
R-Bicalutamide	SO_2	F	H	H	1.1 ± 3.4	273 ± 37.9	NA	NA	NA	NA	229	73.7 ±7.4
A-1	SO_2	CN	H	H	>1000	26.8 ± 1.6	NA	NA	>1000	28.8 ± 1.5	>1000	47.2 ± 9.7
A-2	NH	CN	H	H	>1000	24.8 ± 7.2	>1000	20.9 ± 9.1	47.0	122 ± 26.4	NA	NA
A-3	NH	H	CN	H	>1000	29.8 ± 3.9	828	55.5 ± 11.1	>1000	49.3 ± 6.1	204	64.3 ± 4.5
A-4	NH	H	H	CN	72.3	145 ± 166	NA	NA	34.3	63.6 ± 6.8	>1000	28.9 ± 22.9
A-5	O	H	CN	H	667	76.1 ± 22.7	>1000	15.9 ± 5.3	340	96.8 ± 63.9	>1000	49.6 ± 16.4
A-6	O	H	H	CN	>1000	140 ± 427	NA	NA	3.4	102 ± 3.2	NA	NA
A-8	O	CF_3	H	H	2.6	85.1 ± 8.0	NA	NA	1.0	80.7 ± 5.1	NA	NA
A-9	SO_2	CN	-(CH)4-		NA	NA	>1000	14.5 ± 4.3	>1000	45.6 ± 31.6	604	74.2 ± 0.9
A-10	O	H	-(CH)4-		209	58.9 ± 1.3	NA	NA	>1000	36.2 ± 4.0	NA	NA
A-11	NH	CN	-(CH)4-		2.4	93.1 ± 10.8	NA	NA	3.4	56.1 ± 9.9	784.4	60.5 ± 7.8
A-12	O	CN	-(CH)4-		15.3	110 ± 6.2	NA	NA	18.9	85.0 ± 12.6	NA	NA
A-13	NH	CN	Phenyl	H	>1000	26.8 ± 1.6	>1000	48.3 ± 4.7	>1000	20.6 ± 3.6	79.1	85.6 ± 2.0
A-14	NH	CN	H	Phenyl	1.9	76.7 ± 15.1	305	63.8 ± 13.8	>1000	18.6 ± 0.1	34.3	94.0 ± 0.7
A-15	O	Phenyl	H	H	>1000	33.1 ± 2.2	851	54.2 ± 6.5	>1000	40.7 ± 6.0	221	72.4 ± 6.1

Table 4.2. Functional Activity of Nonsteroidal AR(WT) Antagonists in AR(W741L) and AR(T877A)

Table 4.2 continued

A-21	NCH$_2$(C$_6$H$_5$)	CN	H	H	>1000	26.1 ± 1.7	>1000	47.6 ± 10.0	>1000	17.4 ± 5.4	470	74.8 ± 8.7
A-22	N(CH$_2$)$_2$CH$_3$	CN	H	H	NA	NA	151	81.8 ± 10.1	>1000	20.0 ± 2.3	80.6	70.9 ± 6.0
A-23	NCH$_3$	CN	H	H	NA	NA	260	69.6 ± 4.5	1000	52.5 ± 6.3	245.8	64.3 ± 12.9

The functional activity of each compound was determined by the ability of each ligand to induce (agonist) or suppress (antagonist) AR(W741L)- and AR(T877A) mediated transcriptional activation in a co-transfection system and expressed as a percentage of that induced by DHT. NA: Not applicable.
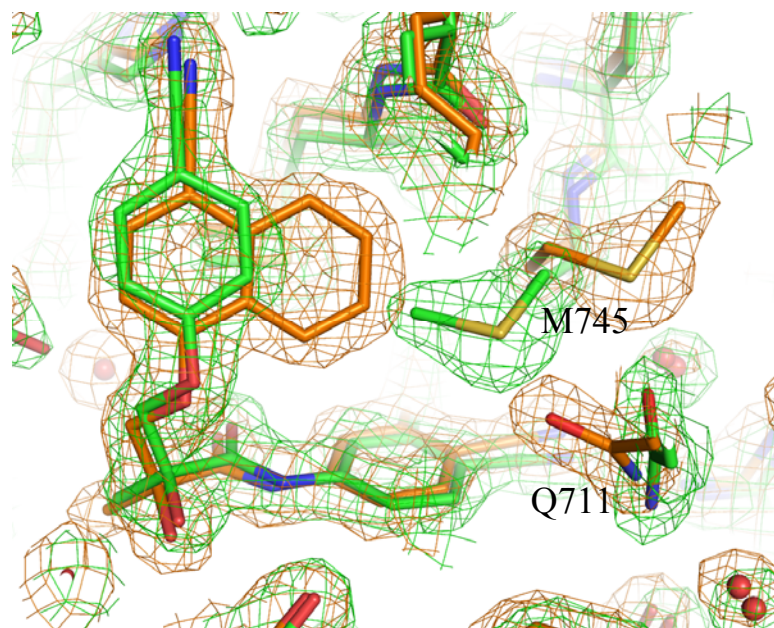
Figure 4.3. Overlaid X-ray Structures of S-22/AR(WT) Complex (green) and A-12 (orange) Co-crystallized with AR(T877A).

The orientation of A-12 is closely overlaid with S-22 and the distal naphthyl ring extends directly away from helix 12 towards M745.
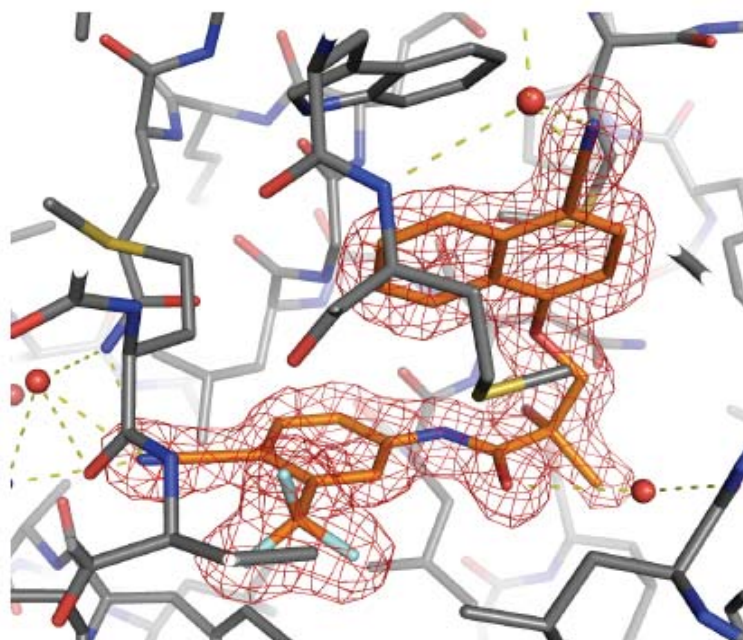
Figure 4.4. X-ray Structure of A-12 Co-crystallized with AR(T877A)

There is an intermolecular π-π interaction between the naphthyl ring of A-12 and the Trp 741 indole ring.

Chapter 5

Effects of SARMs on Dexamethasone-Induced and Hypogonadism-Induced Muscle Atrophy

5.1.   Introduction

Muscle atrophy is a debilitating condition that may result from burns (69), sepsis (70), aging (71), disuse (72), cancer (73), AIDS (74), as well as long-term glucocorticoid administration for the treatment of rheumatoid arthritis (75) and asthma (76). Muscle atrophy often reduces quality of life and prolongs the recovery of these patients. Skeletal muscle catabolism in all of these disparate conditions is the consequence of decreased rates of protein synthesis and accelerated rates of protein degradation. The muscle specific ubiquitin ligases muscle atrophy F-box (*MAFbx* or *atrogin-1*) and muscle ring finger1 (*MuRF1*; (160-165)) that target muscle specific proteins for degradation by the proteasome are upregulated and represent two of the most sensitive genes affected by muscle atrophy (165, 166).

Hypertrophy is in part mediated by insulin-like growth factor 1 (IGF-1) *via* stimulation of the phosphatidylinositol-3 kinase (PI3K)/Akt pathway. *In vivo*, load-induced hypertrophy increases the expression of IGF-1 and stimulates this pathway (167). In transgenic mice, over-expression of IGF-1 and a constitutively active form of Akt are both sufficient to induce hypertrophy in skeletal muscle (168-170). Likewise, addition of IGF-1 to myotubes promotes hypertrophy *in vitro* (171).

Downstream targets of Akt include glycogen synthase kinase 3β (GSK3β), the mammalian target of rapamycin (mTOR), p70 ribosomal protein S6 kinase (p70S6K), as well as the forkhead family transcription factor Forkhead box O (FoxO; (172)). FoxO, when phosphorylated by Akt, is inactive and excluded from the nucleus (173). In myotubes, treatment with dexamethasone (DEX) causes dephosphorylation of FoxO and leads to its subsequent translocation to the nucleus resulting in increased expression of *MAFbx* and *MuRF1* (173, 174). Co-treatment with IGF-1 antagonizes the up-regulation, implicating that the PI3K/Akt pathway induces skeletal muscle hypertrophy not only through increased protein synthesis but also through anti-catabolic effects (173-175). Studies confirm that two

forms of FoxO are involved in muscle atrophy; activation of FoxO3 induces atrophy in myotubes (173) and transgenic mice over-expressing FoxO1 have reduced skeletal muscle mass compared to wild-type control (176).

The anabolic effects of the steroids testosterone and nandrolone have been demonstrated under conditions related to aging men (71), long-term glucocorticoid treatment (77, 78), HIV (79), and severe burns (80). Testosterone administration is associated with a dose-dependent increase in lean muscle mass and maximal voluntary strength and a decrease in fat mass. The increase in lean muscle mass results from decreased rates of protein catabolism, re-establishing a balance between protein synthesis and degradation (71, 80). Under conditions of DEX or denervation-induced atrophy, testosterone and nandrolone, respectively, prevented the up-regulation of muscle specific ubiquitin ligases (177, 178). Similar results were reproduced in myotubes (177). These results indicate that anabolic steroids may inhibit muscle atrophy by reducing the rates of protein catabolism by suppressing muscle specific ubiquitin ligases. However, poor pharmacokinetic profiles and lack of tissue selectivity preclude the frequent use of these steroidal androgens.

In castrated male rats, S-23 maximally maintained the levator ani muscle weight at 129% of intact control and showed significant improvements in BMD, lean mass and fat mass in intact animals (123). These are the first studies to examine the effects of a SARM on signaling involved in protein synthesis and degradation in the levator ani muscle that occurs during DEX-induced and castration-dependent atrophy. The effectiveness of S-23, compared to TP, at inhibiting DEX-induced muscle atrophy and regulating genes and proteins involved in the PI3K/Akt pathway (i.e. *MAFbx*, *MuRF1*, FoxO, *IGF-1*) indicate that SARMs may provide a unique and more selective pharmacologic approach to prevent or treat corticosteroid-induced muscle atrophy.

5.2. Materials and Methods

5.2.1 Animals and Treatment

Male Sprague-Dawley rats were purchased from Harlan Bioproducts for Science (Indianapolis, IN). The animals were maintained on a 12 hour light/dark cycle with food and water available *ad libitum*. All animal studies were conducted under the auspices of an animal protocol approved by the Institutional Laboratory Animal Care and Use Committee at the University of Tennessee. Prior to and at the end of treatment, body fat, lean body mass (LBM), fluids and total water were determined by MRI (EchoMRI 4-in-1 Composition Analyzer, Houston, TX). The animals were 5-6 weeks old and weighed 229-238 grams.

Male rats were randomized according to LBM and assigned to one of four groups (n = 5/group). Animals received daily sc injections (200 μL/d) of the compound of interest for 8 days. Each compound was dispersed in vehicle containing 80% Tween 80 (Sigma-Aldrich, St. Louis, MO) and 20% Captex 200 (Abitec, Columbus, OH). Group 1 was the control group and received vehicle alone. Groups 2-4 received 600 μg/kg/day DEX (Sigma-Aldrich). In addition to receiving DEX, groups 3 and 4 were administered 25 mg/kg/day of TP (Sigma-Aldrich) or S-23, respectively. S-23 (123) was synthesized in our laboratories using described methods (125). Chemical purities were confirmed by MS and NMR and determined to be greater than 99%.

Animals were weighed, anesthetized and sacrificed within 24 hours after the last dose. The ventral prostate and seminal vesicles were removed, cleared of extraneous tissue, and weighed. The levator ani, gastrocnemius (gastroc), extensor digitorum longus (EDL) and soleus muscles were removed (gastroc, EDL and soleus from the left hind limb), weighed, and a segment preserved in RNA*later* (Ambion, Austin, TX) for gene expression analysis, and the other portion immediately frozen in dry ice/ethanol (Sigma-Aldrich) for protein expression analysis. All tissue weights were normalized to total body weight and compared. All muscle samples in RNA*later* and those that were immediately frozen were stored at 4° or -80° C, respectively, until further analysis.

An additional group of male Sprague-Dawley rats was ordered from Harlan Bioproducts for Science for the time-course study. Animals in this study were 5-6 weeks old and ranged from 219-234 grams. Rats were randomized according to weight and assigned to appropriate groups (n = 5/group). Animals were orchidectomized *via* scrotal incision under ketamine/xylazine anesthesia 24 hours before drug treatment and received daily sc injections of S-23 (200 μL/day) at a dose rate of 1 mg/day. S-23 was dissolved in vehicle containing DMSO (Sigma Aldrich) /PEG300 (Sigma Aldrich) [10/90 (vol/vol)]. Additional groups of rats (n = 5/group) with or without castration received vehicle only and served as castrate or intact control groups, respectively. Animals were treated for 3, 7, 10, 14, 21 or 28 days. Animals were weighed, anesthetized, and sacrificed within 24 hours after the last dose. The ventral prostate, seminal vesicles, levator ani, gastroc, EDL and soleus muscles were removed (gastroc, EDL and soleus from the left hind limb), cleared of extraneous tissue, weighed, and preserved in RNA*later* for gene expression analysis. All organ weights were normalized to total body weight and compared. Percent changes were determined by comparison to intact animals.

Lastly, a separate group of animals was randomized according to weight (n = 5/group) to compare DEX treatment versus castration on prostate, levator ani and serum testosterone levels. Animals were 5-6 weeks old and weighed 219-231 grams. Animals were either castrated as described above (ORX group) or left intact (intact and DEX groups). Animals then received daily sc injections of vehicle (intact and ORX groups) or 600 ug/kg/day DEX for 8 days. Animals were weighed, anesthetized and serum collected and stored at -20° C until further analysis. The ventral prostate and levator ani muscles were removed, weighed and normalized to total body weight and compared to the vehicle-treated, intact control group.

5.2.2   Serum Testosterone Analysis

Serum testosterone was quantified using a LC/MS/MS method, using deuterium labeled testosterone as an internal standard. The analyses were performed using a quadrupole ion-trap mass spectrometer coupled with an HPLC system and an electrospray ionization source. The samples were prepared by liquid-liquid extraction, using a 3:2 ratio (v:v) of ethyl acetate:hexane. An aliquot of sample (10 μL) was injected into a C18 column (100 x 2.1 mm, 3 μm; Grace Davison Discovery Sciences Alltima HP) at a flow rate of 0.4 mL/min using a gradient mobile phase. Mobile phase A comprised of 90% water, 10% acetonitrile and 0.1% formic acid. Mobile phase B consisted of 90% acetonitrile, 10% water and 0.1% formic acid. The gradient initiated with 30% B at a flow of 0.4 mL/min and the first three minutes was diverted to waste. After eight minutes, the gradient changed to 90% B, then back to 30% six seconds later, and remained there until the end of the total run time of 13 minutes. The lower limit of quantitation for the method was 0.200 ng/mL.

5.2.3   Cell Culture

Myoblasts from the C2C12 mouse skeletal muscle cell line (ATCC, Manassas, VA) were cultured in growth medium consisting of DMEM supplemented with 10% FBS, 100 units/mL penicillin and 100 μg/mL streptomycin (all purchased from Hyclone, Logan, UT) in a humidified atmosphere containing 5% CO_2 at 37° C. Two, independent experiments were performed for both qPCR and Western blotting, and each were performed in triplicate.

5.2.4   Quantitative Real-Time PCR

C2C12 cells were seeded into 6-well plates in growth medium at a density of 1 million cells/well and allowed to recover for 8 hours. Medium was then replaced with

differentiation medium consisting of DMEM supplemented with 2% horse serum (Hyclone). After 24 hours, cells were transduced with 250 virus particles/cell of an androgen receptor adenovirus (Ad-AR; generated by Welgen, Inc., Worcester, MA) and incubated another 24 hours. Cells were treated with the compound of interest and RNA was isolated 24 hours later, using TRIzol Reagent (Invitrogen, Carlsbad, CA) according to the manufacturer's instructions. For muscle sample analysis, 50 mg of tissue was removed from RNA*later*, homogenized using Lysing Matrix D (MP Biomedicals, Solon, OH) and RNA isolated using TRIzol Reagent. Total RNA was determined by absorbance at 260 nm. RNA (1 μg) was reverse transcribed to produce cDNA (High Capacity cDNA Reverse Transcription Kit with RNase Inhibitor; Applied Biosystems, Foster City, CA). Rat and mouse *Fbxo32*, *Trim63*, and *IGF-1*TaqMan® probes and rat *AR* and *GR* probes were used (Applied Biosystems). qPCR was performed (TaqMan® Fast Universal PCR Master Mix; Applied Biosystems) according to the manufacturer's instructions. To control for any variation in reverse transcription or PCR efficiency, glyceraldehyde-3-phosphate dehydrogenase (*GAPDH*) was used as an internal control. The cycle number at which the reaction crossed an arbitrary threshold (C_T) was determined for each gene and analyzed using the $2^{-\Delta\Delta CT}$ method (179). All PCR runs were performed in duplicate.

5.2.5   Western Blotting

C2C12 cells were seeded into 10 cm dishes in growth medium at a density of 2.5 million cells/dish. Differentiation was induced, cells were transduced, and treated as described above. Cells were washed with Dulbecco's Phosphate Buffered Saline (DPBS; Hyclone) and protein was extracted in buffer containing 1 M potassium phosphate, 10 mM sodium molybdate, 50 mM sodium fluoride, 2 mM EDTA, 2 mM ethylene glycol tetraacetic acid (EGTA), 0.05% monothioglycerol, 1 mg/mL leupeptin, 1 mg/mL antipain dihydrochloride, 1 mg/mL aprotinin, 1 mg/mL benzamidine hydrochloride, 1 mg/mL chymostatin, 1 mg/mL pepstatin, 4 M sodium chloride, and 100 mM phenylmethanesulphonylfluoride (PMSF). The samples were subjected to a freeze/thaw cycle and centrifuged. The supernatant was removed and stored at -80° C until analysis. For muscle sample analysis, 50 mg of tissue was homogenized in 750 μL of homogenization buffer using Lysing Matrix D. The samples were subjected to a freeze/thaw cycle, centrifuged, and the supernatant stored at -80° C. Protein concentrations of the supernatant were determined by the Bio-Rad protein assay (Hercules, CA) using bovine serum albumin (BSA; Sigma-Aldrich) as the standard. The protein samples (50 μg per lane) were mixed

with loading buffer, heated for 5 minutes and resolved by SDS-PAGE on 4-20% tris-glycine gradient gels (Invitrogen) then transferred to polyvinylidene difluoride (PVDF) membranes. Membranes were blocked with 5% nonfat dry milk in Tris-buffered saline with Tween 20 (TBST; 50 mM Tris, 150 mM NaCl and 0.1% Tween 20). The primary antibodies were diluted 1:1000 in 5% BSA (phospho-Akt Ser 473, phospho-mTOR Ser 2488, phospho-GSK-3β Ser 9, phospho-p70 S6 Kinase Thr 389, total Akt, and total FoxO3a all from Cell Signaling Technology, Danvers, MA; phospho-FoxO3a S 253 from Abcam Inc, Cambridge, MA; AR PG21 and anti-actin from Upstate, Billerica, MA; GR from Santa Cruz Biotechnology, Inc., Santa Cruz, CA) and the secondary antibodies 1:2000 in 5% nonfat dry milk (horse-radish peroxidase-conjugated antirabbit IgG and antimouse IgG, Cell Signaling Technology). Immunostaining was visualized by enhanced chemiluminenscence (Amersham ECL Plus™ Western Blotting Detection Reagents, Piscataway, NJ) and captured on photographic film. The protein band densities were quantified using TotalLab TL100 (Nonlinear Dynamics, Durham, NC). β-actin was included for loading control.

5.2.6 Statistical Analyses

All statistical analyses were performed using single-factor ANOVA followed by Dunnett's multiple comparison test. Differences in which $p < 0.05$ were considered statistically significant.

5.3.1 Results

5.3.1 Expression of Muscle Hypertrophy and Atrophy Markers in C2C12 Myotubes

The effects of S-23 and TP on DEX-induced atrophy were examined in differentiated C2C12 myotubes expressing the AR. In the absence of AR in untransfected C2C12 cells, androgens failed to regulate the expression of *MAFbx* or *IGF-1* (data not shown). However, in AR transduced C2C12 cells, overnight incubation with DEX induced a 6.5-fold increase in the expression of *MAFbx* mRNA (Figure 5.1). Co-treatment with TP and S-23 partially but significantly inhibited the up-regulation, with near maximal effect observed at 1 nM. DEX treatment also caused a 13-fold decrease in expression of *IGF-1* mRNA, which was significantly inhibited by TP and S-23 at all concentrations ≥ 1 nM (Figure 5.2).

Addition of DEX to C2C12 myotubes significantly reduced phosphorylation of many proteins involved in the PI3K/Akt pathway (Figure 5.3). Co-treatment with androgens significantly attenuated the effects of DEX on phosphorylation of Akt, GSK3-β, p70S6K, mTOR, FoxO3a and FoxO1. Quantification of band densities revealed significant differences

89

observed in the phosphorylation of Akt at 0.1 and 1 nM for S-23 and TP, respectively (Figure 5.4). Additionally, TP and S-23 increased phosphorylation of FoxO3a above that observed for vehicle control at all concentrations (Figure 5.5).

5.3.2   Dexamethasone-Induced Muscle Atrophy

DEX administration (600 µg/kg/day) significantly reduced the total BW of intact male rats (Figure 5.6A). Co-treatment with 25 mg/kg/day TP or S-23 partially attenuated the effects of DEX on BW. However, the weights were still significantly different from vehicle control. DEX treatment also caused a 5% reduction in LBM after 8 days (Figure 5.6B). S-23 significantly inhibited the loss of LBM with no significant differences observed versus vehicle control, while TP only partially attenuated this loss. DEX also significantly reduced the size of the prostate and seminal vesicles (Figure 5.5.7A and B). Co-administration with TP or S-23 increased the weights of these tissues above that observed for vehicle control (Figure 5.7A and B), with TP significantly increasing the seminal vesicles compared to S-23 ($p < 0.01$). A variety of muscles were also excised to evaluate their response to glucocorticoid and androgen treatment. The levator ani, a highly androgen responsive fast-twitch muscle, decreased by 52% upon DEX administration (Figure 5.8A). TP and S-23 completely inhibited this reduction, maintaining the weight similar to that observed for intact control. The gastrocnemius, a muscle comprised mostly of fast-twitch fibers (94%; (180)), decreased by 37% in response to DEX administration. However, contrary to previously reported data (177), TP and S-23 did not attenuate the effects of DEX on this muscle (Figure 5.8B). The EDL, another fast-twitch muscle, also diminished in size by 34% upon exposure to DEX, with no inhibition observed upon TP or S-23 administration (Figure 5.8C). DEX also caused a reduction in the size of the soleus muscle, a slow-twitch muscle, which was attenuated by S-23, but not TP (Figure 5.8D).

5.3.3   Expression of AR and GR in Muscle

The soleus muscle expresses more *GR* than the other muscles, followed by the gastrocnemius, EDL and the levator ani expressing *GR* the least (Figure 5.9A). A similar trend was observed in protein with the soleus expressing 1.1, 1.5 and 2.6-fold more than the gastrocnemius, EDL, and levator ani muscles, respectively (Figure 5.9B and C). Conversely, the levator ani muscle expresses 5.5, 7.2 and 2.9-fold more *AR* mRNA than the gastrocnemius, EDL and soleus muscles, respectively (Figure 5.10A). A similar trend was also observed with protein levels (Figure 5.10B) and when quantified, the levator ani

expresses 1.9, 1.6 and 6.6-fold more AR than the gastrocnemius, soleus, and EDL muscles, respectively (Fig. 5.10C).

5.3.4   Effects of S-23 and TP on Gene and Protein Expression in Muscle of Intact Rats

Administration of DEX to intact animals resulted in up-regulation of *MAFbx* mRNA in the levator ani, gastrocnemius, EDL and soleus, with the greatest effect observed in the levator ani muscle (60-fold change; Figure 5.11). Co-administration with androgens completely inhibited this up-regulation in the levator ani. In the gastrocnemius, EDL and soleus, the up-regulation of *MAFbx* was slightly attenuated by TP, but S-23 was more effective at inhibiting the up-regulation of *MAFbx* in the gastrocnemius and soleus muscles ($p < 0.05$). A similar trend was observed for *MuRF1*, with a 25-fold increase in mRNA expression in the levator ani, which was completely blocked by TP and S-23 administration. S-23 was statistically more effective than TP at inhibiting *MuRF1* in the soleus ($p < 0.05$, Figure 5.12). DEX treatment decreased the levels of *IGF-1* in the gastrocnemius, EDL, and soleus by 3, 6.5 and 5.5-fold, respectively (Figure 5.13). Although *IGF-1* expression did not decrease in the levator ani, TP and S-23 caused a small but significant increase in expression of *IGF-1* in this tissue. The same trend was observed in other muscles.

Proteins upstream of *MAFbx* and *MuRF1* in the PI3K/Akt pathway, phosphorylated Akt, GSK3β, p70S6K and FoxO3a, decreased in the levator ani muscle upon DEX exposure (Figure 5.14). As was observed in C2C12 myotubes, co-treatment with TP and S-23 maintained phosphorylated levels of GSK3β, p70S6K and Akt (Figures 5.15A). Down-regulation of phosphorylated FoxO3a was attenuated by TP and S-23 (Figure 5.15B).

5.3.5   Hypogonadism-Induced Muscle Atrophy

Castration resulted in an immediate reduction in size of androgen dependent tissues. After just 3 days, the prostate and levator ani muscle reduce to 67 and 79% of intact control, respectively (Figures 5.16B and C). Both tissues continue to decrease in size and reach nadir by 14 days, with sizes of the prostate and levator ani leveling off around 15 and 45% of that observed in intact control, respectively. Conversely, when S-23 is administered to ORX animals, the prostate and levator ani are both maintained, and significant increases are observed through day 28 (Figures 5.16B and C). Castration induces a 40-fold increase in *MAFbx* mRNA expression at 3 days, but drops off 14 days post castration (Figure 5.17A). Administration of S-23 inhibits this up-regulation at 3, 7 and 10 days, but no change is

91

observed after 14 days (Figure 5.17B). Additionally, castration induces a down-regulation in expression of *IGF-1* (Figure 5.18A), which is also attenuated by S-23 (Figure 5.18B).

5.3.6   Comparison of DEX and ORX on BW, Androgen-Dependent Tissues and Serum Testosterone

Significant reductions in body, prostate and levator ani weights were observed after 8 days of DEX administration or castration (Table 5.1). Serum testosterone concentrations measured 3.6 ng/mL in vehicle-treated, intact animals. DEX administration induced no significant change in serum testosterone levels. However, castration reduced serum testosterone levels to below the limit of quantitation (0.20 ng/mL; Table 5.1).

5.4.   Discussion

Corticosteroid-induced protein catabolism predominantly strikes fast-twitch muscle fibers, including the gastrocnemius and levator ani muscles. Atrophy in fast-twitch muscle fibers is highly responsive to androgen administration (81, 181, 182). The Hershberger assay is the method-of-choice for identifying AR-dependent myoanabolic tissue selectivity (183). Our laboratory and many others have shown that the levator ani muscle of rats rapidly atrophies following castration and quickly hypertrophies upon exogenous administration of an anabolic agent (32, 183, 184). Exogenously administered testosterone promotes the growth of anabolic (i.e. muscle) and androgenic (i.e. prostate and seminal vesicles) tissues while SARMs are selectively anabolic. Studies have demonstrated the beneficial effects of testosterone in the DEX-induced animal model of muscle atrophy and signaling effects in the PI3K/Akt pathway (177, 185, 186). In this model, most studies have reported the effects of testosterone on the gastrocnemius muscle (177, 185, 186). The present study provides information regarding the comparative effects of testosterone and a SARM on muscle atrophy and hypertrophy signaling pathways after corticosteroid administration or castration for not only the gastrocnemius, but also the levator ani, extensor digitorum longus, and soleus muscles.

IGF-1 mRNA expression decreased in response to DEX treatment, both *in vitro* and *in vivo* (Figures 5.2 and 5.14), as well as castration (Figure 5.19), corroborating the previous reports that the atrophic effects of glucocorticoids are mediated at least partially *via* suppression of IGF-1 signaling (167-169). This suppression was partially or completely inhibited by TP and S-23. IGF-1 activates the PI3K/Akt pathway and downstream targets associated with protein synthesis include Akt, mTOR, GSK3β, and p70S6K. TP and S-23

completely blocked the DEX-dependent dephosphorylation of Akt and downstream proteins, both in skeletal muscle cells and *in vivo* in the levator ani muscle (Figure 5.3 and 5.15). These results confirm the anabolic effects of TP and S-23 on protein synthesis downstream of IGF-1.

Akt signaling is also involved in inhibiting protein degradation by phosphorylating FoxO and therefore preventing transcription of *MAFbx* and *MuRF1*, muscle specific ubiquitin ligases. Stitt *et al* demonstrated that phosphorylation of FoxO1 is required for inhibition of muscle atrophy *via* the PI3K/Akt pathway (174). Likewise, Sandri *et al* demonstrated that dephosphorylation of FoxO3 is required to activate *MAFbx* (173). In the present study, administration of DEX resulted in dephosphorylation of FoxO1 and FoxO3 in skeletal muscle cells and in the levator ani muscle (Figures 5.3 and 5.15). However, TP and S-23 significantly promoted phosphorylation of FoxO, thereby inhibiting muscle atrophy. Gene expression analysis revealed that dephosphorylation of FoxO by DEX is likely what caused an increase in expression of *MAFbx* and *MuRF1* mRNA, but is attenuated by co-administration with TP or S-23 (Figures 5.1, 5.12 and 5.13). A co-immunoprecipitation assay was performed to determine if there is a direct interaction between the AR and FoxO3a to explain the ability of TP to maintain protein expression of FoxO3a above that of vehicle control (Figure 5.5). However, the results show that the AR and FoxO3a do not directly interact (data not shown).

Interestingly, the AR ligands did not maintain *IGF-1* or *MAFbx* levels at that of control. However, they did bring the proteins downstream of IGF-1 back to the control levels. This indicates that the final effectors of anabolism, such as Akt, FoxO3A and other downstream proteins, are effectively regulated by TP and S-23. Though earlier studies have revealed that there was no change in the proliferation and differentiation rate of C2C12 cells stably transfected with AR in response to DHT (187), myotube diameter and size should have increased in the present study due to the extent of regulation observed with the downstream proteins.

Administration of DEX significantly decreased body weight, which was partially inhibited by androgen administration (Figure 5.6A). There was a significant loss of lean body mass observed in DEX-treated animals, which was only partially inhibited by TP (Figure 5.6B). However, animals co-treated with S-23 maintained lean body mass similar to that observed in vehicle control. The levator ani, gastrocnemius, EDL and soleus muscles all atrophied in response to DEX administration (Figure 5.8). Addition of S-23 completely prevented reduction in weight of the levator ani and soleus muscles. TP only protected

against loss of levator ani muscle weight. Minimal effects were observed in the other muscles. Inconsistent with our results, Zhao *et al* reported that testosterone (28 mg/kg/day) completely protected against loss of gastrocnemius muscle weight at both 1 and 7 days with significant inhibition of *MAFbx* expression (177). In the present study, *MAFbx* expression in the gastrocnemius was only slightly down-regulated by S-23 at 8 days (Figure 5.11). Protein expression data revealed that the levator ani expresses significantly more AR than the soleus muscle (Figure 5.10), and may explain why this muscle responded to TP and S-23 administration more than the others in the present study. Interestingly, the levator ani muscle expresses the least amount of GR (Figure 5.9), but atrophied the most in response to glucocorticoid administration. The gastrocnemius and soleus muscles express comparable GR and AR, however, the slow-twitch muscle fibers of the soleus muscle responded to SARM treatment, whereas the gastrocnemius did not. Analysis of AR expression in the levator ani, gastrocnemius, EDL and soleus muscles at the end of the study revealed that there was no significant change in AR expression in DEX-treated animals or castrated animals treated with S-23. However, castration alone significantly increased AR expression in the levator ani, gastrocnemius, and soleus muscles (data not shown). Additionally, previous studies have shown that DEX administration to rats reduces food consumption (188, 189). The animals in the present study were not pair-fed to account for differences in food intake and therefore this may have an indirect effect on muscle mass and gene expression of animals administered DEX, compared to the other groups.

The levator ani muscle starts atrophying immediately after surgical removal of testosterone and plateaus around 14 days (Figure 5.16C). The greatest up-regulation of *MAFbx* expression in castrated, vehicle treated animals occurs between days 3 and 10 (Figure 17A). S-23 showed the most regulation of this gene through 10 days, with no down-regulation observed days 14-28 (Figure 5.17B). This lack of regulation at the later time points is likely related to the muscle no longer atrophying, with minimal up-regulation of *MAFbx* observed in the ORX animals. Conversely, *IGF-1* declines in ORX animals throughout the 4 weeks, but is up-regulated by S-23 with the greatest regulation observed at 28 days (Figure 5.18).

The levator ani muscle atrophies in response to both castration and DEX administration. Stress-induced elevations in plasma glucocorticoid concentrations inhibit secretion of luteinizing hormone (LH) and therefore reduces testosterone concentrations *in vivo* (190). Studies have also shown that glucocorticoids have a direct inhibitory effect on testicular steroidogenesis (191-193). In humans, significant reductions in circulating

94

testosterone result from DEX administration, as well as *IGF-1* mRNA (194). Yin *et al* reported serum testosterone concentrations that were statistically significant between animals administered testosterone and testosterone combined with DEX, compared to both control and DEX-treated animals (186). In the present study, serum testosterone concentrations reduced by > 95% and the levator ani muscle weight decreased by 28%, 5 days post-castration (Table 1). Due to variability of the data, there was no reduction in serum testosterone induced by DEX in the present study; however, the weight of the levator ani muscle decreased by 17%. The highly androgen responsive levator ani muscle decreased in size in response to both DEX administration and castration possibly due to the reduction in circulating testosterone. This effect may contribute to the myopathy that occurs with glucocorticoid administration.

The mechanisms underlying DEX-induced atrophy appear to be different than castration-induced atrophy. Loss of *IGF-1* in glucocorticoid-induced muscle atrophy does not appear to be as important in levator ani muscle as in the other muscles (Figure 5.13). In glucocorticoid-induced muscle atrophy, expression of *IGF-1* in the levator ani did not decline; however, there was a significant reduction observed in the other muscles. Additionally, the levator ani muscle atrophied the most and displayed the greatest up-regulation of *MAFbx* and *MuRF1* compared to the other muscles (Figures 5.11 and 5.12). The inability of the gastrocnemius, EDL and soleus muscles to maintain *IGF-1* might account for lack of changes in size since the levator ani was able to maintain both *IGF-1* levels and size. In castration-induced atrophy, *IGF-1* mRNA expression declined throughout the 28 day period in the levator ani muscle (Figure 5.18A) and was up-regulated following SARM administration (Figure 5.18B). However, the levator ani muscle also displayed the greatest up-regulation of *MAFbx* compared to the other muscles (data not shown). Our studies suggest that levator ani atrophy caused by hypogonadism (i.e., castration) may be the result of loss of *IGF-1* stimulation, while that caused by glucocorticoid treatment relies almost solely on up-regulation of *MAFbx* and *MuRF1*. Though, the gene expression analyses establish this possibility, the direct correlation that the alteration in these pathways result in muscle loss is lacking. This could be established only using the knockout or transgenic animal models. Studies are ongoing in our laboratories to elucidate the differences in these two mechanisms of muscle atrophy and their response to TP and SARM treatment.

Previous studies have demonstrated that testosterone administration inhibits muscle atrophy by increasing net protein synthesis and reutilizing intracellular amino acids in skeletal muscle (80, 195, 196). Though we have demonstrated that AR ligands induce the

anabolic- and degrade the catabolic- pathway proteins, studies employing radiolabeled amino acids are needed to demonstrate that S-23 has a direct effect on nascent protein synthesis. Importantly, previous publications positively correlate the IGF-1/Akt pathway to protein synthesis in muscle. Recent publications are bringing clarity on the role of ubiquitination and proteasomal degradation of these anabolic proteins (197, 198). Future experiments with radiolabeled amino acids, cyclohexamide or MG-132 will be helpful to determine the direct effects of AR ligands on the biosynthetic pathways.

The doses of S-23 and TP were chosen to result in equal increases in levator ani weight in the DEX-induced model of muscle atrophy (i.e. a dose that would return the levator ani to the same size as observed in intact control). Although a high dose of S-23 was used in this study to determine its mechanistic effects on muscle atrophy, S-23 maintains the levator ani muscle around intact levels at a dose of 0.1 mg/day in castrated animals, whereas the prostate was maintained at less than 30% of that observed in intact control (123). Conversely, at the same dose, TP is non-selective and maintains the weights of both the levator ani and prostate at 70% of intact control (32). Thus, the tissue-selectivity of S-23, like other SARMs, is dose-dependent.

In summary, S-23 and TP maintained the weight of the levator ani muscle in the dexamethasone model of muscle atrophy. S-23 and TP blocked the DEX-induced dephosphorylation of Akt and other proteins involved in protein synthesis, including FoxO. DEX caused a significant up-regulation in the expression of *MAFbx* and *MuRF1* but TP and S-23 administration blocked this effect by phosphorylating FoxO. S-23 also attenuated the up-regulation of *MAFbx* and *MuRF1* in the gastrocnemius, EDL and soleus muscles. Castration induced rapid myopathy of the levator ani muscle, accompanied by up-regulation of ubiquitin ligases and down-regulation of *IGF-1*. S-23 maintained the levator ani muscle at or above intact levels and significantly decreased expression of *MAFbx* and increased expression of *IGF-1* on days 3-10, with minimal regulation observed 14 days post-castration. Given the observed effects on *IGF-1*, *MAFbx* and *Murf1*, these studies suggest that SARMs and TP may stimulate protein synthesis and inhibit protein degradation *via* the IGF-1/PI3K/Akt signaling pathway. SARMs provide the peripheral stimulus necessary to maintain muscle mass with minimal effects on androgenic tissues and represent a viable treatment option for a variety of clinical conditions including glucocorticoid-induced muscle loss and sarcopenia.
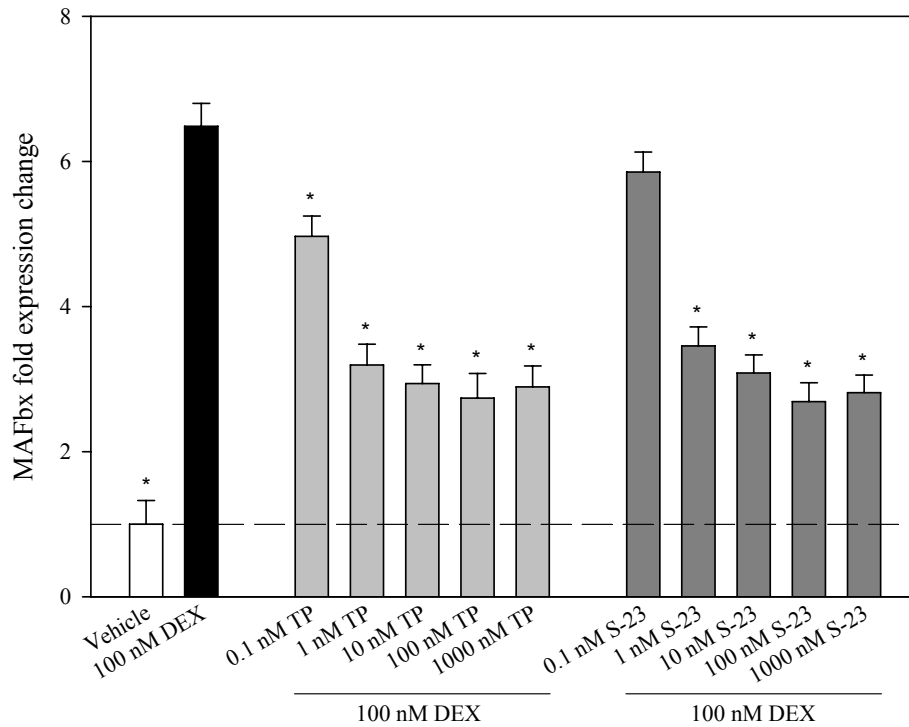
Figure 5.1. *In Vitro* Gene Expression of *MAFbx*

C2C12 cells were transduced with AR, differentiated and myotubes treated as indicated for 24 hours. RNA was isolated, reverse transcribed, and qRT-PCR performed. *GAPDH* was included as internal control. Data was analyzed using the $2^{-\Delta\Delta CT}$ method. Data presented as mean $\pm$ SE (n = 3). * Indicates a significant difference compared to the dexamethasone-treated group, with *p* < 0.05.
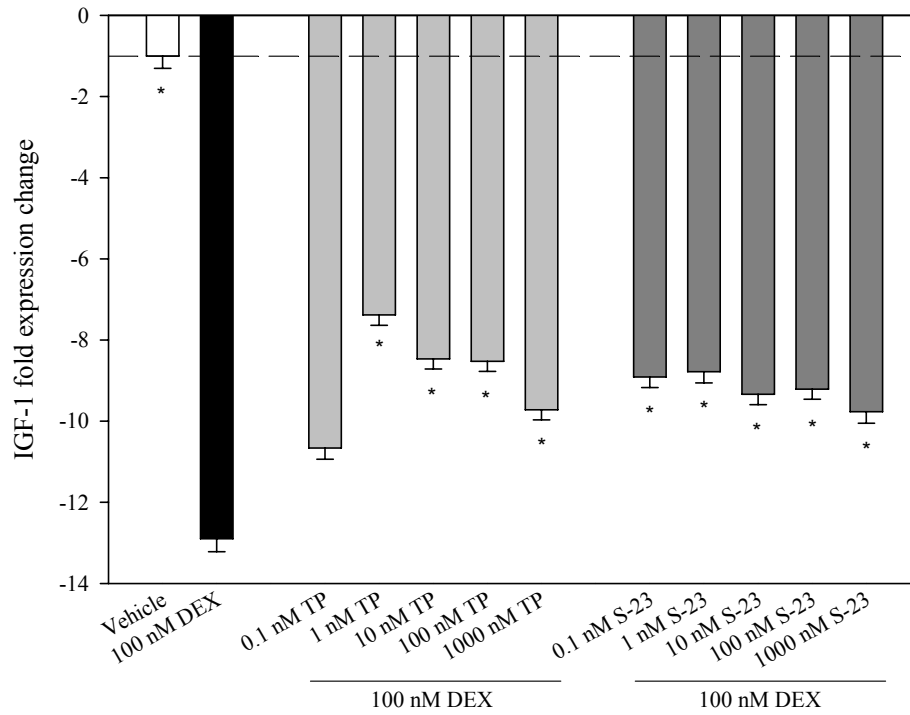
Figure 5.2. *In Vitro* Gene Expression of *IGF-1*

C2C12 cells were transduced with AR, differentiated and myotubes treated as indicated for 24 hours. RNA was isolated, reverse transcribed, and qRT-PCR performed. *GAPDH* was included as internal control. Data was analyzed using the $2^{-\Delta\Delta CT}$ method. Data presented as mean $\pm$ SE (n = 3). * Indicates a significant difference compared to the dexamethasone-treated group, with $p < 0.05$.
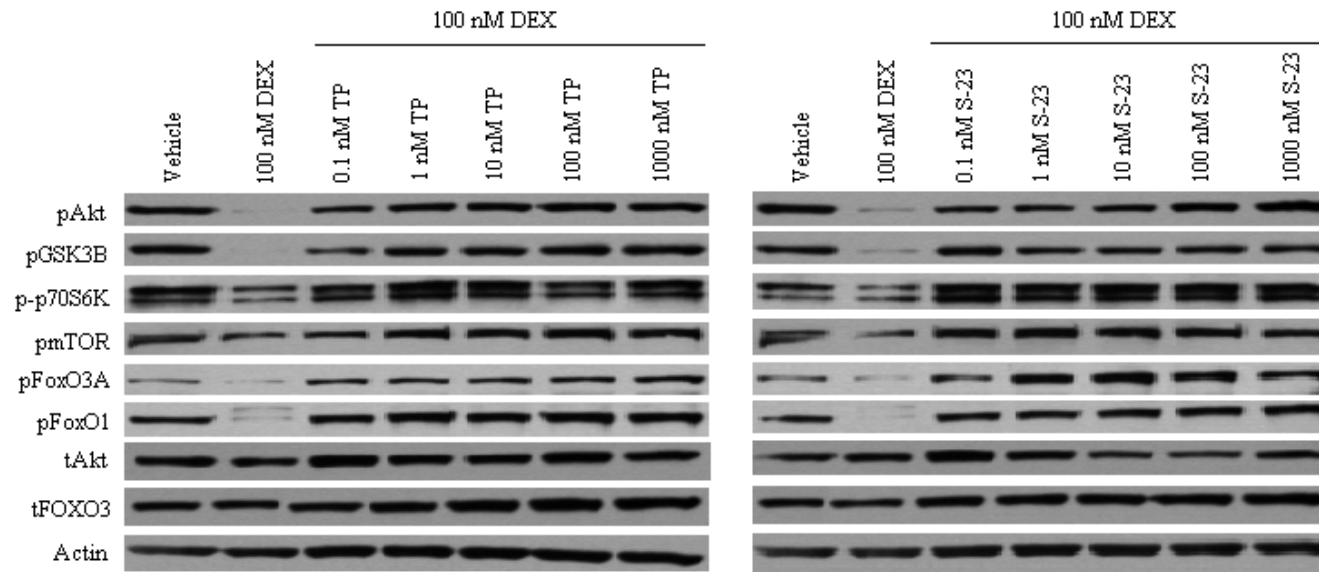
Figure 5.3. *In Vitro* Protein Expression

C2C12 cells were differentiated and myotubes treated as indicated for 24 hours. Protein was extracted, resolved by SDS-PAGE and blotted for the indicated protein. Immunostaining was visualized by enhanced chemiluminenscence, captured on photographic film and band densities quantified. β-actin, total Akt and total FoxO3a included for loading control.

66
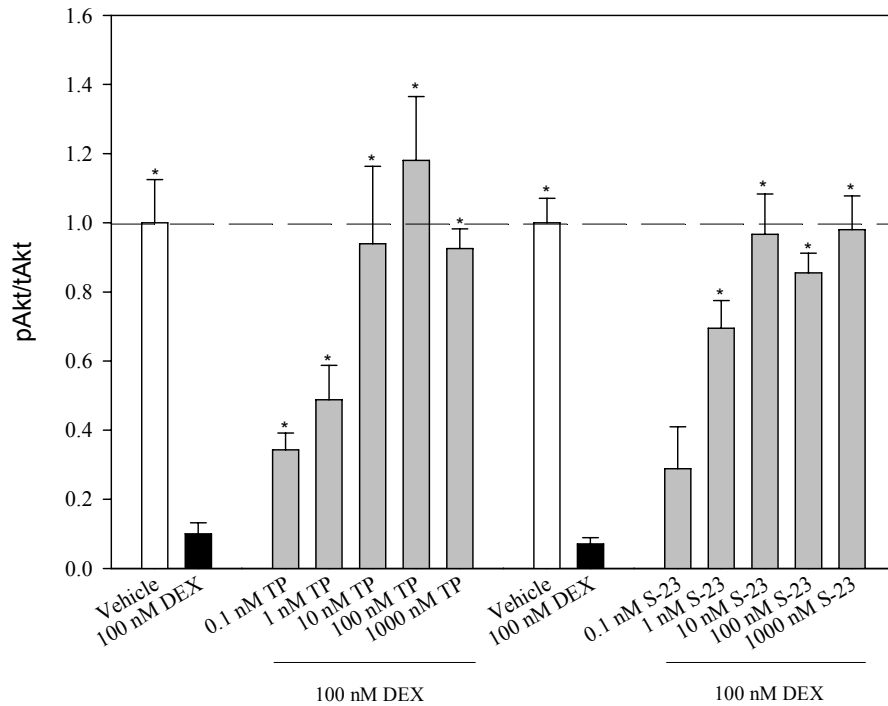
Figure 5.4. Graphical Representation of the Change in Expression of pAkt Compared to Total Akt

C2C12 cells were transduced with the AR, differentiated and myotubes treated as indicated for 24 hours. Protein was extracted, resolved by SDS-PAGE and blotted for pAkt. Immunostaining was visualized by enhanced chemiluminenscence, captured on photographic film and band densities quantified. Total Akt was included for loading control. Data presented as mean ± SE (n = 3). * Indicates a significant difference compared to the dexamethasone-treated group, with $p < 0.05$.
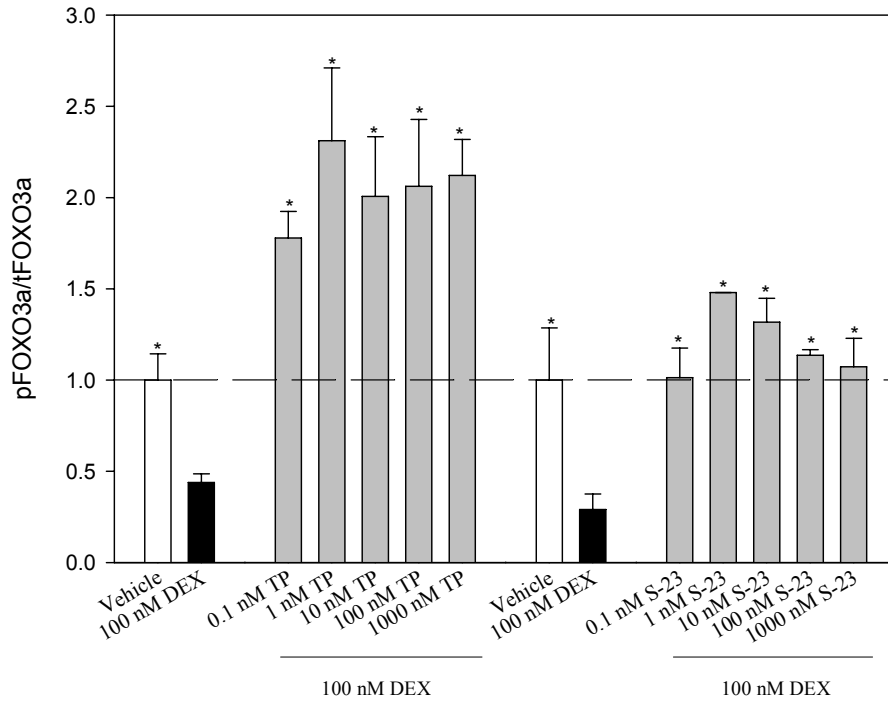
Figure 5.5. Graphical Representation of the Change in Expression of pFoxO3a Compared to Total FoxO3a

C2C12 cells were transduced with the AR, differentiated and myotubes treated as indicated for 24 hours. Protein was extracted, resolved by SDS-PAGE and blotted for pFoxO3a. Immunostaining was visualized by enhanced chemiluminenscence, captured on photographic film and band densities quantified. Total FoxO3a was included for loading control. Data presented as mean ± SE (n = 3). [*] Indicates a significant difference compared to the dexamethasone-treated group, with $p < 0.05$.
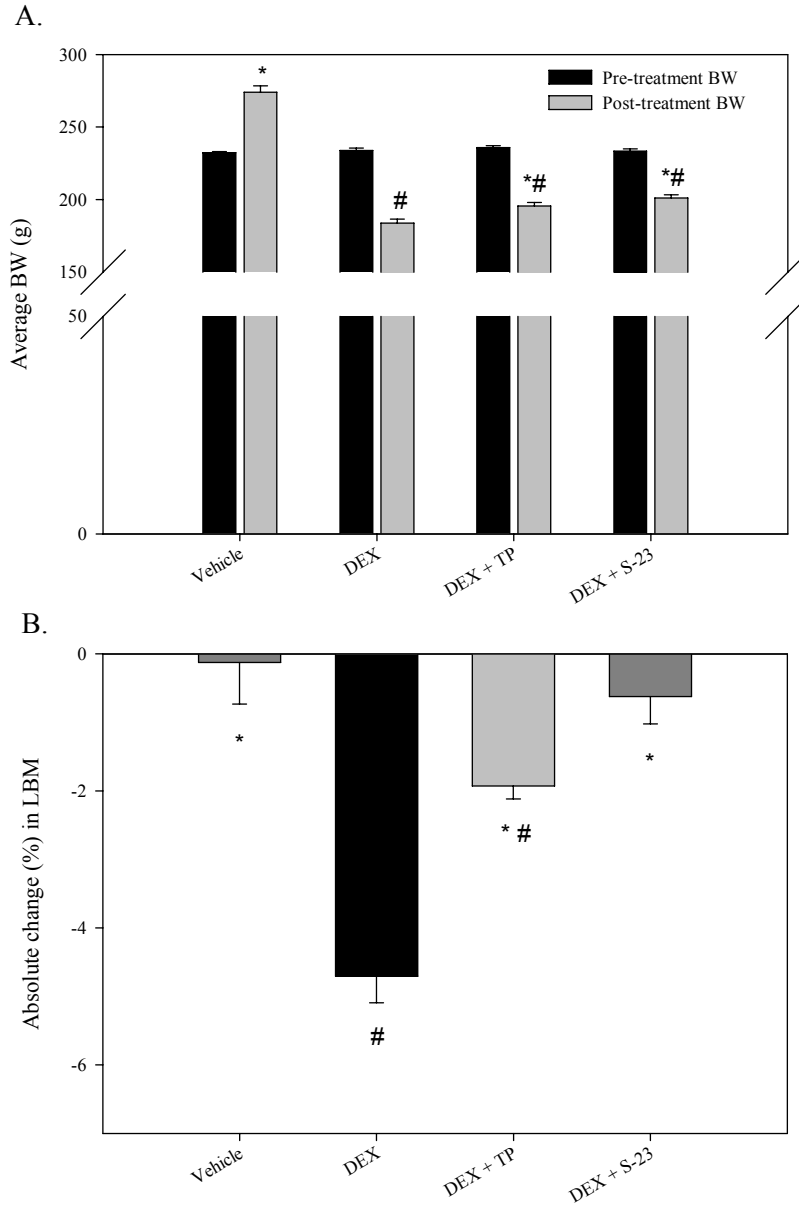
Figure 5.6. Effects of Treatment on Body Weight and Lean Body Mass

Male rats were treated with vehicle, 600 μg/kg/day DEX, DEX plus 25 mg/kg/day TP, or DEX plus 25 mg/kg/day S-23 for 8 days *via* sc injection. Rats were scanned by MRI, weighed, anesthetized and sacrificed within 24 hours after the last dose. Data presented as mean ± SE (n = 5). [#]Indicates a significant difference compared with the vehicle-treated control group, with $p < 0.05$; [*] Indicates a significant difference compared to the dexamethasone-treated group, with $p < 0.05$. A. Average body weight. B. Absolute change in lean body mass.

A.

B.
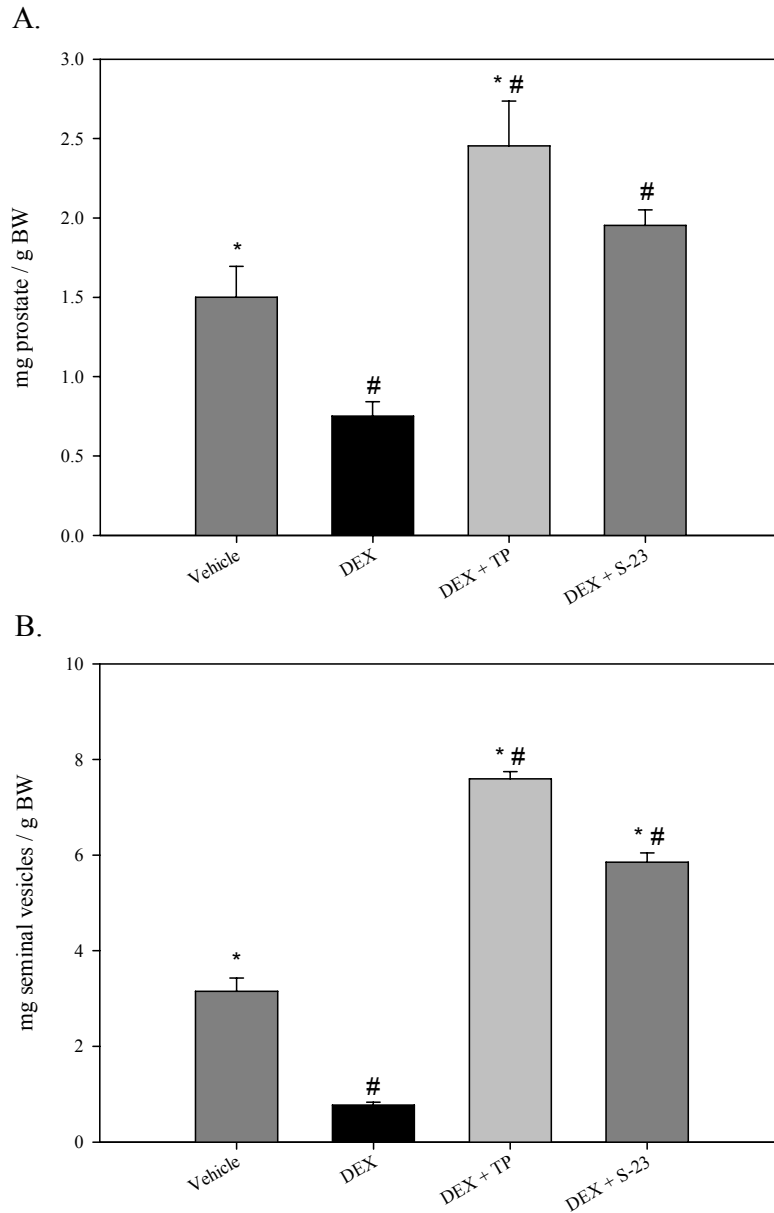
Figure 5.7. Effects of Treatment on Androgenic Tissues

Male rats were treated with vehicle, 600 μg/kg/day DEX, DEX plus 25 mg/kg/day TP, or DEX plus 25 mg/kg/day S-23 for 8 days *via* sc injection. Rats were weighed, anesthetized and sacrificed within 24 hours after the last dose. Tissues were normalized to total body weight and compared. Data presented as mean ± SE (n = 5). [#] Indicates a significant difference compared with the vehicle-treated control group, with $p < 0.05$; [*] Indicates a significant difference compared to the dexamethasone-treated group, with $p < 0.05$. A. Normalized prostate weights. B. Normalized seminal vesicle weights.
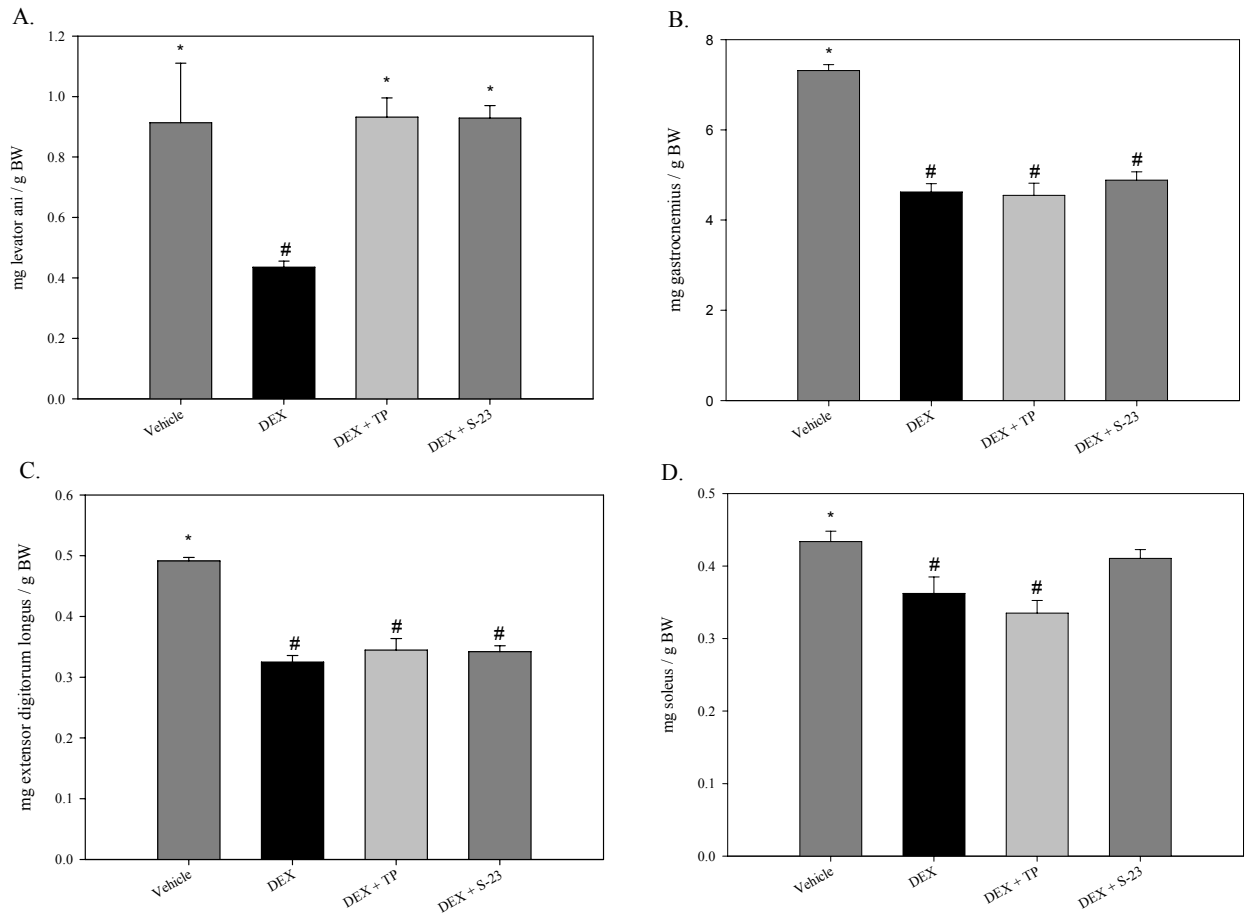
Figure 5.8. Effects of Treatment on Anabolic Tissues

Male rats were treated with vehicle, 600 μg/kg/day DEX, DEX plus 25 mg/kg/day TP, or DEX plus 25 mg/kg/day S-23 for 8 days *via* sc injection. Rats were scanned by MRI, weighed, anesthetized and sacrificed within 24 hours after the last dose. All tissues were normalized to total body weight and compared. Data presented as mean ± SE (n = 5). [#] Indicates a significant difference compared with the vehicle-treated control group, with $p <$ 0.05; [*] Indicates a significant difference compared to the dexamethasone-treated group, with $p < 0.05$. Normalized levator ani weights (A), gastrocnemius, (B), extensor digitorum longus (C), and soleus muscle (D).
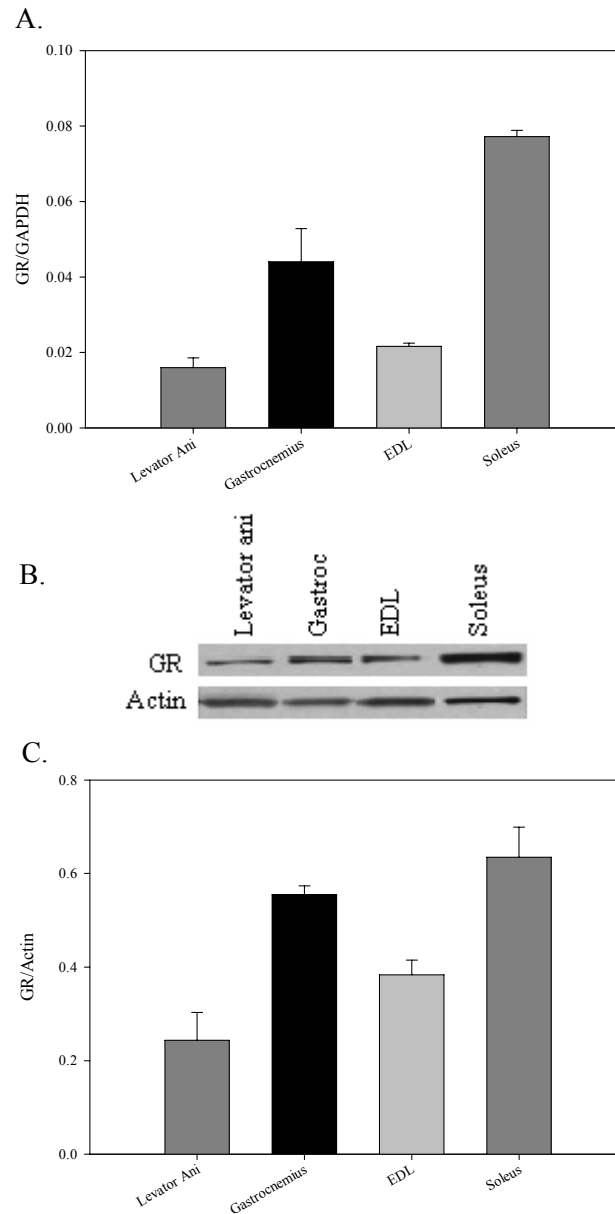
Figure 5.9. Expression of GR in Anabolic Tissues

Male rats were treated with vehicle for 8 days *via* sc injection. A segment of each muscle was preserved in RNA*later* and another portion frozen in dry ice/ethanol. RNA was isolated, reverse transcribed, and qRT-PCR performed. *GAPDH* included as internal control. Data was analyzed using the $2^{-\Delta\Delta CT}$ method. From the portion of the muscle that was flash frozen, protein was extracted, resolved by SDS-PAGE and blotted for the AR or GR. Immunostaining was visualized by enhanced chemiluminenscence, captured on photographic film and band densities quantified. β-actin included for loading control. Data presented as mean ± SE (n = 3). A. mRNA *GR* expression from the levator ani, gastroc, EDL and soleus muscles. B. GR immunoblot in muscle tissues. C. Graphical representation of the expression of GR present in muscles normalized to β-actin.
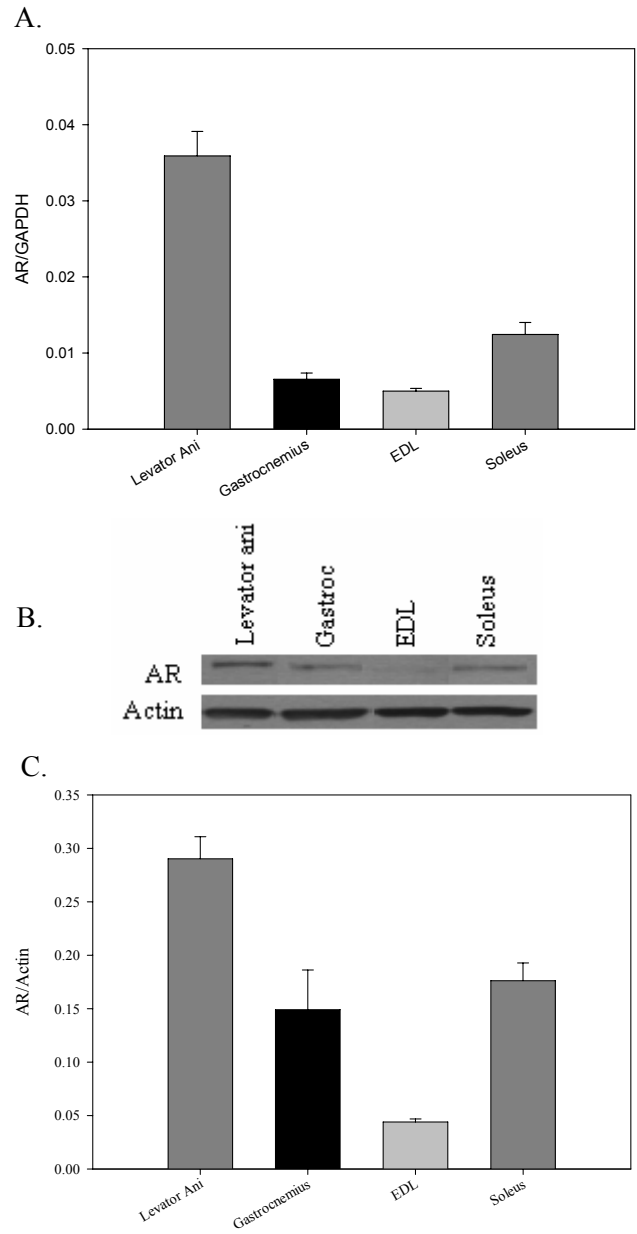
Figure 5.10. Expression AR in Anabolic Tissues

Male rats were treated with vehicle for 8 days *via* sc injection. A segment of each muscle was preserved in RNA*later* and another portion frozen in dry ice/ethanol. RNA was isolated, reverse transcribed, and qRT-PCR performed. *GAPDH* included as internal control. Data was analyzed using the $2^{-\Delta\Delta CT}$ method. From the portion of the muscle that was flash frozen, protein was extracted, resolved by SDS-PAGE and blotted for the AR and GR. Immunostaining was visualized by enhanced chemiluminenscence, captured on photographic film and band densities quantified. β-actin included for loading control. Data presented as mean ± SE (n = 3). A. mRNA *AR* expression from the levator ani, gastroc, EDL and soleus muscles. B. AR immunoblot in muscle tissues. C. Graphical representation of the expression of AR present in muscles normalized to β-actin.
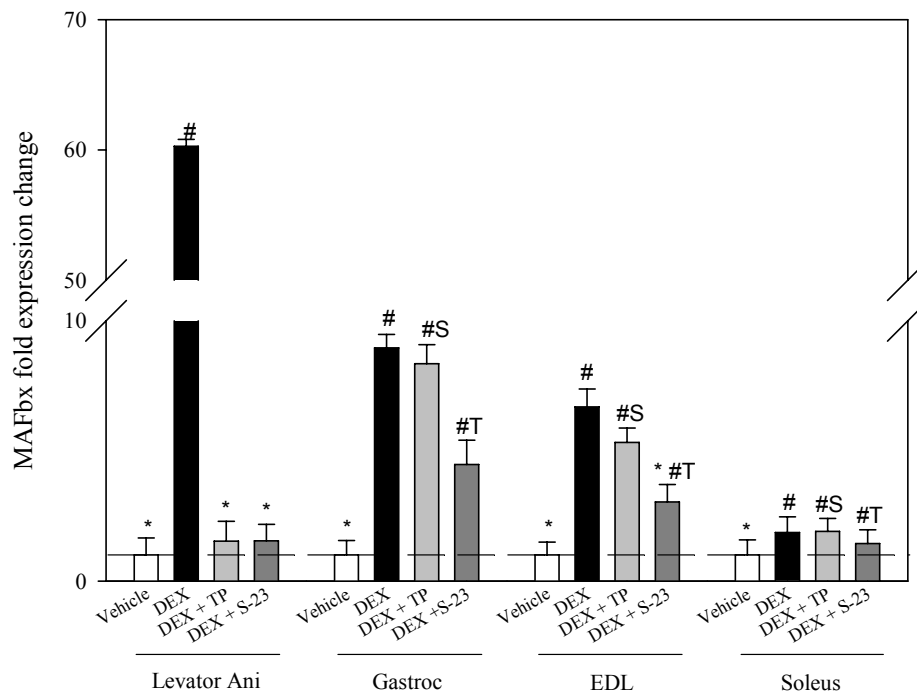
Figure 5.11. Effects of Treatment on *MAFbx* Expression in the Levator Ani, Gastrocnemius, EDL and Soleus Muscles in Intact Male Rats

Male rats were treated with vehicle, 600 μg/kg/day DEX, DEX plus 25 mg/kg/day TP, or DEX plus 25 mg/kg/day S-23 for 8 days *via* sc injection. Rats were scanned by MRI, weighed, anesthetized and sacrificed within 24 hours after the last dose. The levator ani muscles were removed and weighed. RNA was isolated, reverse transcribed, and qRT-PCR performed. *GAPDH* included as internal control. Data was analyzed using the $2^{-\Delta\Delta CT}$ method and presented as mean ± SE (n = 5). # Indicates a significant difference compared with the vehicle-treated control group, with $p < 0.05$; * Indicates a significant difference compared to the dexamethasone-treated group, with $p < 0.05$. S, T Indicates a significant difference compared to the SARM- or TP-treated group, respectively, with $p < 0.05$.

Figure 5.12. Effects of Treatment on *MuRF1* Expression in the Levator Ani, Gastrocnemius, EDL and Soleus Muscles in Intact Male Rats

Male rats were treated with vehicle, 600 μg/kg/day DEX, DEX plus 25 mg/kg/day TP, or DEX plus 25 mg/kg/day S-23 for 8 days *via* sc injection. Rats were scanned by MRI, weighed, anesthetized and sacrificed within 24 hours after the last dose. The levator ani muscles were removed and weighed. RNA was isolated, reverse transcribed, and qRT-PCR performed. *GAPDH* included as internal control. Data was analyzed using the $2^{-\Delta\Delta CT}$ method and presented as mean ± SE (n = 5). [#] Indicates a significant difference compared with the vehicle-treated control group, with $p < 0.05$; [*] Indicates a significant difference compared to the dexamethasone-treated group, with $p < 0.05$. [S, T] Indicates a significant difference compared to the SARM- or TP-treated group, respectively, with $p < 0.05$.

Figure 5.13. Effects of Treatment on *IGF-1* Expression in the Levator Ani, Gastrocnemius, EDL and Soleus Muscles in Intact Male Rats

Male rats were treated with vehicle, 600 μg/kg/day DEX, DEX plus 25 mg/kg/day TP, or DEX plus 25 mg/kg/day S-23 for 8 days *via* sc injection. Rats were scanned by MRI, weighed, anesthetized and sacrificed within 24 hours after the last dose. The levator ani muscles were removed and weighed. RNA was isolated, reverse transcribed, and qRT-PCR performed. *GAPDH* included as internal control. Data was analyzed using the $2^{-\Delta\Delta CT}$ method and presented as mean ± SE (n = 5). $^{\#}$ Indicates a significant difference compared with the vehicle-treated control group, with $p < 0.05$; * Indicates a significant difference compared to the dexamethasone-treated group, with $p < 0.05$. $^{S, T}$ Indicates a significant difference compared to the SARM- or TP-treated group, respectively, with $p < 0.05$.

Figure 5.14. Expression of Hypertrophy and Atrophy Proteins in the Levator Ani of Intact Male Rats

Male rats were treated with vehicle, 600 µg/kg/day DEX, DEX plus 25 mg/kg/day TP, or DEX plus 25 mg/kg/day S-23 for 8 days *via* sc injection. Rats were scanned by MRI, weighed, anesthetized and sacrificed within 24 hours after the last dose. The levator ani muscles were removed and weighed. Protein was extracted, resolved by SDS-PAGE and blotted for the indicated protein. Immunostaining was visualized by enhanced chemiluminenscence and captured on photographic film.
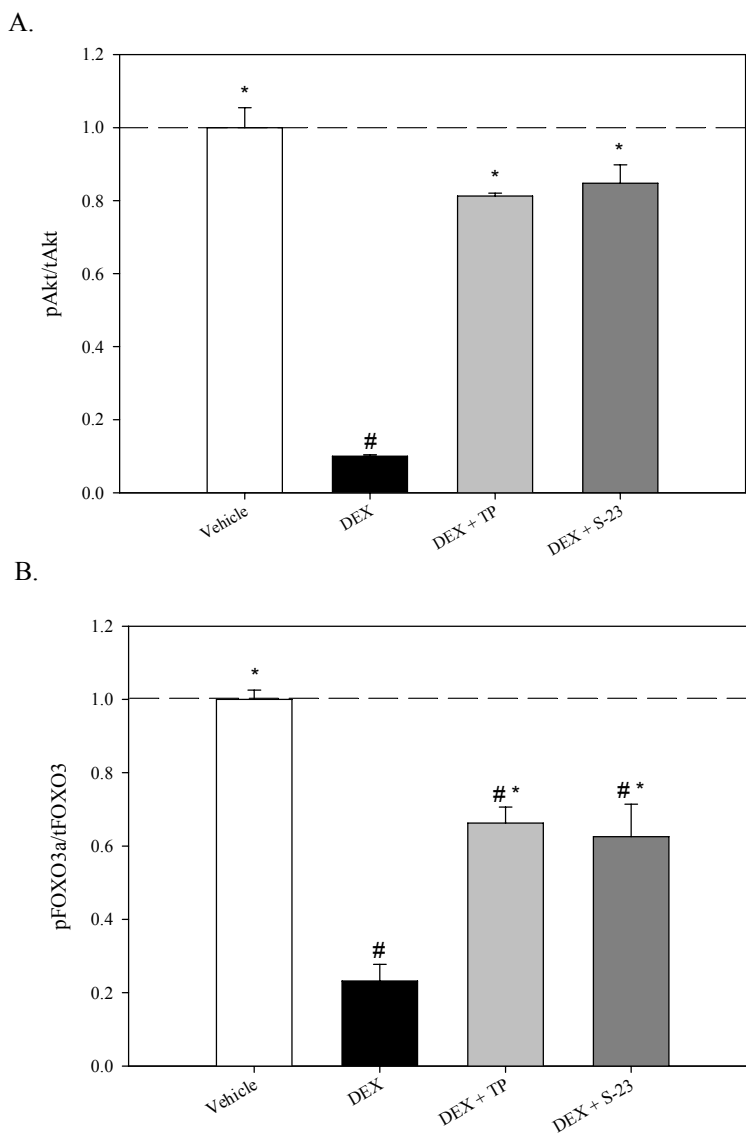
Figure 5.15. Expression of pAkt and pFoxO3a in the Levator Ani of Intact Male Rats

Male rats were treated with vehicle, 600 μg/kg/day DEX, DEX plus 25 mg/kg/day TP, or DEX plus 25 mg/kg/day S-23 for 8 days *via* sc injection. Rats were scanned by MRI, weighed, anesthetized and sacrificed within 24 hours after the last dose. The levator ani muscles were removed and weighed. Protein was extracted, resolved by SDS-PAGE and blotted for pAkt and pFoxO3a. Immunostaining was visualized by enhanced chemiluminenscence, captured on photographic film and band densities quantified. β-actin, total Akt and total FoxO3 included for loading control. Data presented as mean ± SE (n = 3). [#] Indicates a significant difference compared with the vehicle-treated control group, with $p < 0.05$; [*] Indicates a significant difference compared to the dexamethasone-treated group, with $p < 0.05$. Graphical representation of the change in expression of pAkt compared to total Akt (A) and pFoxO3a compared to total FoxO3 (B).
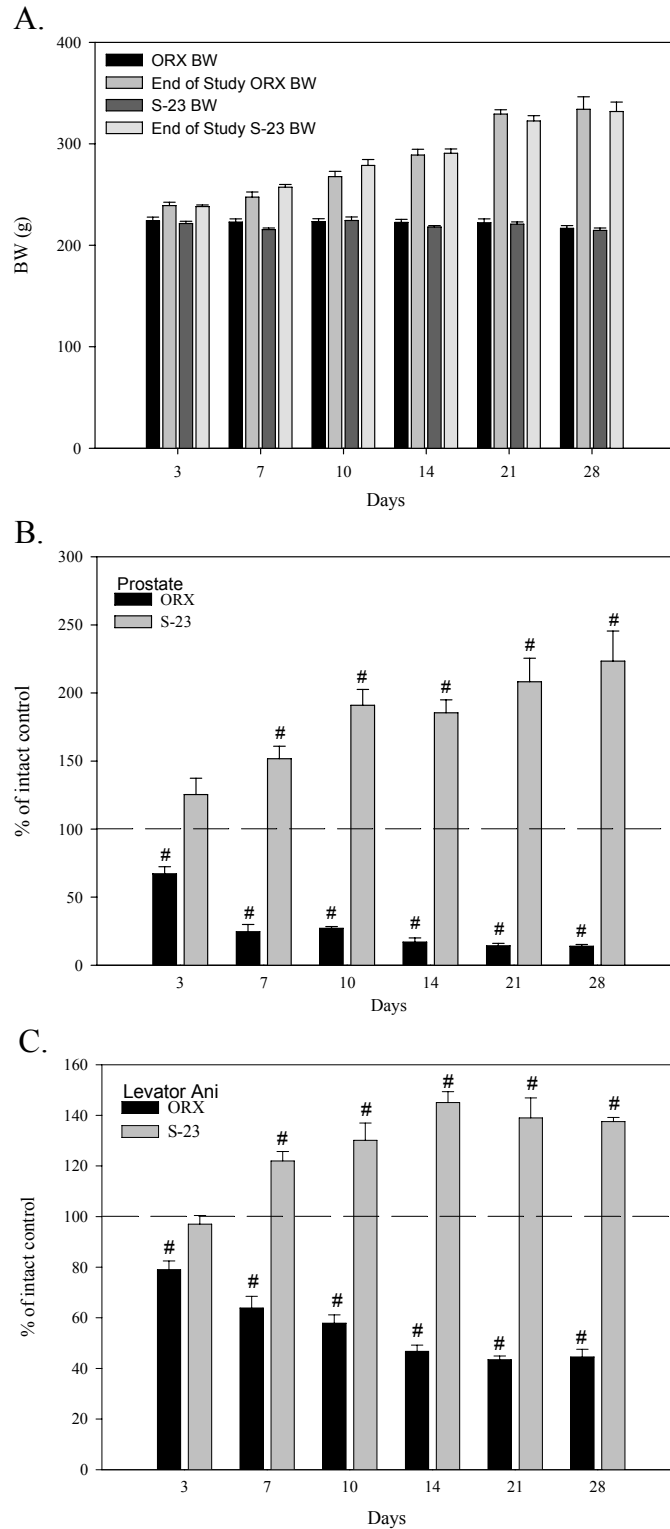
Figure 5.16. Effects of Time and S-23 on Androgenic and Anabolic Tissues in Castrated
Male Rats

Figure 5.16 continued

Male rats were orchidectomized (ORX) *via* scrotal incision under ketamine/xylazine anesthesia 24 hours before drug treatment and received daily sc injections of S-23 at a dose rate of 1 mg/day for 3, 7, 10, 14, 21 or 28 days. Additional groups of animals with or without castration received vehicle only and served as castrate or intact control groups, respectively. Animals were weighed, anesthetized, and sacrificed within 24 hours after the last dose. The ventral prostate, levator ani, gastrocnemius, EDL and soleus were removed and weighed. All tissues were normalized to total body weight and compared. Percent changes were determined by comparison to intact animals. Data presented as mean ± SE (n = 5). [#] Indicates a significant difference compared with the vehicle-treated, intact control group, with $p < 0.05$. A, Body weights of all animal groups before and after treatment. B, Normalized prostate weights of ORX control and S-23-treated animals. C, Normalized levator ani weights of ORX control and S-23-treated animals.
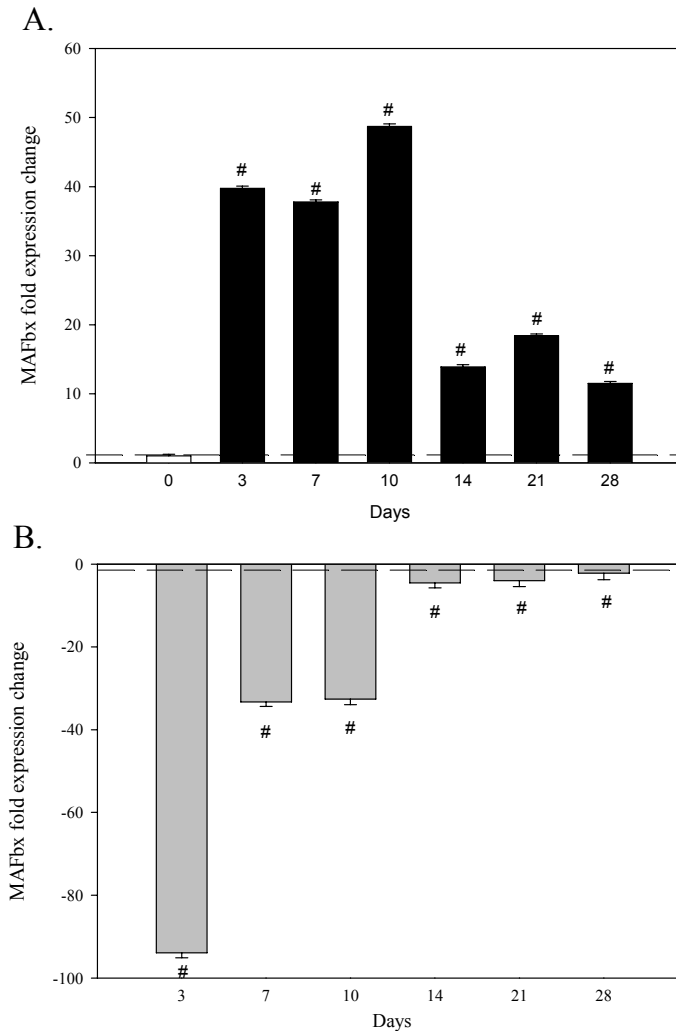
Figure 5.17. Effects of Time and S-23 on *MAFbx* Expression in Castrated Male Rats

Male rats were orchidectomized (ORX) *via* scrotal incision under ketamine/xylazine anesthesia 24 hours before drug treatment and received daily sc injections of S-23 at a dose rate of 1 mg/day for 3, 7, 10, 14, 21 or 28 days. Additional groups of animals with or without castration received vehicle only and served as castrate or intact control groups, respectively. Animals were weighed, anesthetized, and sacrificed within 24 hours after the last dose. The ventral prostate, levator ani, gastrocnemius, EDL and soleus were removed and weighed. A segment of each muscle was preserved in RNA*later*. RNA was isolated, reverse transcribed, and qRT-PCR performed. *GAPDH* was included as internal control. Data was analyzed using the $2^{-\Delta\Delta CT}$ method and presented as mean ± SE (n = 5). Graph A; [#] Indicates a significant difference compared with the vehicle-treated, intact control group, with $p < 0.05$. Graph B; [#] Indicates a significant difference compared with the vehicle-treated, ORX control group on the respective day, with $p < 0.05$. A, Fold expression change of muscle atrophy marker *MAFbx* in ORX animals compared to intact control animals. B, Fold expression change of *MAFbx* in S-23 treated animals compared to ORX at each day.
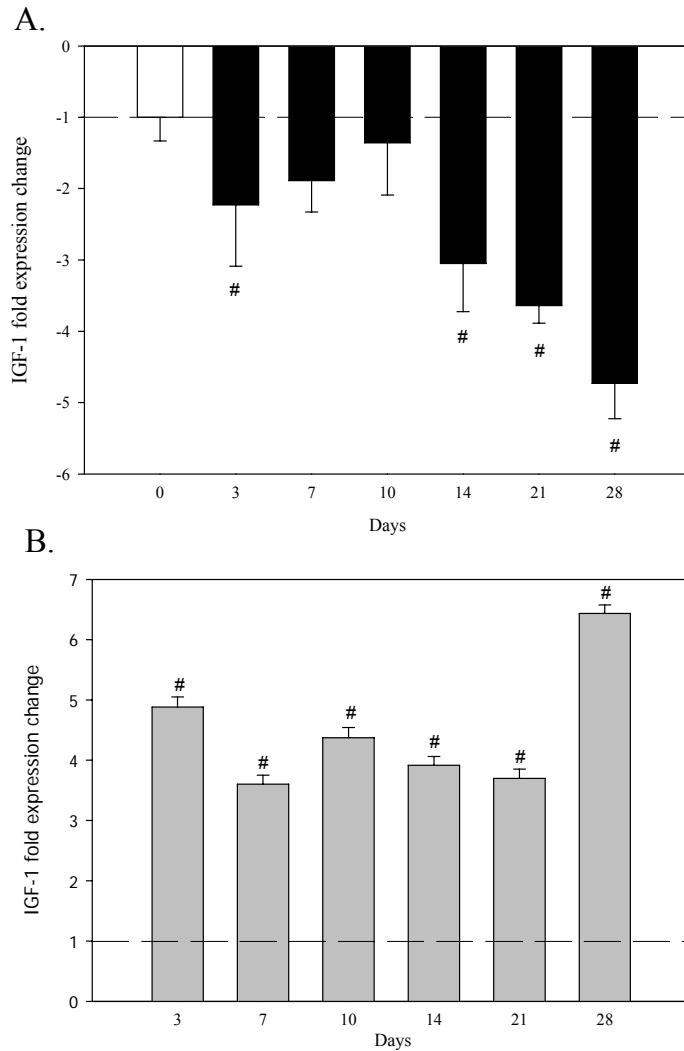
Figure 5.18. Effects of Time and S-23 on *IGF-1* Expression in Castrated Male Rats

Male rats were orchidectomized *via* scrotal incision under ketamine/xylazine anesthesia 24 hours before drug treatment and received daily sc injections of S-23 at a dose rate of 1 mg/day for 3, 7, 10, 14, 21 or 28 days. Additional groups of animals with or without castration received vehicle only and served as castrate or intact control groups, respectively. Animals were weighed, anesthetized, and sacrificed within 24 hours after the last dose. The ventral prostate, levator ani, gastrocnemius, EDL and soleus were removed and weighed. A segment of each muscle was preserved in RNA*later*. RNA was isolated, reverse transcribed, and qRT-PCR performed. *GAPDH* included as internal control. Data was analyzed using the $2^{-\Delta\Delta CT}$ method and presented as mean ± SE (n = 5). Graph A, [#] Indicates a significant difference compared with the vehicle-treated, intact control group, with $p < 0.05$. Graph B; [#] Indicates a significant difference compared with the vehicle-treated, ORX control group on the respective day, with $p < 0.05$. A, Fold expression change of muscle hypertrophy marker *IGF-1* in ORX animals compared to intact control animals. B, Fold expression change of *IGF-1* in S-23 treated animals compared to ORX at each day.

Group	BW (g)	Prostate (mg/g BW)	Levator ani (mg/g BW)	Serum testosterone (ng/mL)
Intact	251 ± 2.7	0.72 ± 0.1	0.76 ± 0.04	3.6 ± 0.3
DEX	$198 \pm 2.2*$	0.56 ± 0.04	$0.63 \pm 0.02*$	2.6 ± 0.7
ORX	$232 \pm 4.9*$	$0.18 \pm 0.05*$	$0.55 \pm 0.04*$	$< 0.20*$

Table 5.1. Effects of DEX and Castration on BW, Prostate, Levator Ani and Serum Testosterone

Animals in the ORX group were castrated on day 0. On days 1-8, animals in the intact and ORX groups received daily sc injections of vehicle and the DEX group received 600 μg/kg/day dexamethasone. Prostate and levator ani muscle weights were measured and normalized to BW. Serum testosterone concentrations were determined by LC/MS. Data are presented as mean ± SE (n=5). *Indicates a significant difference compared with the vehicle-treated, intact control group, with $p < 0.05$.

Chapter 6
Summary and Conclusions

The objectives and conclusions of this dissertation are as follows:

I.   To determine if a SARM (S-23) is an effective and reversible hormonal male contraceptive agent.

   S-23 was identified as a potent and efficacious SARM in castrated male rats with significantly higher anabolic activity than androgenic activity. S-23 also demonstrated high oral bioavailability (96%). In intact male rats, the combination of S-23 and estradiol benzoate (EB) functioned efficiently as a hormonal male contraceptive agent. S-23 in combination with EB effectively suppressed the HPG axis achieving a complete or maximal inhibition of sperm in the testis. A 100% infertility rate was observed at 0.1 mg/day. This effective therapy selectively decreased weights of the prostate, seminal vesicles, testis, and epdidymides, retained muscle weight, percentage of fat and fat-free mass, and increased bone mineral density (BMD). After termination of treatment, serum hormones and mean sperm counts returned to that of control, resulting in 100% pregnancy rates in all treatment groups. These results indicate that the effect of the S-23 and EB combination on spermatogenesis is completely reversible. This is the first study to show that sperm synthesis can be completely inhibited by EB-SARM combination therapy, in which, EB was used to maintain libido without affecting quantitative spermatogenesis. However, given the narrow therapeutic window observed with SARM administration, use of an androgen alone for male contraception may be problematic. However, combination of an orally available SARM (S-23) with an orally available progestin (to suppress LH and thus widen the therapeutic window for SARM action) represents a logical and likely feasible way to achieve oral male contraception.

II.   To determine if a series of arylpropionamide SARMs are effective in maintaining sexual motivation in ovariectomized female rats.

Structural modifications to the *meta-* and *para-* positions of the B-ring of the SARM pharmacophore resulted in a wide range of *in vitro* AR binding affinities (RBAs range from 3.2 to 27%) and functional activities (65-101% of DHT). With the exception of S-23, all of the SARMs tested were prostate sparing and selectively maintained the size of the levator ani muscle in castrated male rats. Most nonsteroidal SARMs improved sexual motivation of OVX female rats in a partner preference paradigm, comparable to testosterone propionate (TP), while maintaining uterine weights at less than 50% of intact control. The observed increase in uterine size following TP and SARM administration is due to growth of the myometrium, the smooth muscle of the uterus, but not the endometrium. SARMs do not significantly cross-react with the estrogen receptor and are non-aromatizable, indicating that androgens play an important role in female libido. Co-administration of an anti-androgen with TP reduced the sexual preference of the female for an intact male, also implying that the AR is involved in female sexual behavior. These studies indicate that it is possible to develop a SARM that selectively maintains sexual motivation without any adverse effects on the endometrium (e.g. S-30). SARMs, with many advantages over traditional steroidal androgen preparations, could be beneficial in the clinical treatment of hypoactive sexual desire disorder.

III.   To determine if AR pan-antagonists can be developed by adding bulk to the B-ring.

A variety of structural modifications were made to the arylpropionamide backbone that resulted in relative binding affinities ranging from 0.25 to 3% and AR(WT) antagonist potency and inhibition peaking at 7 nM and 94%, respectively. We investigated the possibility of increasing bulk on the B-ring to inhibit receptor folding following ligand binding. The amine-linked naphthyl derivative displayed the greatest potency of this substitution although its IC_{50} was only 193 nM, approximately 10-fold less potent than R-bicalutamide. However, potency and efficacy comparable to R-bicalutamide (A-13) was achieved when bulk was introduced through a phenyl ring, which exhibited considerably more flexibility than the naphthyl-substituted compounds. Unfortunately, these molecules did not display any significant antagonist properties in the two mutated ARs. The crystal structure of A-12 in the AR(T877A) mutation showed that the antagonist properties of A-12 in the AR(WT) were not the result of added bulk on the B-ring and the linker must therefore explain the differences in agonist and antagonist activity of these nonsteroidal ligands. Amine-linked molecules were 6-fold less potent in the AR(WT) than R-bicalutamide. This linkage, however, added pan-antagonist activity in the 100 nM range.

These studies suggest that replacing the sulfonyl linkage of bicalutamide with a substituted amine may provide feasible template for the development of pan-antagonists for the AR. Designing molecules that combine the wild-type AR activity of the B-ring *meta*-phenyl group with the mutant AR antagonist activity of the amine-substitution may be a more potent approach to antagonize the wild-type AR and its mutations. With further knowledge of how these molecules bind in the AR(WT), AR(W741L) and AR(T877A), more potent and efficacious AR pan-antagonists could be developed and would be a major breakthrough in the treatment of prostate cancer.

IV.   To determine the mechanism by which SARMs inhibit glucocorticoid- and castration-induced muscle atrophy.

S-23 maintained the weight of the levator ani muscle in the dexamethasone model of muscle atrophy. It also blocked the DEX-induced dephosphorylation of Akt and other proteins involved in protein synthesis, including FoxO. While DEX caused a significant up-regulation in the expression of *MAFbx* and *MuRF1*, administration of S-23 blocked this effect likely by phosphorylating FoxO. S-23 also attenuated the up-regulation of *MAFbx* and *MuRF1* in the gastrocnemius, EDL and soleus muscles. Castration induced rapid myopathy of the levator ani muscle, accompanied by up-regulation of ubiquitin ligases and down-regulation of *IGF-1*. S-23 maintained the levator ani muscle at or above intact levels and significantly decreased expression of *MAFbx* and increased expression of *IGF-1* between days 3 and 10, with minimal regulation observed 14 days post-castration. Our studies suggest that levator ani atrophy caused by hypogonadism (i.e. castration) may be the result of loss of *IGF-1* stimulation, while the atrophy caused by glucocorticoid treatment relies almost solely on up-regulation of *MAFbx* and *MuRF1*. Given the observed effects on *IGF-1*, *MAFbx* and *MuRF1*, these studies suggest that SARMs and TP may stimulate protein synthesis and inhibit protein degradation *via* the IGF-1/PI3K/Akt signaling pathway. However, this observation would be further supported with knowledge of the direct effect of SARMs on protein synthetic and degradation rates. SARMs provide the peripheral stimulus necessary to maintain muscle mass with minimal effects on androgenic tissues and represent a viable treatment option for a variety of clinical conditions including glucocorticoid-induced muscle loss and sarcopenia.

References

1.   **Hiort O** 2002 Androgens and puberty. Best Pract Res Clin Endocrinol Metab 16:31-41

2.   **Mooradian AD, Morley JE, Korenman SG** 1987 Biological actions of androgens. Endocr Rev 8:1-28

3.   **Ganong WF** 2005 The Gonads: Development and Function of the Reproductive System. In: Review of medical Physiology, 22 ed. McGraw-Hill Companies, Inc., New York

4.   **Jenster G, van der Korput HA, van Vroonhoven C, van der Kwast TH, Trapman J, Brinkmann AO** 1991 Domains of the human androgen receptor involved in steroid binding, transcriptional activation, and subcellular localization. Mol Endocrinol 5:1396-404

5.   **Smith CL, O'Malley BW** 2004 Coregulator function: a key to understanding tissue specificity of selective receptor modulators. Endocr Rev 25:45-71

6.   **Pratt WB, Toft DO** 1997 Steroid receptor interactions with heat shock protein and immunophilin chaperones. Endocr Rev 18:306-60

7.   **Freedman LP** 1998 Molecular biology of steroid and nuclear hormone receptors. Birkhauser, Boston, MA

8.   **Heinlein CA, Chang C** 2002 Androgen receptor (AR) coregulators: an overview. Endocr Rev 23:175-200

9.   **Shang Y, Myers M, Brown M** 2002 Formation of the androgen receptor transcription complex. Mol Cell 9:601-10

10.   **Matias PM, Donner P, Coelho R, Thomaz M, Peixoto C, Macedo S, Otto N, Joschko S, Scholz P, Wegg A, Basler S, Schafer M, Egner U, Carrondo MA** 2000 Structural evidence for ligand specificity in the binding domain of the human androgen receptor. Implications for pathogenic gene mutations. J Biol Chem 275:26164-71

11.   **Lutz LB, Jamnongjit M, Yang WH, Jahani D, Gill A, Hammes SR** 2003 Selective modulation of genomic and nongenomic androgen responses by androgen receptor ligands. Mol Endocrinol 17:1106-16

12.   **Zagar Y, Chaumaz G, Lieberherr M** 2004 Signaling cross-talk from Gbeta4 subunit to Elk-1 in the rapid action of androgens. J Biol Chem 279:2403-13

13.   **Unni E, Sun S, Nan B, McPhaul MJ, Cheskis B, Mancini MA, Marcelli M** 2004 Changes in androgen receptor nongenotropic signaling correlate with transition of LNCaP cells to androgen independence. Cancer Res 64:7156-68

14.   **Estrada M, Espinosa A, Muller M, Jaimovich E** 2003 Testosterone stimulates intracellular calcium release and mitogen-activated protein kinases via a G protein-coupled receptor in skeletal muscle cells. Endocrinology 144:3586-97

15.   **Norman AW, Mizwicki MT, Norman DP** 2004 Steroid-hormone rapid actions, membrane receptors and a conformational ensemble model. Nat Rev Drug Discov 3:27-41

16.   **Kang HY, Cho CL, Huang KL, Wang JC, Hu YC, Lin HK, Chang C, Huang KE** 2004 Nongenomic androgen activation of phosphatidylinositol 3-kinase/Akt signaling pathway in MC3T3-E1 osteoblasts. J Bone Miner Res 19:1181-90

17.   **Davis SR, McCloud P, Strauss BJ, Burger H** 2008 Testosterone enhances estradiol's effects on postmenopausal bone density and sexuality. Maturitas 61:17-26

18.   **Nieschlag E, Cuppers HJ, Wickings EJ** 1977 Influence of sex, testicular development and liver function on the bioavailability of oral testosterone. Eur J Clin Invest 7:145-7

19.   **Nieschlag E B, HM** (ed) 2004 Testosterone: Action, Deficiency, Substitution, 3rd ed. Cambridge University Press, New York, NY

20.   **Schurmeyer T, Wickings EJ, Freischem CW, Nieschlag E** 1983 Saliva and serum testosterone following oral testosterone undecanoate administration in normal and hypogonadal men. Acta Endocrinol (Copenh) 102:456-62

21.   **Neri R, Florance K, Koziol P, Van Cleave S** 1972 A biological profile of a nonsteroidal antiandrogen, SCH 13521 (4'-nitro-3'trifluoromethylisobutyranilide). Endocrinology 91:427-37

22.   **Neri R, Peets E, Watnick A** 1979 Anti-androgenicity of flutamide and its metabolite Sch 16423. Biochem Soc Trans 7:565-9

23.   **Neri RO, Peets EA** 1975 Biological aspects of antiandrogens. J Steroid Biochem 6:815-9

24.   **Harris MG, Coleman SG, Faulds D, Chrisp P** 1993 Nilutamide. A review of its pharmacodynamic and pharmacokinetic properties, and therapeutic efficacy in prostate cancer. Drugs Aging 3:9-25

25.   **Moguilewsky M, Bertagna C, Hucher M** 1987 Pharmacological and clinical studies of the antiandrogen Anandron. J Steroid Biochem 27:871-5

26.	**Raynaud JP, Bonne C, Moguilewsky M, Lefebvre FA, Belanger A, Labrie F** 1984 The pure antiandrogen RU 23908 (Anandron), a candidate of choice for the combined antihormonal treatment of prostatic cancer: a review. Prostate 5:299-311

27.	**Furr BJ, Valcaccia B, Curry B, Woodburn JR, Chesterson G, Tucker H** 1987 ICI 176,334: a novel non-steroidal, peripherally selective antiandrogen. J Endocrinol 113:R7-9

28.	**Kaisary AV** 1994 Current clinical studies with a new nonsteroidal antiandrogen, Casodex. Prostate Suppl 5:27-33

29.	**Lunglmayr G** 1995 Efficacy and tolerability of Casodex in patients with advanced prostate cancer. International Casodex Study Group. Anticancer Drugs 6:508-13

30.	**Dalton JT, Mukherjee A, Zhu Z, Kirkovsky L, Miller DD** 1998 Discovery of nonsteroidal androgens. Biochem Biophys Res Commun 244:1-4

31.	**Yin D, Xu H, He Y, Kirkovsky LI, Miller DD, Dalton JT** 2003 Pharmacology, pharmacokinetics, and metabolism of acetothiolutamide, a novel nonsteroidal agonist for the androgen receptor. J Pharmacol Exp Ther 304:1323-33

32.	**Yin D, Gao W, Kearbey JD, Xu H, Chung K, He Y, Marhefka CA, Veverka KA, Miller DD, Dalton JT** 2003 Pharmacodynamics of selective androgen receptor modulators. J Pharmacol Exp Ther 304:1334-40

33.	**Yin D, He Y, Perera MA, Hong SS, Marhefka C, Stourman N, Kirkovsky L, Miller DD, Dalton JT** 2003 Key structural features of nonsteroidal ligands for binding and activation of the androgen receptor. Mol Pharmacol 63:211-23

34.	**Negro-Vilar A** 1999 Selective androgen receptor modulators (SARMs): a novel approach to androgen therapy for the new millennium. J Clin Endocrinol Metab 84:3459-62

35.	**Chang CY, McDonnell DP** 2002 Evaluation of ligand-dependent changes in AR structure using peptide probes. Mol Endocrinol 16:647-60

36.	**Kazmin D, Prytkova T, Cook CE, Wolfinger R, Chu TM, Beratan D, Norris JD, Chang CY, McDonnell DP** 2006 Linking ligand-induced alterations in androgen receptor structure to differential gene expression: a first step in the rational design of selective androgen receptor modulators. Mol Endocrinol 20:1201-17

37.	**Narayanan R, Coss CC, Yepuru M, Kearbey JD, Miller DD, Dalton JT** 2008 Steroidal androgens and nonsteroidal, tissue-selective androgen receptor modulator, S-22, regulate androgen receptor function through distinct genomic and nongenomic signaling pathways. Mol Endocrinol 22:2448-65

38.	**Pavlou SN, Brewer K, Farley MG, Lindner J, Bastias MC, Rogers BJ, Swift LL, Rivier JE, Vale WW, Conn PM, et al.** 1991 Combined administration of a gonadotropin-releasing hormone antagonist and testosterone in men induces reversible azoospermia without loss of libido. J Clin Endocrinol Metab 73:1360-9

39.   **Prasad MR, Rajalakshmi M** 1976 Target sites for suppressing fertility in the male. Adv Sex Horm Res 2:263-87

40.   1990 Contraceptive efficacy of testosterone-induced azoospermia in normal men. World Health Organization Task Force on methods for the regulation of male fertility. Lancet 336:955-9

41.   1996 Contraceptive efficacy of testosterone-induced azoospermia and oligozoospermia in normal men. Fertil Steril 65:821-9

42.   **Gu YQ, Wang XH, Xu D, Peng L, Cheng LF, Huang MK, Huang ZJ, Zhang GY** 2003 A multicenter contraceptive efficacy study of injectable testosterone undecanoate in healthy Chinese men. J Clin Endocrinol Metab 88:562-8

43.   **Kamischke A, Ploger D, Venherm S, von Eckardstein S, von Eckardstein A, Nieschlag E** 2000 Intramuscular testosterone undecanoate with or without oral levonorgestrel: a randomized placebo-controlled feasibility study for male contraception. Clin Endocrinol (Oxf) 53:43-52

44.   **von Eckardstein S, Noe G, Brache V, Nieschlag E, Croxatto H, Alvarez F, Moo-Young A, Sivin I, Kumar N, Small M, Sundaram K** 2003 A clinical trial of 7 alpha-methyl-19-nortestosterone implants for possible use as a long-acting contraceptive for men. J Clin Endocrinol Metab 88:5232-9

45.   **Wenk M, Nieschlag E** 2006 Male contraception: a realistic option? Eur J Contracept Reprod Health Care 11:69-80

46.   **Glasier AF, Anakwe R, Everington D, Martin CW, van der Spuy Z, Cheng L, Ho PC, Anderson RA** 2000 Would women trust their partners to use a male pill? Hum Reprod 15:646-9

47.   **Martin CW, Anderson RA, Cheng L, Ho PC, van der Spuy Z, Smith KB, Glasier AF, Everington D, Baird DT** 2000 Potential impact of hormonal male contraception: cross-cultural implications for development of novel preparations. Hum Reprod 15:637-45

48.   **Chen J, Hwang DJ, Bohl CE, Miller DD, Dalton JT** 2005 A selective androgen receptor modulator for hormonal male contraception. J Pharmacol Exp Ther 312:546-53

49.   **Sherwin BB, Gelfand MM** 1987 The role of androgen in the maintenance of sexual functioning in oophorectomized women. Psychosom Med 49:397-409

50.   **Dennerstein L, Dudley E, Burger H** 2001 Are changes in sexual functioning during midlife due to aging or menopause? Fertil Steril 76:456-60

51.   **McCoy NL, Davidson JM** 1985 A longitudinal study of the effects of menopause on sexuality. Maturitas 7:203-10

52.   **Shifren JL, Davis SR, Moreau M, Waldbaum A, Bouchard C, DeRogatis L, Derzko C, Bearnson P, Kakos N, O'Neill S, Levine S, Wekselman K, Buch A,**

Rodenberg C, Kroll R 2006 Testosterone patch for the treatment of hypoactive sexual desire disorder in naturally menopausal women: results from the INTIMATE NM1 Study. Menopause 13:770-9

53.   **Nathorst-Boos J, von Schoultz B** 1992 Psychological reactions and sexual life after hysterectomy with and without oophorectomy. Gynecol Obstet Invest 34:97-101

54.   **Zussman L, Zussman S, Sunley R, Bjornson E** 1981 Sexual response after hysterectomy-oophorectomy: recent studies and reconsideration of psychogenesis. Am J Obstet Gynecol 140:725-9

55.   **Judd HL, Judd GE, Lucas WE, Yen SS** 1974 Endocrine function of the postmenopausal ovary: concentration of androgens and estrogens in ovarian and peripheral vein blood. J Clin Endocrinol Metab 39:1020-4

56.   **Davis S, Papalia MA, Norman RJ, O'Neill S, Redelman M, Williamson M, Stuckey BG, Wlodarczyk J, Gard'ner K, Humberstone A** 2008 Safety and efficacy of a testosterone metered-dose transdermal spray for treating decreased sexual satisfaction in premenopausal women: a randomized trial. Ann Intern Med 148:569-77

57.   **Buster JE, Kingsberg SA, Aguirre O, Brown C, Breaux JG, Buch A, Rodenberg CA, Wekselman K, Casson P** 2005 Testosterone patch for low sexual desire in surgically menopausal women: a randomized trial. Obstet Gynecol 105:944-52

58.   **Simon J, Braunstein G, Nachtigall L, Utian W, Katz M, Miller S, Waldbaum A, Bouchard C, Derzko C, Buch A, Rodenberg C, Lucas J, Davis S** 2005 Testosterone patch increases sexual activity and desire in surgically menopausal women with hypoactive sexual desire disorder. J Clin Endocrinol Metab 90:5226-33

59.   **Wierman ME, Basson R, Davis SR, Khosla S, Miller KK, Rosner W, Santoro N** 2006 Androgen therapy in women: an Endocrine Society Clinical Practice guideline. J Clin Endocrinol Metab 91:3697-710

60.   **Smith MR, Goode M, Zietman AL, McGovern FJ, Lee H, Finkelstein JS** 2004 Bicalutamide monotherapy versus leuprolide monotherapy for prostate cancer: effects on bone mineral density and body composition. J Clin Oncol 22:2546-53

61.   **Klotz L** 2008 Maximal androgen blockade for advanced prostate cancer. Best Pract Res Clin Endocrinol Metab 22:331-40

62.   **Scher HI, Kelly WK** 1993 Flutamide withdrawal syndrome: its impact on clinical trials in hormone-refractory prostate cancer. J Clin Oncol 11:1566-72

63.   **Linja MJ, Visakorpi T** 2004 Alterations of androgen receptor in prostate cancer. J Steroid Biochem Mol Biol 92:255-64

64.   **Buchanan G, Greenberg NM, Scher HI, Harris JM, Marshall VR, Tilley WD** 2001 Collocation of androgen receptor gene mutations in prostate cancer. Clin Cancer Res 7:1273-81

65. **Suzuki H, Akakura K, Komiya A, Aida S, Akimoto S, Shimazaki J** 1996 Codon 877 mutation in the androgen receptor gene in advanced prostate cancer: relation to antiandrogen withdrawal syndrome. Prostate 29:153-8

66. **Hara T, Miyazaki J, Araki H, Yamaoka M, Kanzaki N, Kusaka M, Miyamoto M** 2003 Novel mutations of androgen receptor: a possible mechanism of bicalutamide withdrawal syndrome. Cancer Res 63:149-53

67. **Bohl CE, Gao W, Miller DD, Bell CE, Dalton JT** 2005 Structural basis for antagonism and resistance of bicalutamide in prostate cancer. Proc Natl Acad Sci U S A 102:6201-6

68. **Zhou J, Liu B, Geng G, Wu JH** Study of the impact of the T877A mutation on ligand-induced helix-12 positioning of the androgen receptor resulted in design and synthesis of novel antiandrogens. Proteins 78:623-37

69. **Przkora R, Herndon DN, Suman OE** 2007 The effects of oxandrolone and exercise on muscle mass and function in children with severe burns. Pediatrics 119:e109-16

70. **Nystrom G, Pruznak A, Huber D, Frost RA, Lang CH** 2009 Local insulin-like growth factor I prevents sepsis-induced muscle atrophy. Metabolism 58:787-97

71. **Ferrando AA, Sheffield-Moore M, Yeckel CW, Gilkison C, Jiang J, Achacosa A, Lieberman SA, Tipton K, Wolfe RR, Urban RJ** 2002 Testosterone administration to older men improves muscle function: molecular and physiological mechanisms. Am J Physiol Endocrinol Metab 282:E601-7

72. **de Boer MD, Selby A, Atherton P, Smith K, Seynnes OR, Maganaris CN, Maffulli N, Movin T, Narici MV, Rennie MJ** 2007 The temporal responses of protein synthesis, gene expression and cell signalling in human quadriceps muscle and patellar tendon to disuse. J Physiol 585:241-51

73. **Zilbermint MF, Dobs AS** 2009 Nonsteroidal selective androgen receptor modulator Ostarine in cancer cachexia. Future Oncol 5:1211-20

74. **Scott WB, Oursler KK, Katzel LI, Ryan AS, Russ DW** 2007 Central activation, muscle performance, and physical function in men infected with human immunodeficiency virus. Muscle Nerve 36:374-83

75. **Dore RK, Cohen SB, Lane NE, Palmer WR, Shergy W, Zhou L, Wang H, Tsuji W, Newmark R** 2009 Effects of denosumab on bone mineral density and bone turnover in patients with rheumatoid arthritis receiving concurrent glucocorticoids or bisphosphonates. Ann Rheum Dis

76. **Cordina M, Fenech AG, Vassallo J, Cacciottolo JM** 2009 Anxiety and the management of asthma in an adult outpatient population. Ther Adv Respir Dis 3:227-33

77. **Crawford BA, Liu PY, Kean MT, Bleasel JF, Handelsman DJ** 2003 Randomized placebo-controlled trial of androgen effects on muscle and bone in men requiring long-term systemic glucocorticoid treatment. J Clin Endocrinol Metab 88:3167-76

78. **Van Balkom RH, Dekhuijzen PN, Folgering HT, Veerkamp JH, Van Moerkerk HT, Fransen JA, Van Herwaarden CL** 1998 Anabolic steroids in part reverse glucocorticoid-induced alterations in rat diaphragm. J Appl Physiol 84:1492-9

79. **Knapp PE, Storer TW, Herbst KL, Singh AB, Dzekov C, Dzekov J, LaValley M, Zhang A, Ulloor J, Bhasin S** 2008 Effects of a supraphysiological dose of testosterone on physical function, muscle performance, mood, and fatigue in men with HIV-associated weight loss. Am J Physiol Endocrinol Metab 294:E1135-43

80. **Ferrando AA, Sheffield-Moore M, Wolf SE, Herndon DN, Wolfe RR** 2001 Testosterone administration in severe burns ameliorates muscle catabolism. Crit Care Med 29:1936-42

81. **Gao W, Reiser PJ, Coss CC, Phelps MA, Kearbey JD, Miller DD, Dalton JT** 2005 Selective androgen receptor modulator treatment improves muscle strength and body composition and prevents bone loss in orchidectomized rats. Endocrinology 146:4887-97

82. **Kearbey JD, Gao W, Narayanan R, Fisher SJ, Wu D, Miller DD, Dalton JT** 2007 Selective Androgen Receptor Modulator (SARM) treatment prevents bone loss and reduces body fat in ovariectomized rats. Pharm Res 24:328-35

83. **Hardman J** 1996 Goodman and Gilman's Pharmacological Basis of Therapeutics, 9th ed. McGraw Hill, New York, NY

84. **Nieschlag E** 1998 Testosterone: action, deficiency, substitution, 2 ed. Springer, New York

85. **Gao W, Kim J, Dalton JT** 2006 Pharmacokinetics and pharmacodynamics of nonsteroidal androgen receptor ligands. Pharm Res 23:1641-58

86. **Amory JK, Page ST, Bremner WJ** 2006 Drug insight: Recent advances in male hormonal contraception. Nat Clin Pract Endocrinol Metab 2:32-41

87. **Kamischke A, Nieschlag E** 2004 Progress towards hormonal male contraception. Trends Pharmacol Sci 25:49-57

88. **Kim J, Wu D, Hwang DJ, Miller DD, Dalton JT** 2005 The para substituent of S-3-(phenoxy)-2-hydroxy-2-methyl-N-(4-nitro-3-trifluoromethyl-phenyl)-prop ionamides is a major structural determinant of in vivo disposition and activity of selective androgen receptor modulators. J Pharmacol Exp Ther 315:230-9

89. **Lodder J, Baum MJ** 1977 Facilitation of mounting behavior by dihydrotestosterone propionate in castrated estradiol benzoate-treated male rats following pudendectomy. Behav Biol 20:141-8

90. **Baum MJ, Vreeburg JT** 1973 Copulation in castrated male rats following combined treatment with estradiol and dihydrotestosterone. Science 182:283-5

91.   **Feder HH** 1971 The comparative actions of testosterone propionate and 5 -
        androstan-17 -ol-3-one propionate on the reproductive behaviour, physiology and
        morphology of male rats. J Endocrinol 51:241-52

92.   **McDonald P, Beyer C, Newton F, Brien B, Baker R, Tan HS, Sampson C,
        Kitching P, Greenhill R, Pritchard D** 1970 Failure of 5alpha-dihydrotestosterone to
        initiate sexual behaviour in the castrated male rat. Nature 227:964-5

93.   **Jones ME, Boon WC, Proietto J, Simpson ER** 2006 Of mice and men: the evolving
        phenotype of aromatase deficiency. Trends Endocrinol Metab 17:55-64

94.   **Carani C, Rochira V, Faustini-Fustini M, Balestrieri A, Granata AR** 1999 Role
        of oestrogen in male sexual behaviour: insights from the natural model of aromatase
        deficiency. Clin Endocrinol (Oxf) 51:517-24

95.   **Hechter O, Mechaber D, Zwick A, Campfield LA, Eychenne B, Baulieu EE,
        Robel P** 1983 Optimal radioligand exchange conditions for measurement of occupied
        androgen receptor sites in rat ventral prostate. Arch Biochem Biophys 224:49-68

96.   **Chen J, Hwang DJ, Chung K, Bohl CE, Fisher SJ, Miller DD, Dalton JT** 2005 In
        vitro and in vivo structure-activity relationships of novel androgen receptor ligands
        with multiple substituents in the B-ring. Endocrinology 146:5444-54

97.   **Anderson RA, Baird DT** 2002 Male contraception. Endocr Rev 23:735-62

98.   **Maffei L, Murata Y, Rochira V, Tubert G, Aranda C, Vazquez M, Clyne CD,
        Davis S, Simpson ER, Carani C** 2004 Dysmetabolic syndrome in a man with a
        novel mutation of the aromatase gene: effects of testosterone, alendronate, and
        estradiol treatment. J Clin Endocrinol Metab 89:61-70

99.   **Herrmann BL, Saller B, Janssen OE, Gocke P, Bockisch A, Sperling H, Mann
        K, Broecker M** 2002 Impact of estrogen replacement therapy in a male with
        congenital aromatase deficiency caused by a novel mutation in the CYP19 gene. J
        Clin Endocrinol Metab 87:5476-84

100.   **Miner JN, Chang W, Chapman MS, Finn PD, Hong MH, Lopez FJ, Marschke
        KB, Rosen J, Schrader W, Turner R, van Oeveren A, Viveros H, Zhi L, Negro-
        Vilar A** 2007 An orally active selective androgen receptor modulator is efficacious
        on bone, muscle, and sex function with reduced impact on prostate. Endocrinology
        148:363-73

101.   **Oshima H, Wakabayashi K, Tamaoki BI** 1967 The effect of synthetic estrogen
        upon the biosynthesis in vitro of androgeng and luteinizing hormone in the rat.
        Biochim Biophys Acta 137:356-66

102.   **Verjans HL, de Jong FH, Cooke BA, van der Molen HJ, Eik-Nes KB** 1974 Effect
        of oestradiol benzoate on pituitary and testis function in the normal adult male rat.
        Acta Endocrinol (Copenh) 77:636-42

103.   **Hislop MS, Ratanjee BD, Soule SG, Marais AD** 1999 Effects of anabolic-androgenic steroid use or gonadal testosterone suppression on serum leptin concentration in men. Eur J Endocrinol 141:40-6

104.   **Watanobe H, Suda T** 1999 A detailed study on the role of sex steroid milieu in determining plasma leptin concentrations in adult male and female rats. Biochem Biophys Res Commun 259:56-9

105.   **Pinilla L, Seoane LM, Gonzalez L, Carro E, Aguilar E, Casanueva FF, Dieguez C** 1999 Regulation of serum leptin levels by gonadal function in rats. Eur J Endocrinol 140:468-73

106.   **Chen J GN, Chung K, Miller DD, Dalton JT** 2002 Modulation of hormonal biomarkers and target organ weights *in vivo* by selective androgen receptor modulators (SARMs) AAPS Pharm Sci

107.   **Gao W, Kearbey JD, Nair VA, Chung K, Parlow AF, Miller DD, Dalton JT** 2004 Comparison of the pharmacological effects of a novel selective androgen receptor modulator, the 5alpha-reductase inhibitor finasteride, and the antiandrogen hydroxyflutamide in intact rats: new approach for benign prostate hyperplasia. Endocrinology 145:5420-8

108.   **Turner TT, Jones CE, Howards SS, Ewing LL, Zegeye B, Gunsalus GL** 1984 On the androgen microenvironment of maturing spermatozoa. Endocrinology 115:1925-32

109.   **Jarow JP, Zirkin BR** 2005 The androgen microenvironment of the human testis and hormonal control of spermatogenesis. Ann N Y Acad Sci 1061:208-20

110.   **Zirkin BR, Santulli R, Awoniyi CA, Ewing LL** 1989 Maintenance of advanced spermatogenic cells in the adult rat testis: quantitative relationship to testosterone concentration within the testis. Endocrinology 124:3043-9

111.   **Walsh PC, Swerdloff RS** 1973 Biphasic effect of testosterone on spermatogenesis in the rat. Invest Urol 11:190-3

112.   **Awoniyi CA, Santulli R, Chandrashekar V, Schanbacher BD, Zirkin BR** 1989 Quantitative restoration of advanced spermatogenic cells in adult male rats made azoospermic by active immunization against luteinizing hormone or gonadotropin-releasing hormone. Endocrinology 125:1303-9

113.   **Awoniyi CA, Sprando RL, Santulli R, Chandrashekar V, Ewing LL, Zirkin BR** 1990 Restoration of spermatogenesis by exogenously administered testosterone in rats made azoospermic by hypophysectomy or withdrawal of luteinizing hormone alone. Endocrinology 127:177-84

114.   **Awoniyi CA, Zirkin BR, Chandrashekar V, Schlaff WD** 1992 Exogenously administered testosterone maintains spermatogenesis quantitatively in adult rats actively immunized against gonadotropin-releasing hormone. Endocrinology 130:3283-8

115. **Saito K, O'Donnell L, McLachlan RI, Robertson DM** 2000 Spermiation failure is a major contributor to early spermatogenic suppression caused by hormone withdrawal in adult rats. Endocrinology 141:2779-85

116. **Beardsley A, O'Donnell L** 2003 Characterization of normal spermiation and spermiation failure induced by hormone suppression in adult rats. Biol Reprod 68:1299-307

117. **Palacios A, McClure RD, Campfield A, Swerdloff RS** 1981 Effect of testosterone enanthate on testis size. J Urol 126:46-8

118. **Meachem SJ, Wreford NG, Stanton PG, Robertson DM, McLachlan RI** 1998 Follicle-stimulating hormone is required for the initial phase of spermatogenic restoration in adult rats following gonadotropin suppression. J Androl 19:725-35

119. **Ewing LL, Desjardins C, Irby DC, Robaire B** 1977 Synergistic interaction of testosterone and oestradiol inhibits spermatogenesis in rats. Nature 269:409-11

120. **Handelsman DJ, Wishart S, Conway AJ** 2000 Oestradiol enhances testosterone-induced suppression of human spermatogenesis. Hum Reprod 15:672-9

121. **Schmidt C** 1994 Diagnostic and statistical namual of mental disorders, 4th ed. American Psychiatric Association, Washington, DC

122. **Blasberg ME, Robinson S, Henderson LP, Clark AS** 1998 Inhibition of estrogen-induced sexual receptivity by androgens: role of the androgen receptor. Horm Behav 34:283-93

123. **Jones A, Chen J, Hwang DJ, Miller DD, Dalton JT** 2009 Preclinical characterization of a (S)-N-(4-cyano-3-trifluoromethyl-phenyl)-3-(3-fluoro, 4-chlorophenoxy)-2-hydroxy-2-methyl-propanamide: a selective androgen receptor modulator for hormonal male contraception. Endocrinology 150:385-95

124. **Mukherjee A, Kirkovsky L, Yao XT, Yates RC, Miller DD, Dalton JT** 1996 Enantioselective binding of Casodex to the androgen receptor. Xenobiotica 26:117-22

125. **Marhefka CA, Gao W, Chung K, Kim J, He Y, Yin D, Bohl C, Dalton JT, Miller DD** 2004 Design, synthesis, and biological characterization of metabolically stable selective androgen receptor modulators. J Med Chem 47:993-8

126. **Mukherjee A, Kirkovsky LI, Kimura Y, Marvel MM, Miller DD, Dalton JT** 1999 Affinity labeling of the androgen receptor with nonsteroidal chemoaffinity ligands. Biochem Pharmacol 58:1259-67

127. **He Y, Yin D, Perera M, Kirkovsky L, Stourman N, Li W, Dalton JT, Miller DD** 2002 Novel nonsteroidal ligands with high binding affinity and potent functional activity for the androgen receptor. Eur J Med Chem 37:619-34

128. **Kirkovsky L, Mukherjee A, Yin D, Dalton JT, Miller DD** 2000 Chiral nonsteroidal affinity ligands for the androgen receptor. 1. Bicalutamide analogues bearing electrophilic groups in the B aromatic ring. J Med Chem 43:581-90

129. **Bohl CE, Wu Z, Chen J, Mohler ML, Yang J, Hwang DJ, Mustafa S, Miller DD, Bell CE, Dalton JT** 2008 Effect of B-ring substitution pattern on binding mode of propionamide selective androgen receptor modulators. Bioorg Med Chem Lett 18:5567-70

130. **Hamann LG, Higuchi RI, Zhi L, Edwards JP, Wang XN, Marschke KB, Kong JW, Farmer LJ, Jones TK** 1998 Synthesis and biological activity of a novel series of nonsteroidal, peripherally selective androgen receptor antagonists derived from 1,2-dihydropyridono[5,6-g]quinolines. J Med Chem 41:623-39

131. **Ishioka T, Kubo A, Koiso Y, Nagasawa K, Itai A, Hashimoto Y** 2002 Novel non-steroidal/non-anilide type androgen antagonists with an isoxazolone moiety. Bioorg Med Chem 10:1555-66

132. **Morris JJ, Hughes LR, Glen AT, Taylor PJ** 1991 Non-steroidal antiandrogens. Design of novel compounds based on an infrared study of the dominant conformation and hydrogen-bonding properties of a series of anilide antiandrogens. J Med Chem 34:447-55

133. **Teutsch G, Goubet F, Battmann T, Bonfils A, Bouchoux F, Cerede E, Gofflo D, Gaillard-Kelly M, Philibert D** 1994 Non-steroidal antiandrogens: synthesis and biological profile of high-affinity ligands for the androgen receptor. J Steroid Biochem Mol Biol 48:111-9

134. **Tucker H, Crook JW, Chesterson GJ** 1988 Nonsteroidal antiandrogens. Synthesis and structure-activity relationships of 3-substituted derivatives of 2-hydroxypropionanilides. J Med Chem 31:954-9

135. **Higuchi RI, Thompson AW, Chen JH, Caferro TR, Cummings ML, Deckhut CP, Adams ME, Tegley CM, Edwards JP, Lopez FJ, Kallel EA, Karanewsky DS, Schrader WT, Marschke KB, Zhi L** 2007 Potent, nonsteroidal selective androgen receptor modulators (SARMs) based on 8H-[1,4]oxazino[2,3-f]quinolin-8-ones. Bioorg Med Chem Lett 17:5442-6

136. **Li JJ, Sutton JC, Nirschl A, Zou Y, Wang H, Sun C, Pi Z, Johnson R, Krystek SR, Jr., Seethala R, Golla R, Sleph PG, Beehler BC, Grover GJ, Fura A, Vyas VP, Li CY, Gougoutas JZ, Galella MA, Zahler R, Ostrowski J, Hamann LG** 2007 Discovery of potent and muscle selective androgen receptor modulators through scaffold modifications. J Med Chem 50:3015-25

137. **Long YO, Higuchi RI, Caferro TR, Lau TL, Wu M, Cummings ML, Martinborough EA, Marschke KB, Chang WY, Lopez FJ, Karanewsky DS, Zhi L** 2008 Selective androgen receptor modulators based on a series of 7H-[1,4]oxazino[3,2-g]quinolin-7-ones with improved in vivo activity. Bioorg Med Chem Lett 18:2967-71

138. **Manfredi MC, Bi Y, Nirschl AA, Sutton JC, Seethala R, Golla R, Beehler BC, Sleph PG, Grover GJ, Ostrowski J, Hamann LG** 2007 Synthesis and SAR of tetrahydropyrrolo[1,2-b][1,2,5]thiadiazol-2(3H)-one 1,1-dioxide analogues as highly potent selective androgen receptor modulators. Bioorg Med Chem Lett 17:4487-90

139. **Martinborough E, Shen Y, Oeveren A, Long YO, Lau TL, Marschke KB, Chang WY, Lopez FJ, Vajda EG, Rix PJ, Viveros OH, Negro-Vilar A, Zhi L** 2007 Substituted 6-(1-pyrrolidine)quinolin-2(1H)-ones as novel selective androgen receptor modulators. J Med Chem 50:5049-52

140. **Nirschl AA, Zou Y, Krystek SR, Jr., Sutton JC, Simpkins LM, Lupisella JA, Kuhns JE, Seethala R, Golla R, Sleph PG, Beehler BC, Grover GJ, Egan D, Fura A, Vyas VP, Li YX, Sack JS, Kish KF, An Y, Bryson JA, Gougoutas JZ, DiMarco J, Zahler R, Ostrowski J, Hamann LG** 2009 N-aryl-oxazolidin-2-imine muscle selective androgen receptor modulators enhance potency through pharmacophore reorientation. J Med Chem 52:2794-8

141. **Zhang X, Li X, Allan GF, Sbriscia T, Linton O, Lundeen SG, Sui Z** 2007 Design, synthesis, and in vivo SAR of a novel series of pyrazolines as potent selective androgen receptor modulators. J Med Chem 50:3857-69

142. **Zhao S, Shen Y, van Oeveren A, Marschke KB, Zhi L** 2008 Discovery of a novel series of nonsteroidal androgen receptor modulators: 5- or 6-oxachrysen-2-ones. Bioorg Med Chem Lett 18:3431-5

143. **Zhou C, Wu G, Feng Y, Li Q, Su H, Mais DE, Zhu Y, Li N, Deng Y, Yang D, Wang MW** 2008 Discovery and biological characterization of a novel series of androgen receptor modulators. Br J Pharmacol 154:440-50

144. **Ng RA, Lanter JC, Alford VC, Allan GF, Sbriscia T, Lundeen SG, Sui Z** 2007 Synthesis of potent and tissue-selective androgen receptor modulators (SARMs): 2-(2,2,2)-Trifluoroethyl-benzimidazole scaffold. Bioorg Med Chem Lett 17:1784-7

145. **van Oeveren A, Motamedi M, Martinborough E, Zhao S, Shen Y, West S, Chang W, Kallel A, Marschke KB, Lopez FJ, Negro-Vilar A, Zhi L** 2007 Novel selective androgen receptor modulators: SAR studies on 6-bisalkylamino-2-quinolinones. Bioorg Med Chem Lett 17:1527-31

146. **Bohl CE, Chang C, Mohler ML, Chen J, Miller DD, Swaan PW, Dalton JT** 2004 A ligand-based approach to identify quantitative structure-activity relationships for the androgen receptor. J Med Chem 47:3765-76

147. **Edwards DA, Pfeifle JK** 1983 Hormonal control of receptivity, proceptivity and sexual motivation. Physiol Behav 30:437-43

148. **Erskine MS** 1989 Solicitation behavior in the estrous female rat: a review. Horm Behav 23:473-502

149. **Allan GF, Tannenbaum P, Sbriscia T, Linton O, Lai MT, Haynes-Johnson D, Bhattacharjee S, Zhang X, Sui Z, Lundeen SG** 2007 A selective androgen receptor

modulator with minimal prostate hypertrophic activity enhances lean body mass in male rats and stimulates sexual behavior in female rats. Endocrine 32:41-51

150.   **Tazuke S, Khaw KT, Barrett-Connor E** 1992 Exogenous estrogen and endogenous sex hormones. Medicine (Baltimore) 71:44-51

151.   **Abraham GE** 1974 Ovarian and adrenal contribution to peripheral androgens during the menstrual cycle. J Clin Endocrinol Metab 39:340-6

152.   **Fisher S** 2004 Identification of structure-activity relationships of selective androgen receptor modulators in preclinical animal models Pharmacy. The Ohio State University, Columbus

153.   **Kim J** 2006 Pharmacokinetics, metabolism, and pharmacologic activities of nonsteroidal selective androgen receptor modulators and their potential application to osteoporosis Pharmacy. The Ohio State University, Columbus

154.   **Tran C, Ouk S, Clegg NJ, Chen Y, Watson PA, Arora V, Wongvipat J, Smith-Jones PM, Yoo D, Kwon A, Wasielewska T, Welsbie D, Chen CD, Higano CS, Beer TM, Hung DT, Scher HI, Jung ME, Sawyers CL** 2009 Development of a second-generation antiandrogen for treatment of advanced prostate cancer. Science 324:787-90

155.   **Brzozowski AM, Pike AC, Dauter Z, Hubbard RE, Bonn T, Engstrom O, Ohman L, Greene GL, Gustafsson JA, Carlquist M** 1997 Molecular basis of agonism and antagonism in the oestrogen receptor. Nature 389:753-8

156.   **Bohl CE, Miller DD, Chen J, Bell CE, Dalton JT** 2005 Structural basis for accommodation of nonsteroidal ligands in the androgen receptor. J Biol Chem 280:37747-54

157.   **Yoshida T, Kinoshita H, Segawa T, Nakamura E, Inoue T, Shimizu Y, Kamoto T, Ogawa O** 2005 Antiandrogen bicalutamide promotes tumor growth in a novel androgen-dependent prostate cancer xenograft model derived from a bicalutamide-treated patient. Cancer Res 65:9611-6

158.   **Brunger AT, Adams PD, Clore GM, DeLano WL, Gros P, Grosse-Kunstleve RW, Jiang JS, Kuszewski J, Nilges M, Pannu NS, Read RJ, Rice LM, Simonson T, Warren GL** 1998 Crystallography & NMR system: A new software suite for macromolecular structure determination. Acta Crystallogr D Biol Crystallogr 54:905-21

159.   **Jones TA, Zou JY, Cowan SW, Kjeldgaard M** 1991 Improved methods for building protein models in electron density maps and the location of errors in these models. Acta Crystallogr A 47 (Pt 2):110-9

160.   **Dehoux MJ, van Beneden RP, Fernandez-Celemin L, Lause PL, Thissen JP** 2003 Induction of MafBx and Murf ubiquitin ligase mRNAs in rat skeletal muscle after LPS injection. FEBS Lett 544:214-7

161. **DeRuisseau KC, Kavazis AN, Deering MA, Falk DJ, Van Gammeren D, Yimlamai T, Ordway GA, Powers SK** 2005 Mechanical ventilation induces alterations of the ubiquitin-proteasome pathway in the diaphragm. J Appl Physiol 98:1314-21

162. **Gomes MD, Lecker SH, Jagoe RT, Navon A, Goldberg AL** 2001 Atrogin-1, a muscle-specific F-box protein highly expressed during muscle atrophy. Proc Natl Acad Sci U S A 98:14440-5

163. **Latres E, Amini AR, Amini AA, Griffiths J, Martin FJ, Wei Y, Lin HC, Yancopoulos GD, Glass DJ** 2005 Insulin-like growth factor-1 (IGF-1) inversely regulates atrophy-induced genes via the phosphatidylinositol 3-kinase/Akt/mammalian target of rapamycin (PI3K/Akt/mTOR) pathway. J Biol Chem 280:2737-44

164. **Li YP, Chen Y, Li AS, Reid MB** 2003 Hydrogen peroxide stimulates ubiquitin-conjugating activity and expression of genes for specific E2 and E3 proteins in skeletal muscle myotubes. Am J Physiol Cell Physiol 285:C806-12

165. **Bodine SC, Latres E, Baumhueter S, Lai VK, Nunez L, Clarke BA, Poueymirou WT, Panaro FJ, Na E, Dharmarajan K, Pan ZQ, Valenzuela DM, DeChiara TM, Stitt TN, Yancopoulos GD, Glass DJ** 2001 Identification of ubiquitin ligases required for skeletal muscle atrophy. Science 294:1704-8

166. **Murton AJ, Constantin D, Greenhaff PL** 2008 The involvement of the ubiquitin proteasome system in human skeletal muscle remodelling and atrophy. Biochim Biophys Acta 1782:730-43

167. **DeVol DL, Rotwein P, Sadow JL, Novakofski J, Bechtel PJ** 1990 Activation of insulin-like growth factor gene expression during work-induced skeletal muscle growth. Am J Physiol 259:E89-95

168. **Coleman ME, DeMayo F, Yin KC, Lee HM, Geske R, Montgomery C, Schwartz RJ** 1995 Myogenic vector expression of insulin-like growth factor I stimulates muscle cell differentiation and myofiber hypertrophy in transgenic mice. J Biol Chem 270:12109-16

169. **Musaro A, McCullagh K, Paul A, Houghton L, Dobrowolny G, Molinaro M, Barton ER, Sweeney HL, Rosenthal N** 2001 Localized Igf-1 transgene expression sustains hypertrophy and regeneration in senescent skeletal muscle. Nat Genet 27:195-200

170. **Lai KM, Gonzalez M, Poueymirou WT, Kline WO, Na E, Zlotchenko E, Stitt TN, Economides AN, Yancopoulos GD, Glass DJ** 2004 Conditional activation of akt in adult skeletal muscle induces rapid hypertrophy. Mol Cell Biol 24:9295-304

171. **Rommel C, Bodine SC, Clarke BA, Rossman R, Nunez L, Stitt TN, Yancopoulos GD, Glass DJ** 2001 Mediation of IGF-1-induced skeletal myotube hypertrophy by PI(3)K/Akt/mTOR and PI(3)K/Akt/GSK3 pathways. Nat Cell Biol 3:1009-13

172.   **Glass DJ** 2005 Skeletal muscle hypertrophy and atrophy signaling pathways. Int J Biochem Cell Biol 37:1974-84

173.   **Sandri M, Sandri C, Gilbert A, Skurk C, Calabria E, Picard A, Walsh K, Schiaffino S, Lecker SH, Goldberg AL** 2004 Foxo transcription factors induce the atrophy-related ubiquitin ligase atrogin-1 and cause skeletal muscle atrophy. Cell 117:399-412

174.   **Stitt TN, Drujan D, Clarke BA, Panaro F, Timofeyva Y, Kline WO, Gonzalez M, Yancopoulos GD, Glass DJ** 2004 The IGF-1/PI3K/Akt pathway prevents expression of muscle atrophy-induced ubiquitin ligases by inhibiting FOXO transcription factors. Mol Cell 14:395-403

175.   **Sacheck JM, Ohtsuka A, McLary SC, Goldberg AL** 2004 IGF-I stimulates muscle growth by suppressing protein breakdown and expression of atrophy-related ubiquitin ligases, atrogin-1 and MuRF1. Am J Physiol Endocrinol Metab 287:E591-601

176.   **Kamei Y, Miura S, Suzuki M, Kai Y, Mizukami J, Taniguchi T, Mochida K, Hata T, Matsuda J, Aburatani H, Nishino I, Ezaki O** 2004 Skeletal muscle FOXO1 (FKHR) transgenic mice have less skeletal muscle mass, down-regulated Type I (slow twitch/red muscle) fiber genes, and impaired glycemic control. J Biol Chem 279:41114-23

177.   **Zhao W, Pan J, Zhao Z, Wu Y, Bauman WA, Cardozo CP** 2008 Testosterone protects against dexamethasone-induced muscle atrophy, protein degradation and MAFbx upregulation. J Steroid Biochem Mol Biol 110:125-9

178.   **Zhao J, Zhang Y, Zhao W, Wu Y, Pan J, Bauman WA, Cardozo C** 2008 Effects of nandrolone on denervation atrophy depend upon time after nerve transection. Muscle Nerve 37:42-9

179.   **Livak KJ, Schmittgen TD** 2001 Analysis of relative gene expression data using real-time quantitative PCR and the 2(-Delta Delta C(T)) Method. Methods 25:402-8

180.   **Dumas JF, Simard G, Roussel D, Douay O, Foussard F, Malthiery Y, Ritz P** 2003 Mitochondrial energy metabolism in a model of undernutrition induced by dexamethasone. Br J Nutr 90:969-77

181.   **Dekhuijzen PN, Gayan-Ramirez G, Bisschop A, De Bock V, Dom R, Decramer M** 1995 Corticosteroid treatment and nutritional deprivation cause a different pattern of atrophy in rat diaphragm. J Appl Physiol 78:629-37

182.   **Roy RR, Gardiner PF, Simpson DR, Edgerton VR** 1983 Glucocorticoid-induced atrophy in different fibre types of selected rat jaw and hind-limb muscles. Arch Oral Biol 28:639-43

183.   **Eisenberg E, Gordan GS** 1950 The levator ani muscle of the rat as an index of myotrophic activity of steroidal hormones. J Pharmacol Exp Ther 99:38-44

184.   **Hershberger LG, Shipley EG, Meyer RK** 1953 Myotrophic activity of 19-nortestosterone and other steroids determined by modified levator ani muscle method. Proc Soc Exp Biol Med 83:175-80

185. **Zhao W, Pan J, Wang X, Wu Y, Bauman WA, Cardozo CP** 2008 Expression of the muscle atrophy factor muscle atrophy F-box is suppressed by testosterone. Endocrinology 149:5449-60

186. **Yin HN, Chai JK, Yu YM, Shen CA, Wu YQ, Yao YM, Liu H, Liang LM, Tompkins RG, Sheng ZY** 2009 Regulation of signaling pathways downstream of IGF-I/insulin by androgen in skeletal muscle of glucocorticoid-treated rats. J Trauma 66:1083-90

187. **Meksumpun C, Meksumpun S** 2008 Integration of aquatic ecology and biological oceanographic knowledge for development of area-based eutrophication assessment criteria leading to water resource remediation and utilization management: a case study in Tha Chin, the most eutrophic river of Thailand. Water Sci Technol 58:2303-11

188. **Ma K, Mallidis C, Bhasin S, Mahabadi V, Artaza J, Gonzalez-Cadavid N, Arias J, Salehian B** 2003 Glucocorticoid-induced skeletal muscle atrophy is associated with upregulation of myostatin gene expression. Am J Physiol Endocrinol Metab 285:E363-71

189. **Savary I, Debras E, Dardevet D, Sornet C, Capitan P, Prugnaud J, Mirand PP, Grizard J** 1998 Effect of glucocorticoid excess on skeletal muscle and heart protein synthesis in adult and old rats. Br J Nutr 79:297-304

190. **Briski KP, Vogel KL, McIntyre AR** 1995 The antiglucocorticoid, RU486, attenuates stress-induced decreases in plasma-luteinizing hormone concentrations in male rats. Neuroendocrinology 61:638-45

191. **Hales DB, Payne AH** 1989 Glucocorticoid-mediated repression of P450scc mRNA and de novo synthesis in cultured Leydig cells. Endocrinology 124:2099-104

192. **Srivastava RK, Taylor MF, Mann DR** 1993 Effect of immobilization stress on plasma luteinizing hormone, testosterone, and corticosterone concentrations and on 3 beta-hydroxysteroid dehydrogenase activity in the testes of adult rats. Proc Soc Exp Biol Med 204:231-5

193. **Welsh TH, Jr., Bambino TH, Hsueh AJ** 1982 Mechanism of glucocorticoid-induced suppression of testicular androgen biosynthesis in vitro. Biol Reprod 27:1138-46

194. **Inder WJ, Jang C, Obeyesekere VR, Alford FP** 2009 Dexamethasone administration inhibits skeletal muscle expression of the androgen receptor and IGF-1 - implications for steroid-induced myopathy. Clin Endocrinol (Oxf)

195. **Urban RJ, Bodenburg YH, Gilkison C, Foxworth J, Coggan AR, Wolfe RR, Ferrando A** 1995 Testosterone administration to elderly men increases skeletal muscle strength and protein synthesis. Am J Physiol 269:E820-6

196. **Ferrando AA, Tipton KD, Doyle D, Phillips SM, Cortiella J, Wolfe RR** 1998 Testosterone injection stimulates net protein synthesis but not tissue amino acid transport. Am J Physiol 275:E864-71

197. **Jogo M, Shiraishi S, Tamura TA** 2009 Identification of MAFbx as a myogenin-engaged F-box protein in SCF ubiquitin ligase. FEBS Lett 583:2715-9

198. **Yang WL, Wang J, Chan CH, Lee SW, Campos AD, Lamothe B, Hur L, Grabiner BC, Lin X, Darnay BG, Lin HK** 2009 The E3 ligase TRAF6 regulates Akt ubiquitination and activation. Science 325:1134-8